FABRIC

Feasibility analysis and development of on-road charging solutions for future electric vehicles

Architecture definition

Deliverable No.		D3.5.1	
Work package No.	WP3.5	Work package Title	Architecture
Authors		D. Parena, P. Napolitano (AMET), H. Bludszuweit, J. Sallán (CIRCE), P. Guglielmi, G. Piccoli (POLITO), S. Laporte (VEDECOM), D. Roiu (CRF), M. Emre, P. Vermaat (TRL), T. Theodoropoulos, Y. Damousis (ICCS)	
Status		Final	
Dissemination level		Public	
Project start date and duration		01 January 2014, 48 Months	
Revision date		25 September 2017	
Submission date		25 September 2017	

This project has received funding from the European Union's Seventh Framework Programme for research, technological development and demonstration under grant agreement no 605405

TABLE OF CONTENTS

LIST OF FIGURES

LIST OF TABLES

LIST OF ABBREVIATIONS

ABBREVIATION	DESCRIPTION
AD	Automated Driving
BMS	Battery Management System
BOM	Bill of Materials
CAD	Computer Aided Design
CAE	Computer Aided Engineering
CO2	Carbon Dioxide
COG	Centre Of Gravity
CWD	Charge While Driving
DGPS	Differential Global Positioning System
DOF	Degree Of Freedom
DOW	Description of Work
DSM	Durability Strength and Misuse
DWPT	Dynamic Wireless Power Transfer
DX.X.X	Deliverable X.X.X
DSO	Distribution System Operator
EcoFEV	Efficient COoperative infrastructure for Fully Electric Vehicles
EM	Electromagnetic
EMF	Electromagnetic field
EMC	Electromagnetic Compatibility
ERG	External Reference Group
EV	Electric Vehicle
FABRIC	FeAsiBility analysis and development of on-Road chargIng solutions for

	future electric vehiCles
FE	Finite Element
FRF	Frequency Response Function
GNSS	Global Navigation Satellite System
HDV	Heavy Duty Vehicle
HV	High Voltage
I2I	Infrastructure to Infrastructure
ICT	Information and Communication Technology
IGBT	Insulated Gate Bipolar Transistor
JSON	Javascript Object Notation
LDV	Light Duty Vehicle
LTE	Long Term Evolution
LV	Low Voltage
MF-WPT	Magnetic Field Wireless Power Transfer
MV	Medium Voltage
MX	Month X
NIST	National Institute of Standards and Technology
NVH	Noise vibration and harshness
OCPP	Open Charge Point Protocol
OEM	Original Equipment Manufacturers
OSCP	Open Smart Charging Protocol
PWM	Pulse Width Modulation
RES	Renewable Energy Sources
RFID	Radio Frequency Identification
RTK GPS	Real Time Kinematic Global Positioning System

RSSI	Received Signal Strength Indication
RMS	Root Mean Square (effective value of AC quantities)
SP	Sub-Project
TCP/IP	Transmission Control Protocol / Internet Protocol
THD	Total Harmonic Distortion
TSO	Transport System Operator
TX.X.X	Task X.X.X
UC	Use Case
UL	Underwriters Laboratories
V2G	Vehicle to Grid
V2I	Vehicle to Infrastructure
V2V	Vehicle to Vehicle
VDSC	Vehicle Detection and Segment Control (system)
WP	Work Package
WPC	Wayside Power Converter
WPT	Wireless Power Transfer

EXECUTIVE SUMMARY

The vision of FABRIC is the large-scale adoption of pure Electric Vehicles (EVs) in future transportation systems, so it addresses the technological feasibility, economic and environmental sustainability of dynamic on-road charging of electric vehicles.

This document is the deliverable D3.5.1 - “Architecture Definition“- and summarizes the WP35 outcomes of the FABRIC Project. The objective of this document is to present and analyse the results of evaluations for the proposed dynamic power transfer architectures, to be used in the project. The WP35 work has been carried out on the basis of inputs provided by linked WPs, in particular WP32 and WP34, provided in deliverables D3.2.1 “Technical and user requirements” and D3.4.1 “Specifications document”.

This investigation covers the architecture of vehicle equipment, road-side and in-road equipment, and the interface of the charging infrastructure to the feeding electricity grid. Special focus is given to the specific solutions at each test site, but also the perspective of feasibility of large-scale implementation is kept in mind.

Concerning the vehicle equipment, the results of the investigation on the POLITO receiving structure behaviour, in some specific load conditions, support the conclusion that the system does not undergo any structural problems in normal vehicle operation conditions. However, some areas for improvement were identified in the equipment: first of all, a significant weight reduction of the system would be desirable. Further improvements can be achieved regarding the fastening of suspended solution and the choice of materials that are critical points, due to the need to find the best compromise between electromagnetic, thermal and mechanical requirements.

A generic architecture for roadside and in-road (for inductive systems) equipment has been considered. The transfer of power from the roadside to significant numbers of vehicles, particularly heavy vehicles, will require considerable roadside infrastructure due to the power levels involved, with power conversion capability in close proximity to ultimate power transfer equipment (coils, cables or rails). The generic architecture presented covers a range of implementation options. A more detailed architecture cannot be defined, due to the need to ensure compatibility with the different methods of power transfer.

The architectural issues of in-road equipment (e.g. buried coils) are considered while the vehicle is equipped with an on-board receiving structure. This kind of technology is potentially safer than other recharge systems with no exposed high-voltage equipment. However at this stage a generic architecture for in-road installation cannot be defined, due to the readiness level of viable solutions, and to the uncertainties of key design aspects.

Regarding the architecture of the interface to the energy network, existing solutions of WPT and railway applications have been analysed. A main conclusion was that power distribution of an electric road will be very similar if not identical to current railway systems. Light railway architectures are most likely to be a suitable solution. The actual interface to the grid is the converter station (including transformer). Here the study was focussed on the grid-tied converter which will feed the DC distribution line. Due to the power levels at the test sites, two generic converter topologies are presented, based on PWM IGBT devices. Total Harmonic distortion (THD) has been found to be a critical parameter, especially if the feeding grid is not strong enough.

1 INTRODUCTION

1.1 Generalities

As stated by the DoW, this deliverable covers the output of all tasks in WP35 (Define architecture), namely:

- Task 3.5.1 – Vehicle equipment architecture;
- Task 3.5.2 – In-road equipment architecture;
- Task 3.5.3 – Interface with the energy distribution network architecture.

The aim of WP35 was to define architectures for on-road charging solutions and the architecture definition and performance analysis are based on technical and user requirements, stated in D3.2.1, and on the specifications document (D3.4.1).

1.2 Contribution to FABRIC objectives

The aim of WP35 was to define on-road charging solution architectures, for each use case, in terms of Energy distribution network (or grid) interface, road infrastructure interface and vehicle interface.

Where possible, the architecture has been defined to be transferable, scalable and common across the various use cases, and in order to remain within the scope and budget of the project, the architecture utilises as much of the existing on-road charging solution design as possible.

On-road charging solution suppliers have supported the task, in order to ensure that proposed architectures are achievable, complying with the specifications from WP34.

Finally, the architecture definition also took into account inputs from SP4 (Integration, Infrastructure & Testing), to ensure that proposed architectures can be implemented in the specific test sites.

1.3 Deliverable structure

This deliverable is structured according to the three tasks which are defined within WP35:

- Chapter 1: includes a general introduction to the scope of the document and describes its structure;
- Chapter 2: describes the outcomes from Task 3.5.1 – Vehicle equipment architecture;
- Chapter 3: describes the outcomes from Task 3.5.2 – In-road equipment architecture;
- Chapter 4: describes the outcomes from Task 3.5.3 – Interface with the energy distribution network architecture;
- Chapter 5: describes general aspects relevant to shielding
- Chapter 6: includes the results summary and conclusions.

2 VEHICLE EQUIPMENT ARCHITECTURE

2.1 Introduction

This chapter describes the outcomes of Task 3.5.1 in the frame of deliverable D3.5.1, “Architecture Definition” as stated in DoW.

The aim of Task 3.5.1 “Vehicle equipment architecture”, is the vehicle architecture definition, both for the use cases and for the assessment in SP5, taking into account the specifications, as proposed in WP34.

However, only one vehicle architecture, in particular concerning the structural issues, is analysed in the document. This is in accordance with the FABRIC Project DoW, which states that the existing solutions have to be investigated, in order to identify the architectural aspects suitable for the application under study and which changes and improvement are required for further design, on the basis of a single vehicle perspective.

FABRIC solution 1 is based on a proprietary DWPT solution, produced by Qualcomm. The conditions under which they joined the project mean that the IP contained in their solution is confidential, and will not be published or released to other project partners. This constraint is also imposed by IP restrictions regarding the Qualcomm on-board system.

Hence the work presented here is focussed on the CRF vehicle layout, with considerations from solution 1 where appropriate.

In cooperation with the OEMs and charging solution providers, the architecture definition has been discussed to ensure it is realistic and achievable within the scope of the project (in the case of those proposed for SP4), and viable for those being defined to feed into SP5. Independent review of the general parameters of charging requirements/vehicle operation has been undertaken here, as well as the other vehicle equipment identified, which is required for the different use cases implementation.

Concerning the description of the examined available solutions, it has to be pointed out that not all solutions can be analysed and described with the same level of detail, due to the different stage of development and readiness level of the solutions, as well as differing contractual arrangements with suppliers and partners and the resulting in differences in the level of detail in the available data.

In the context of a feasibility study, the work aimed to define system architecture addresses the technical choices, in view of the system implementation and execution of tests, in line with the specification document.

A detailed layout study has been performed to define the correct installation of the system on the vehicle, and performance analysis, both in terms of NVH and Passive Safety for the CRF vehicle, has been carried out to check the developed layout, with CRF Partner support.

Other contributions to this task come from ICCS, regarding the architecture of shielding for EMF emissions and EMC issues, and from MECT, addressing the aspects of battery storage architecture. OEM and charging solution providers have contributed specific inputs regarding the architecture of their vehicles.

Project partner POLITO, as a solution provider, covered aspects such as fastening of the receiver to the vehicle, analysis of vehicle dynamics and definition of the electric power train architecture.

Finally, VEDECOM supported the definition of system architecture providing industry perspective and practical considerations.

It is noted that the vehicle architecture for conductive power transfer systems is not included in this deliverable as the major complexity for inductive power transfer systems lies in the power control and pick-up systems. The pick-up systems for conductive system are highly dependent on the type of system, so a generic architecture would need to be at such a high level as to be of little value.

The architectural specifications for the vehicle equipment are mainly driven by the specification defined in D3.4.1 “Specifications document”. As also stated in D3.4.1, since there is no standardization available regarding the dynamic wireless power transfer the proposed vehicle architectures in this document are different for CRF and VEDECOM vehicles. The proposed CRF vehicle architecture covers two different on-road power transfer solutions, POLITO and SAET, since the receiver part and the on-board components and ECUs are the same.

2.2 Methodology

2.2.1 Vehicle Architecture, POLITO Receiving Structure

The work presented in this section is focussed on the charging solution provided by Partner POLITO and it analyses the on-board system installation for CRF vehicle, evaluating structural performances and Passive Safety aspects.

Politecnico di Torino (POLITO) has designed a dynamic power transfer system (indicated as “Solution 2” in the DoW), which is installed in a short roadway section and has modified a hybrid vehicle enabling 20 kW of wireless power transfer into the battery across a 130 mm air gap, in the frame of EcoFEV Project.

The design work envisaged in WP36 is focussed on modifying this baseline system in order to meet the requirements defined in FABRIC, without a major redesign of the sub-systems, but by means of component re-selection and software improvement.

In the following figures the structure and components of the power receiving system are shown: the system consists of a receiving coil, two ferrite “I” cores, laid on Lexan plates and covered by aluminium shielding, supported by two aluminium shielding beams (see Figure 1 and Figure 2).

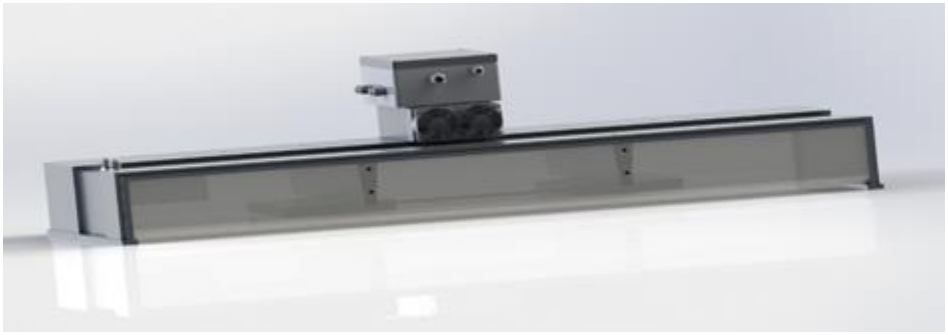

Figure 1: Receiving structure and Power Electronics on Board.

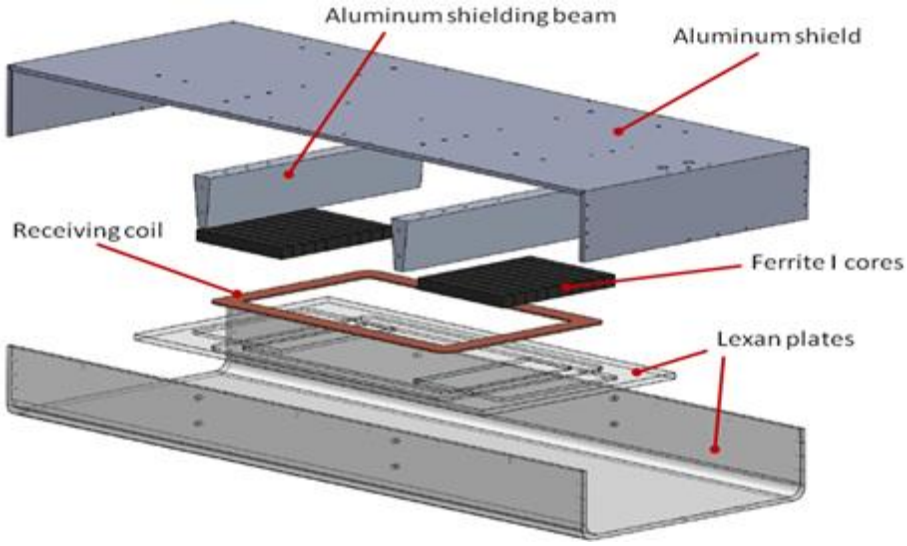

Figure 2: Receiving structure components.

2.2.2 Vehicle (on-board) equipment – system installation

The CRF vehicle designated for installation is the Iveco Daily Electric (see Figure 3). Electrical, mechanical and functional specifications for this vehicle have been defined in Deliverable D3.4.1 - “Specifications document”, as well as the protection requirements and communication interface specifications. [1].

Figure 3: Test vehicle for WP3.5 analysis and development.

The Iveco Daily Electric can have different layouts according to the desired range of autonomy and load capacity. For this reason different modular battery packs (ranging from 2 to 4) can be installed to fit different mission ranges (from 90 to 130 km), on two different Daily configurations, with different weights and, consequently different ranges.

For the choice of the coil placement the following data, shown originally in in D34.1, and in Table 1, have to be considered:

Table 1: Main mechanical parameters for coil placement on CRF vehicle.

Parameter	Value
Secondary coil dimension	140x80x15 cm
Number of coils	1
Placement of the AC/DC converter system	Over the coil box
Power converter overall weight	10 kg
Secondary coil overall weight	70 kg
Cooling system	Forced air (TBC)
Air gap variations in different vehicle load conditions	No load 30 cm Full load 24 cm

These parameters are the ones that impact on the choice of the coil placement and, consequently, on the mechanical performances of the system.

The receiving structure will be installed in the rear part of the vehicle (behind the rear axle, on the rear overhang – see Figure 4): the possibility to avoid the installation of the third optional battery pack (see Figure 5) makes this area the most acceptable for the coil placement, since there are no moving parts, nor other electrical/electronic (E/E) systems that could be in conflict with the new system.

Figure 4: Receiving structure on-board positioning.

As already pointed out in the Specifications Document, while the rear overhang is the most convenient place for charging coils for this particular vehicle, in general, for most vehicles this may not be the most suitable location. For dynamic charging, coils can be placed anywhere on the centreline of the vehicle, but for static and stationary cases, a standardised charging coil location within a charging bay should be defined, suitable for the greatest number of vehicles.

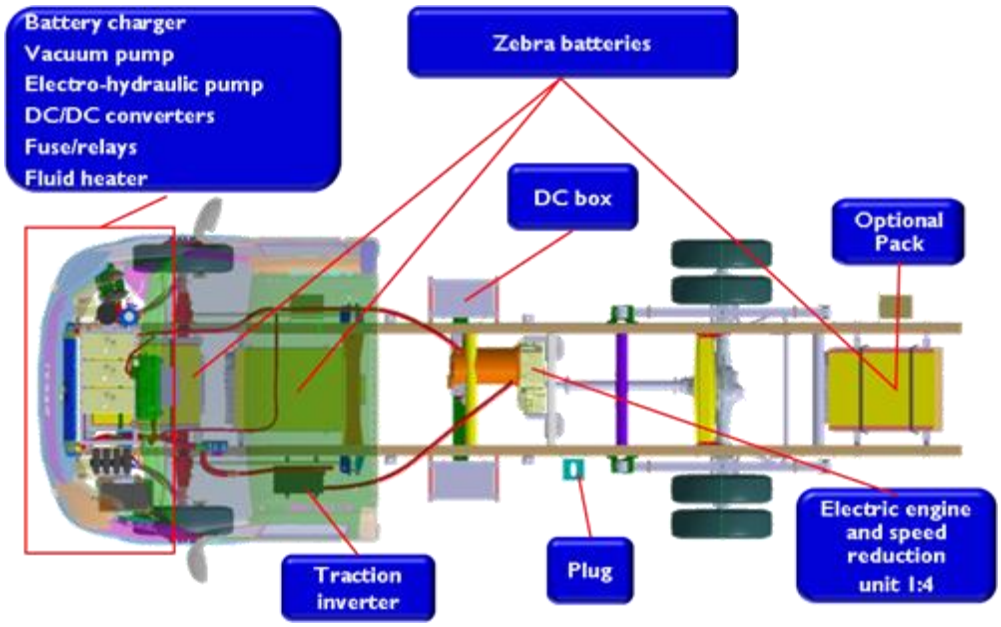

Figure 5: System layout of Iveco electric Daily, as a basis for secondary device installation.

Figure 5 shows the plan diagram of the system layout for the CRF vehicle, highlighting components, such as the Zebra battery packs, that impact on the installation of on-board equipment.

Installation of added parts on the vehicle requires an assessment of dimensions and displacements with respect to the ground, in order to ensure that there is no interference (see Figure 6)

Figure 6

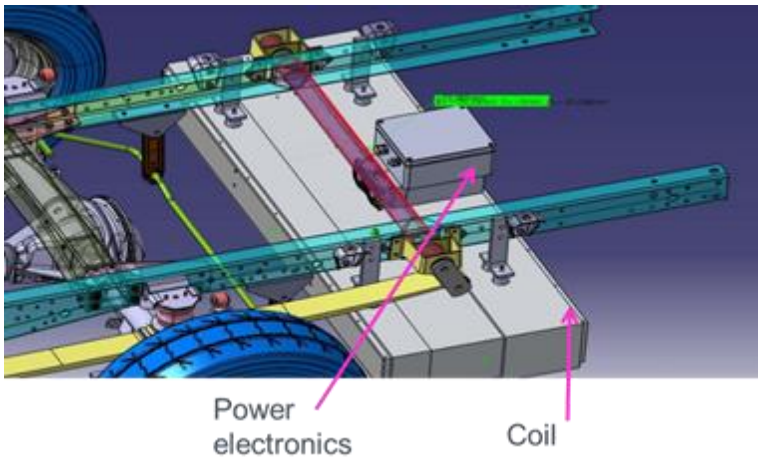

Figure 6: Added parts on existing vehicle and installation.

Figure 7 shows the real vehicle and the E/E functional on-road architecture.

Figure 7: Vehicle E/E functional architecture.

Figure 8 shows the Charging System's functional architecture on vehicle side.

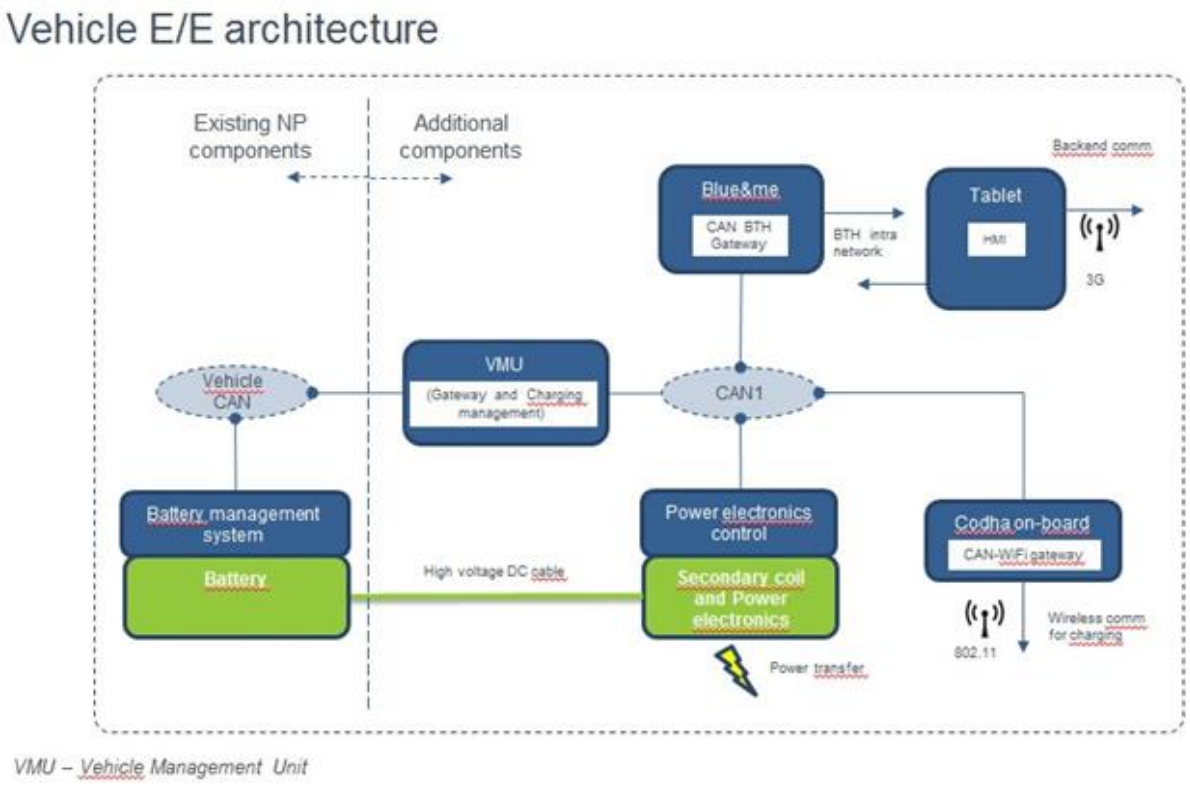

Figure 8: Vehicle E/E functional architecture.

2.2.3 GLOBAL VEHICULAR ARCHITECTURE FOR VEDECOM CAR PROTOTYPES

As stated in the description of work (DoW) page 95, “since the Qualcomm Halo IPT systems are not yet commercial products, a specific contract between VeDeCoM and Qualcomm will be signed to define the specifications and the delivery and installation conditions of the Qualcomm Halo IPT systems on the Satory test track (emitter pads), and on the passenger cars (Renault and PSA) that will be used at the Satory test site. This contract will also cover confidentiality, intellectual property rights and liability issues between the parties, and with respect to other partners of the FABRIC consortium. More specifically Qualcomm will loan to VeDeCoM sufficient Qualcomm Halo base pad systems to power 100m of track and two Qualcomm Halo vehicle pad systems to VeDeCoM for installation into PSA and Renault cars controlled by VeDeCoM”

The contract was concluded between VEDECOM and QUALCOMM Halo IPT in December 2015. It was agreed that two prototypes vehicles provided by RSA would be equipped with Qualcomm system for the tests (Renault Kangoo). The overview of the components supplied by Qualcomm can be summarized as follows :

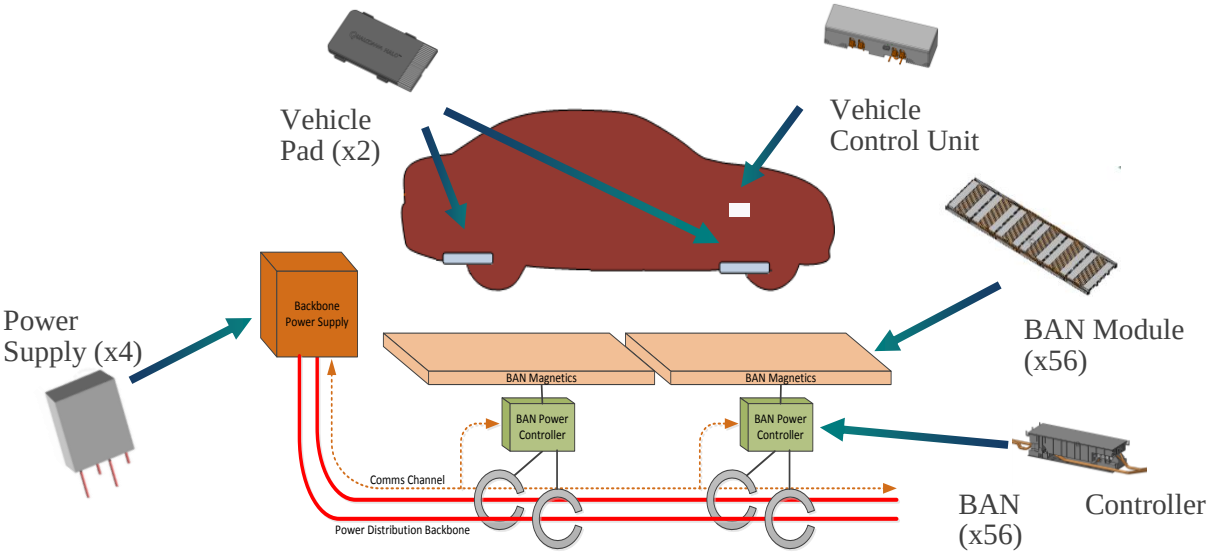

Figure 9: Overview of Qualcomm system provided to VEDECOM

A first vehicular power architecture was agreed with RSA on the basis of information supplied by Qualcomm Halo IPT.

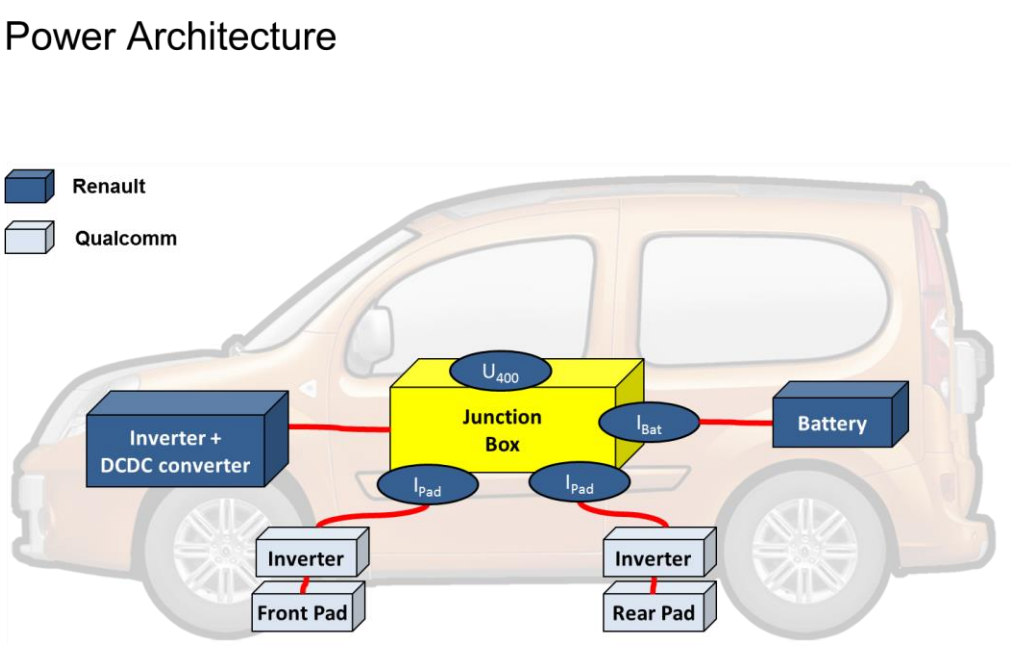

Figure 10: High-level Vehicle power architecture

The above architecture was agreed to be common on the two prototype vehicles. In order to optimize costs, it was decided to have one vehicle fully instrumented and the second vehicle with minimal instrumentation (power measurement only through Ubat and Ibat). The complete high-level architecture with partners perimeter is represented in the following figure:

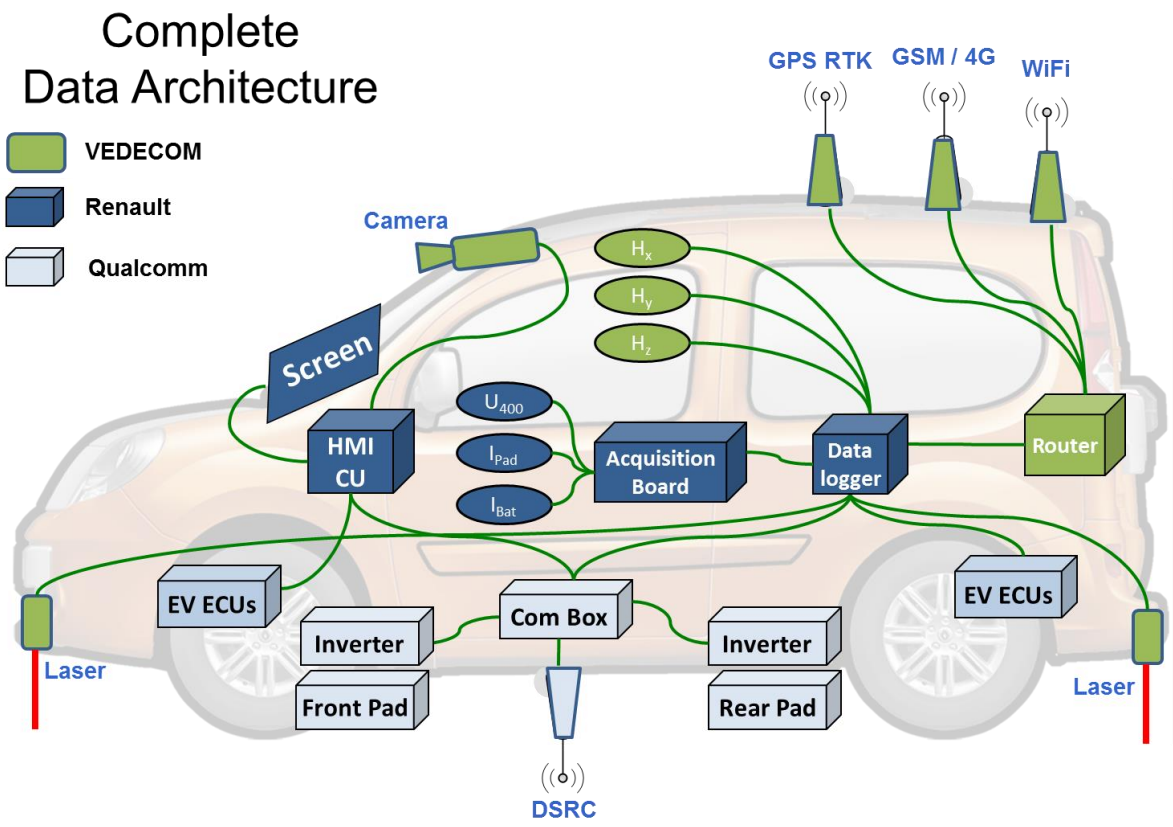

Figure 11: High level complete architecture of VEDECOM instrumented car prototype

2.2.4 Detailed EE and COM in-board architecture for the French vehicle

As of November 2015, the architecture for the VEDECOM experimental cars prepared by RSA (Renault Kangoo) has been defined as shown in Figure 12 and Figure 13.

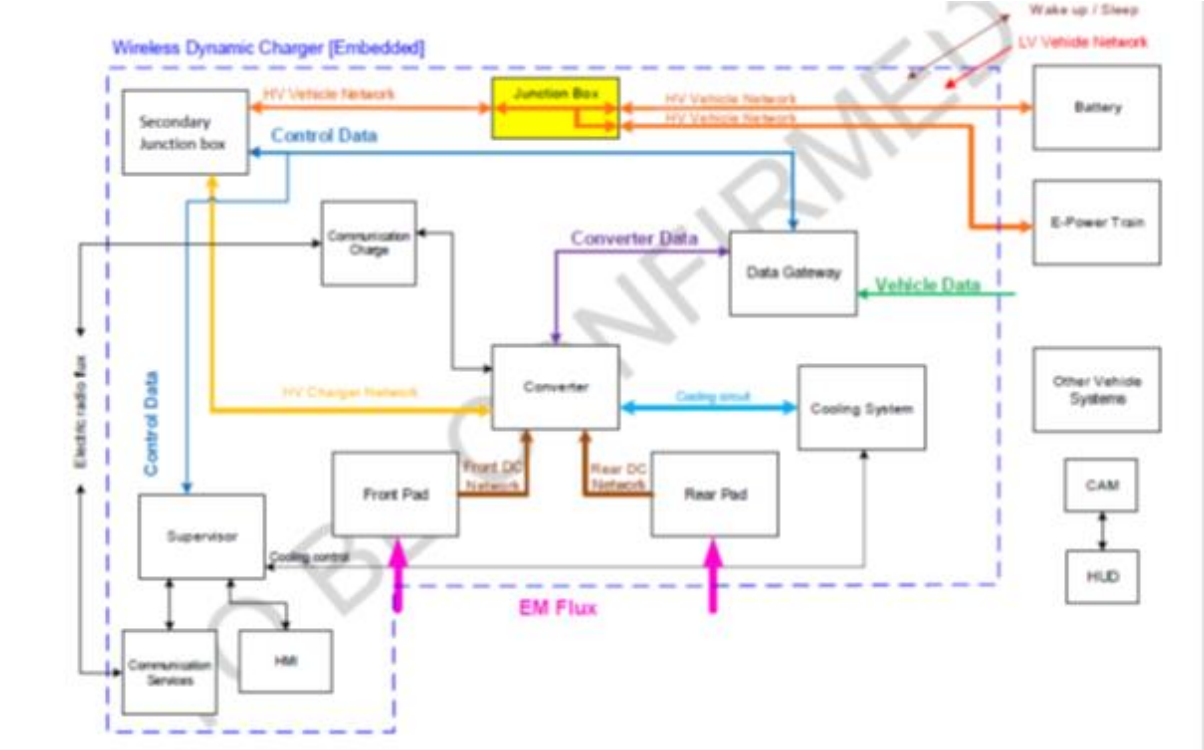

Figure 12: On-board COM architecture for VEDECOM experimental car.

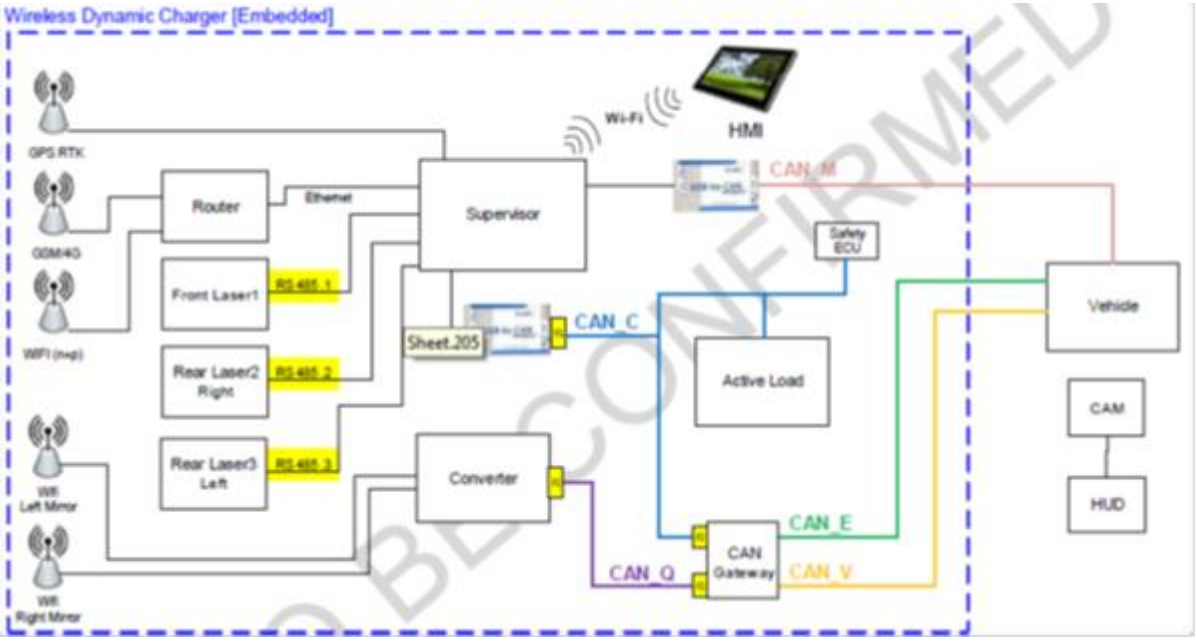

Figure 13: On-board COM architecture for VEDECOM experimental car.

2.3 Structural Performance Analysis of vehicle equipment

The aim of this section is to present the results of an investigation of the receiving structure behaviour in some specific load conditions, where the term “load condition” implies a specific operating condition, during the device’s life cycle.

The static analysis uses a numerical method to investigate how the device under test moves due to an external force. The first hypothesis will be the “static load hypothesis”, according to which all load will be considered acting independently from time and the inertial behaviour will be neglected (e.g. no mass is needed for static analysis).

In particular, the analysis will focus on two kinds of load condition:

1. The first one is the normal use condition during the life cycle: this condition is expected to induce a deformation of the test object which can be neglected. So, the device should easily withstand this condition.
2. The second one is an extreme condition, for example a crash, not expected during the normal operation. The object is expected to crash in a safe way, without danger to passengers.

For the first case two load conditions have been considered: the first is simply the applied gravity field, so that the only load acting on the object is its weight. The second one is a 3g force applied perpendicularly to the road plane. This condition will simulate a bump of the vehicle which causes an overweight on the object.

An extreme load condition considered the hypothesis of a car crash, with both front and side impacts.

Before the static analysis, a modal analysis was performed on the whole model, in order to verify there were no errors or free components in the model and to investigate the normal modes (or eigenvalues) of the structure. A normal mode of an oscillating system is a pattern of motion in which all parts of the system oscillate with the same frequency and with a fixed phase relation. The free motion described by the normal modes takes place at the fixed frequencies, which are indicated as the natural frequencies or resonant frequencies of the system. A physical object has a set of normal modes and related natural frequencies that depend on its structure, materials and boundary conditions.

So, the normal modes occur at certain frequencies, for which the structure is particularly easy to excite. The importance of knowing these frequencies is strictly related to the common practice in engineering of avoiding a dynamic load with an exciting frequency near to a normal mode frequency of the structure. Knowing the normal frequencies of interest, it is possible to dimension loads in order to be far away from them.

2.3.1 FE Method: overview

The Finite element (FE) method is a numerical tool for structural analysis. The basic idea of the FE method is that every structure can be divided into a great number of smaller sub-structures, each of which is called an “element”. A suitable number of elements are connected together, in order to represent the real structure.

Each element is defined by a proper number of nodes (commonly three or four) and by a function describing how the element reacts to a force. An element defined by three nodes is called a “triangular element” and the Optistruct code defines it as CTRIA3. If the element is described by four nodes, the element is “quadrangular” and it is called CQUAD4. These elements are called “first order elements”, because they have nodes only in vertex. If a node is placed in the middle of every element edge, the element is termed a “second order element” and it is identified as CTRIA6 and CQUAD8.

When a load is applied on the structure, it is decomposed in many smaller loads and then divided among the elements. The main feature of the FE method is that the load is applied on nodes and not on elements. Pressure loads, usually defined as force on a surface, are applied in nodes too.

For each node, a matrix which contains the applied loads is defined (zero value if no load is applied on a particular node) as is a second matrix called “stiffness matrix”. The stiffness matrix represents an element’s property and is a known function based on element type. Once the load matrix and the stiffness matrix are known, the displacement is calculated for each node with a mathematical algorithm. The displacements are calculated according to constraints applied to the model.

Constraint means, generally speaking, a motion law for a specific node.

From nodal displacement, using the element function, displacements and other derived quantities are calculated, for all elements.

To ensure an acceptable level of accuracy in the calculation, the division of the structure in the elements, which is called the mesh, must have a regular geometry, but in practice it is impossible that this condition is satisfied for all structures, so the element geometry is slightly deformed. The FE equations are still valid if the deformation is small.

To check the element geometry some parameters are available, such as “Warpage” and “Jacobian” which are a measure of how the element is deformed.

A good mesh should respect Warpage and Jacobian criteria to provide the accuracy required.

2.3.2 FE Model set up meshing guidelines: overview

Figure 14 shows the FE model for Charging System’s receiving structure.

In order to perform the analysis on the model, a first meshing phase has been performed to discretise the whole receiving structure. Components in the model were divided into two groups: the first one consisting of shell components; the second one of solid components.

For shell components, the middle surface has been extracted and meshed using shell CTRIA3 (less than 15%) and CQUAD4 elements. The average size of the elements is about 10 millimetres.

For solid components, Tetra and Brick elements were used (according with a penta percentage of less than 15%) with a mean size governed by the component. The mesh quality was checked evaluating the Jacobian (> 0.7 for shell and > 0.5 for solid) and Warpage (< 10 deg for shell and < 15 deg for solid) criteria in the first instance. A second

check was performed on elements' angles (45-135 deg for CQUAD4 and 30-150 deg for CTRIA3. For solid elements a check on tetra collapse was performed (> 0.2). During mesh phase the component under investigation was translated according to its spatial position with respect to the underbody on which it is attached.

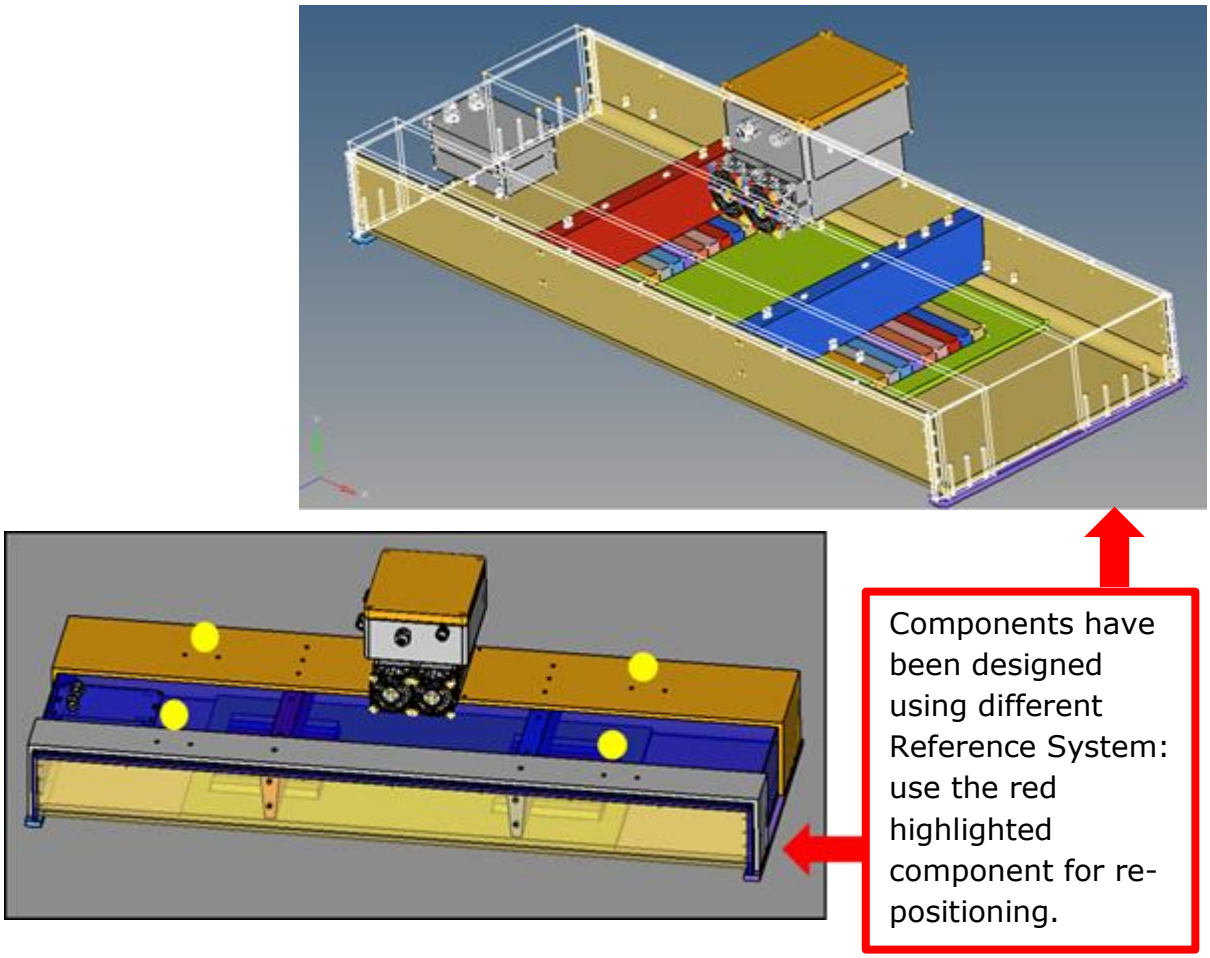

Figure 14: Charging system – Receiving structure FE model.

The connection between the charging box and underbody was guaranteed by four brackets (see Figure 15).

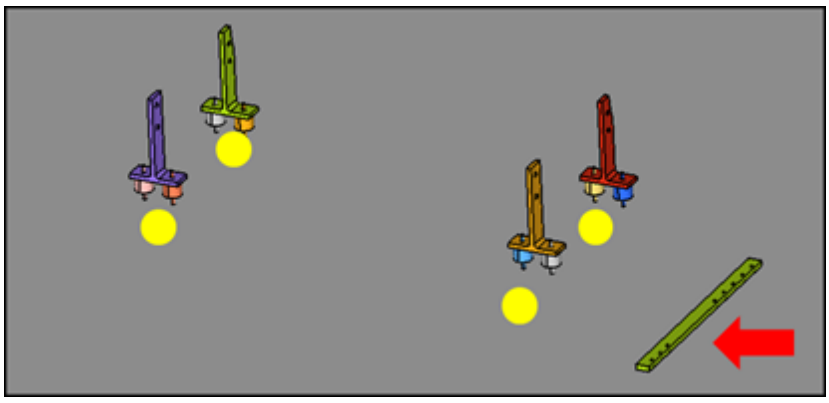

Figure 15: Bracket to connect Pack to Under Body.

2.3.3 FE Model set up meshing guidelines: shell mesh remarks

The mesh operation on components has been done according to the components' own properties.

Some approximations have been introduced, based on the available data:

1. The first one deals with the green component in Figure 16: since the same components are shown with different thickness areas, all these areas are divided in specific components with the same thickness;

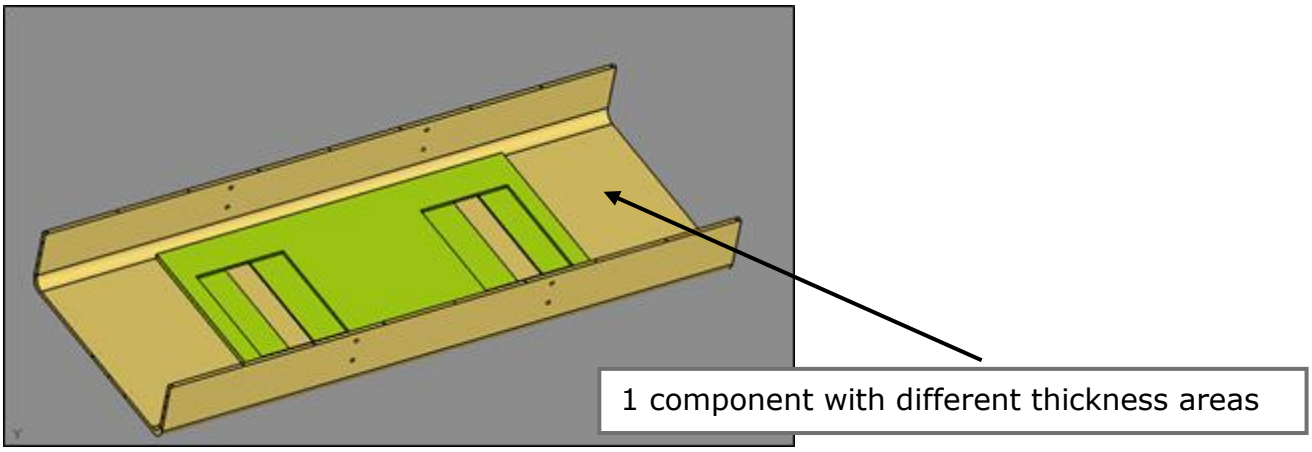

Figure 16: Component with different thickness areas.

2. The second one concerns the damping system with connection brackets linked to a charging box. Since no data are available for damping schematisation (material, mass, damping coefficient, elastic modulus) they are considered rigid and not modelled (see Figure 17).

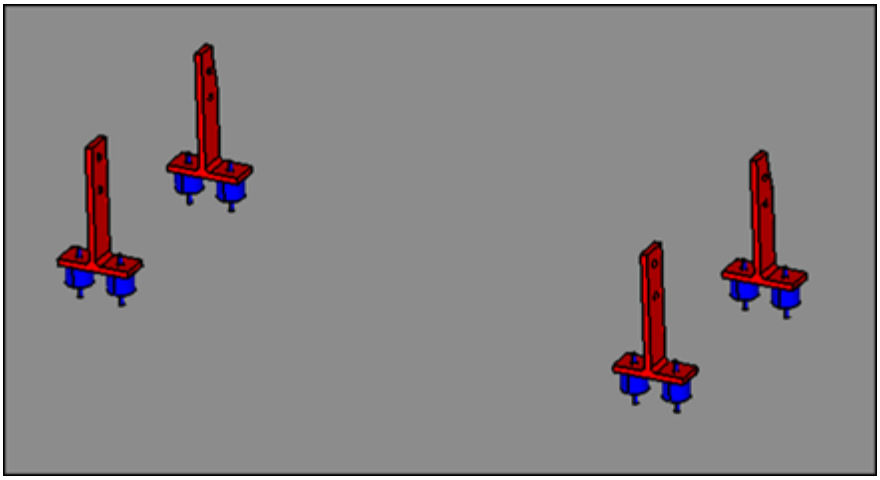

Figure 17: Dampers not included in Mesh – 1D Rigid Elements modelled.

2.3.4 FE Model set up meshing guidelines: solid mesh remarks

The components meshed as solid are shown in Figure 18 (blue and red star components plus bars). All the bars have been divided into two components (one for each side of the box).

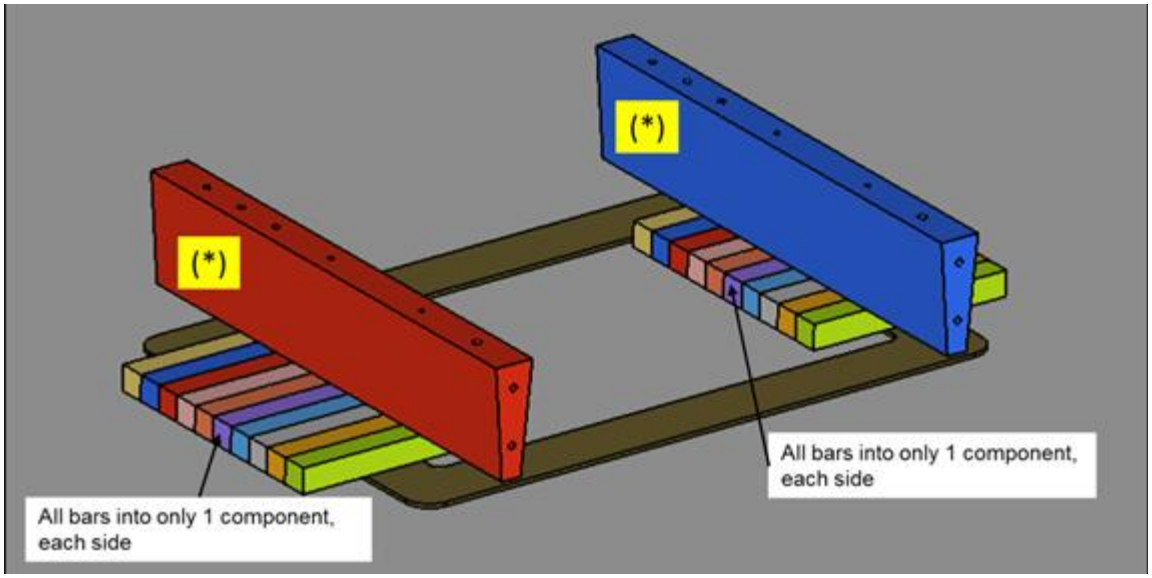

Figure 18: Ferrite bars.

General mesh remarks

Some non-relevant components have been schematised for inertial contribution to the system behaviour. These components are shown in Figure 19:

For these components only mass and inertial behaviour is considered. To guarantee a correct interface between components, a node to node mesh is preferred over faced components. This makes the connection phase easier and faster (Figure 20).

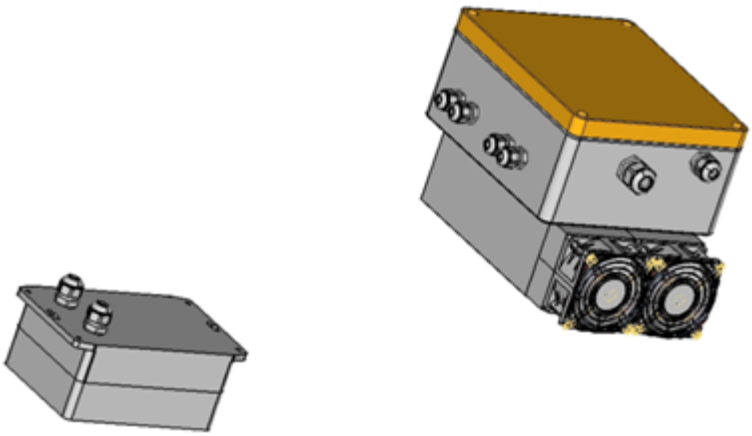

Figure 19: Simplified geometry: parts relevant only for inertial contribution.

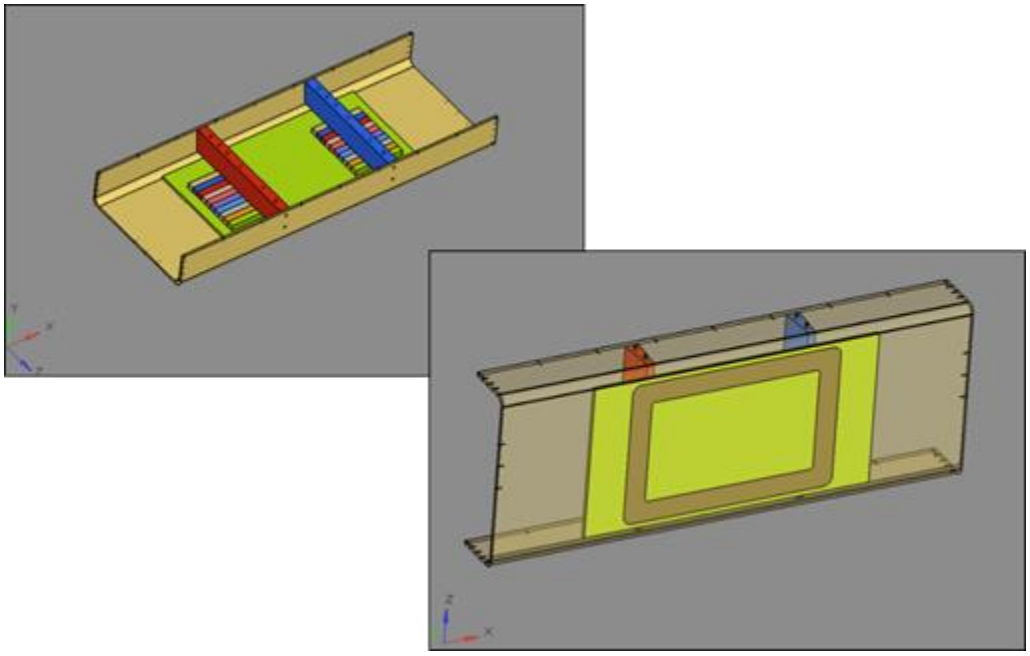

Figure 20: Top and bottom components.

2.3.5 FE Model set up modelling guidelines: overview

A single FE model is provided for both NVH (Noise Vibration and Hardness) and DSM (Durability Strength and Misuse) analysis. On the same model static and dynamic load cases are executed, using Optistruct as a reference code.

As previously mentioned, some components (see Figure 21) have been meshed keeping in account mass and inertial properties only. The components are considered as non-deformable (rigid). The components are modelled by means of a concentrated mass (CONM2 element) in the COG position (note that the COG position is not known and is assumed to be equivalent to geometrical COG); the mass applied is calculated from CAD and BOM for real components and is linked to a charging box with RBE3 elements.

A second modelling aspect looks at a magnetic system (Figure 22): the material is assumed to be ferrite and, in model analysis, it is considered in terms of its contribution to mass and stiffness of the system; the coils have been considered as non-structural components. The mesh is solid for encumbrance only and a dummy material is applied. The real mass requirement is fulfilled with a non-structural mass, added to the component.

The last assumption during the schematisation phase is related to the plastic material of the charging box: a PPO (modelled as DuPont material) was chosen, missing real material properties.

PPO material proved to be suitable for the purpose, since it has excellent electrical properties, is flame resistant, has good toughness, is dimensionally rigid and resistant to detergent. It is already used for electrical parts, TV back covers, car dashboards, washing m/c parts.

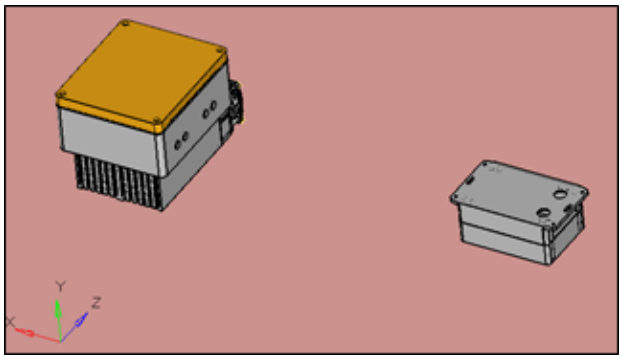

Figure 21: Electric System.

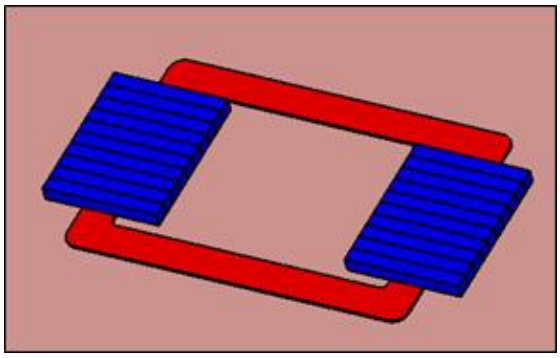

Figure 22: Magnetic System.

In the table of Figure 23 is shown the Bill of Materials used for the FEM model.

Structural Non-deformable (Rigid) Components: Mass to fulfill

Total Mass to fulfill

#	Weight, each comp	CAD Part Name	Material	Quantity	Weight, all similar comps	Weight whole system
Num. articolo	Massa per unità	–	Descrizione	QUANTITà	Massa totale per componenti	Massa totale
1	4.96 kg	C_alluminio	Alluminio	1	4.96 kg	
2	4.37 kg	Trave_trapezia_destra	Alluminio	1	4.37 kg	
3	4.37 kg	Trave_trapezia	Alluminio	1	4.37 kg	
4	10.86 kg	Lexan	Lexan	1	10.86 kg	
5	0.67 kg	Ferrite_core	Ferrite	20	13.4 kg	
6	3.95 kg	Receiving_coil	Rame	1	3.95 kg	
7	0.71 kg	CELEM_capacitor	Rame	2	1.42 kg	
8	3.21 kg	Lexan_supporto	Lexan	1	3.21 kg	
9	0.17 kg	scatola_1	Plastica	1	0.17 kg	
10	0.16 kg	scatola_2	Plastica	1	0.16 kg	
11	9.29 kg	C_supporto_seconda	Alluminio	1	9.29 kg	
12	4.64 kg	C_supporto	Alluminio	1	4.64 kg	
13	0.5 kg	Supporto inferiore	Alluminio	1	0.5 kg	
14	0.5 kg	Supporto inferiore destra	Alluminio	1	0.5 kg	
15	0	PG11 (Ø10)-Long_Body	Plastica	2	0	
16	0	PG11-Cap	Plastica	2	0	
17	0.33 kg	Staffa_a_T	Alluminio	2	0.66 kg	70.64 kg
18	0.2 kg	Silent block	Gomma+Alluminio	8	1.6 kg	
19	0.32 kg	Staffa_a_T_posteriore	Alluminio	2	0.64 kg	
20	1.73 kg	Staffa	Alluminio	1	1.73 kg	
21	0.03 kg	Staffa_frontale_tot	Alluminio	1	0.03 kg	
22	0.03 kg	Staffa_frontale	Alluminio	1	0.03 kg	
23	0.03 kg	Staffa_frontale_particolare	Alluminio	1	0.03 kg	
24	0.03 kg	Staffa_frontale_particolare_seconda	Alluminio	1	0.03 kg	
25	3.85 kg	LA10	Alluminio	1	3.85 kg	
26	0.06 kg	supporto_LA10	Alluminio	2	0.12 kg	
27	0.07 kg	Fan-House_8212JH4_ebm-papst	Plastica	2	0.14 kg	
28		Fan_8212JH4_ebm-papst	Plastica	2		
29	0	PG16 (Ø14)-Std_Body	Plastica	1	0	
30	0	PG16-Cap	Plastica	1	0	
31	0	PG9 (Ø8)-Std_Body	Plastica	4	0	
32	0	PG9-Cap	Plastica	4	0	
33	0.52 kg	Z231BOX1	Alluminio	1	0.52 kg	
34	0.29 kg	Z231Lid1	Alluminio	1	0.29 kg	

Rame = Cu

Figure 23: BoM of materials.

2.3.6 FE Model set up modelling guidelines: connections

The connection between different components was provided in two different ways:

- The first one is a glue connection between faced components (see Figure 25);
- For some others components the connection is simulated with bolts between elements (Figure 24).

Both glue and bolts are modelled as a node to node connection between parts because connections are not under investigation in this model. As remarked previously, it should be noted that the Electric/Fan Box to Main Box connection is currently with four 1D Rigid Elements.

Looking at Figure 26, the yellow component is not attached to the pink component (that represents the plastic box).

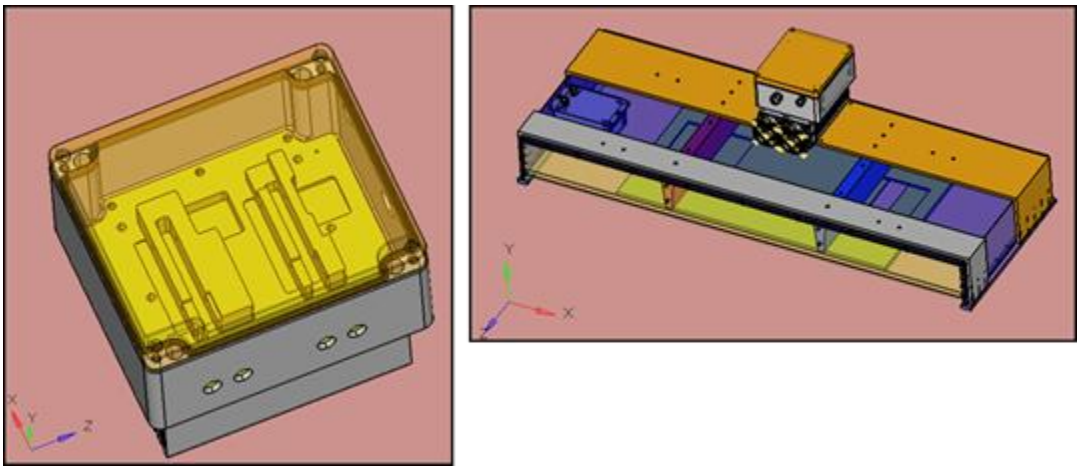

Figure 24: Holes, location for Bolted Parts.

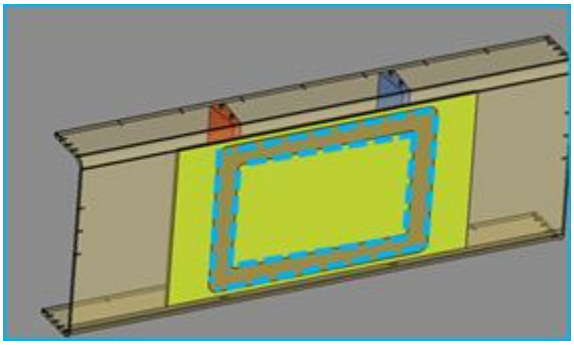

Figure 25: Dotted Light-Blue Lines, Glue location – along edges: FEM as Merged Nodes.

Figure 26: Glue location – side view.

2.3.7 Load case set up: overview

The analysis performed on the model has been divided into two groups:

- the first for NVH requirements verification;
- the second for static requirements verification.

In the following section, the chart flow followed during the analysis phase is described and in the overview section the load cases analysed are listed. It is important to notice that the load case for the FRF calculation is skipped for two reasons: missing information about damping (see previous chapters) and missing information about vibration target for mounted components.

Background

CAE structural assessment has been performed both in terms of the stiffness/strength and vibration on the receiving system installed on the vehicle; the goal is to verify whether the system is stiff enough and insulated sufficiently against vibrations. Target values are not quantified.

Overview

The receiving system has been assessed, mounted on a CRF Commercial Vehicle: the principal idea is to assess performances via simplified tests, such as linear dynamic and static load cases, reproducing critical event conditions.

The specific items are listed below:

- Description of the FE Model (masses and connections) and set-up, as previously defined;
- Packaging verification;
- Normal Modes assessment with receiving system installed;
- Gravity;
- 3g Gravity (Vertical Bump);
- 25g x-acceleration (Front Impact);
- 25g y-acceleration (Side Impact);
- 25g x-acceleration combined with 1g in (-z) direction;
- 25g y-acceleration combined with 1g in (-z) direction.

Keys to tune for performances

For performance improvement, it is possible to tune some parameters of the receiving system:

- The mounting position of the receiving structure can be moved in x direction, on the centreline of the vehicle, according to the packaging;
- Thickness of metal/polymeric sheet parts (the box containing magnetic coils) and Transversal Bars (blocking ferrite blocks) can be varied: lexan thickness ≤ 10 mm;
- Thickness, length and shape of brackets between the receiving structure and the vehicle can be resized.

2.3.8 Load case set up: packaging verification

Before running analysis on the model, a final check was performed to verify all the assumptions and schematisations done during the model phase. In the following section, the main steps during pre-run check phase are listed.

The subject of this check was the Receiving System installed on the rear area of the CRF Vehicle, the Iveco Daily Electric.

The light blue vehicle equipment in Figure 27 had to be removed and reference points for mounting are highlighted in yellow on Figure 28; currently the vehicle equipment is mounted by means of bolts.

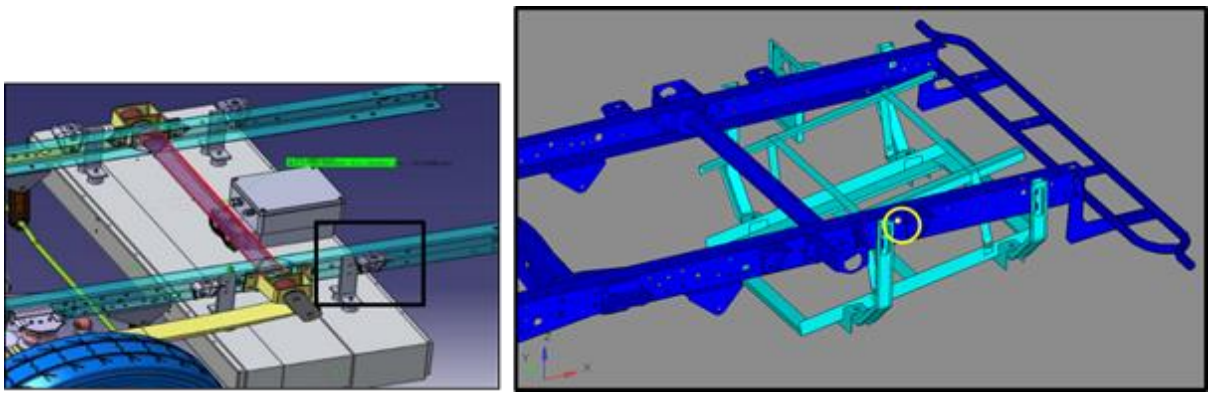

Figure 27: On-board system installation.

2.3.9 Load case set up: NVH/DSM assessment

A more detailed list of load cases and analysis tasks is provided in this section, according to load case division of previous chapters (NVH or DSM).

The FRF calculation was not carried out on the model, so the dynamic analysis is restricted to the normal modes calculation.

Normal modes for the receiving structure installed on the vehicle have been calculated for frequency values from 0 to 100 Hz with the FE Model of the receiving structure as per nominal design, identifying main local modes of the installed device.

Gravity effects for the receiving structure installed on the vehicle have been calculated:

- **Gravity**: analysis with 1g in a vertical direction has been carried out in order to assess the status of a stationary vehicle;
- **Vertical Bump**: analysis with 3g in a vertical direction has been carried out in order to assess when the vehicle meets a bump on the road;
- **Front Impact**: analysis with frontal 25g along the y direction (plus 1g vertical) has been carried out in order to assess the effects of a front impact;
- **Side Impact**: Analysis with lateral 25g along the y direction (plus 1g vertical) in order to assess the effects of a side impact.

Impact analysis included identifying possible risks related to physical deformations and failures under load conditions, finding out the stress distribution within the structure of the

receiving system, for each of the load cases. Furthermore, the highest stress levels reached in every load case are specified, identifying the maximum values and the most strained components.

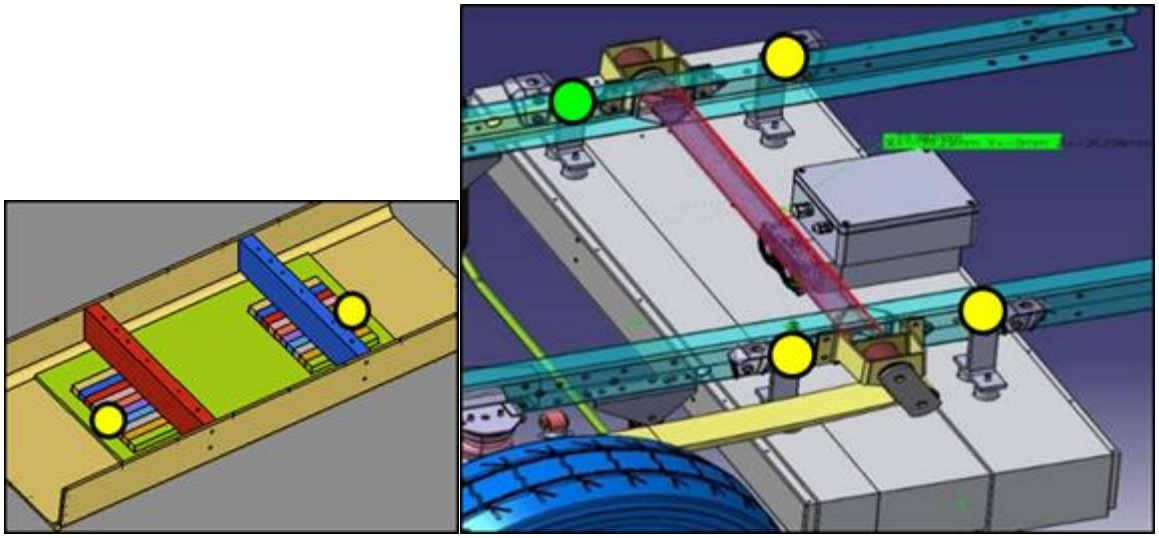

Figure 28: Reference points for mounting (highlighted in yellow).

In Figure 29, the final model of the charging box is shown and some final considerations can be drawn, taking into account analysis during the modelling phase and results evaluation:

1. The first one is about the weight of the whole object, since the FE model weight is 70.6 kg instead of 70.64 kg derived from BOM.

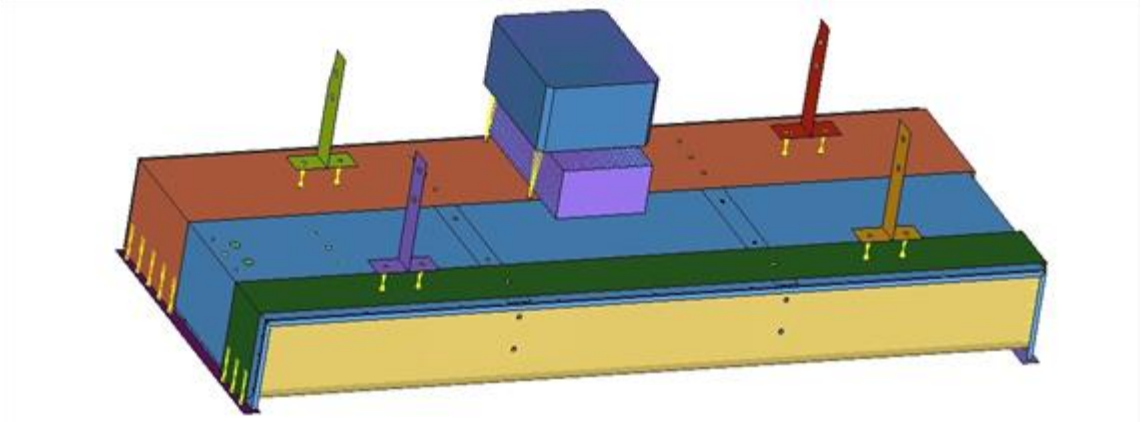

Figure 29: Final charging box model.

2. The second consideration is about the material distribution: in Table 2 below the structural materials used in the model with their parameters (Young modulus, Poisson modulus and density) are listed.

Table 2: Material Characteristics.

	E (Mpa)	Nu	Rho (t/mm3)
Aluminium	7.1e4	0.35	2.7e-9
Lexan	2200	0.37	1.05e-9
Ferrite	1.8e5	0.28	5e-9
Rame (Cu)	1.1e5	0.34	8.9e-9

In Figure 30, the material distribution in the model is shown, component by component. It has to be pointed out that Lexan's properties are obtained from a public datasheet and that the use of Lexan is an assumption, also due to the lack of information available about the actual material and its properties.

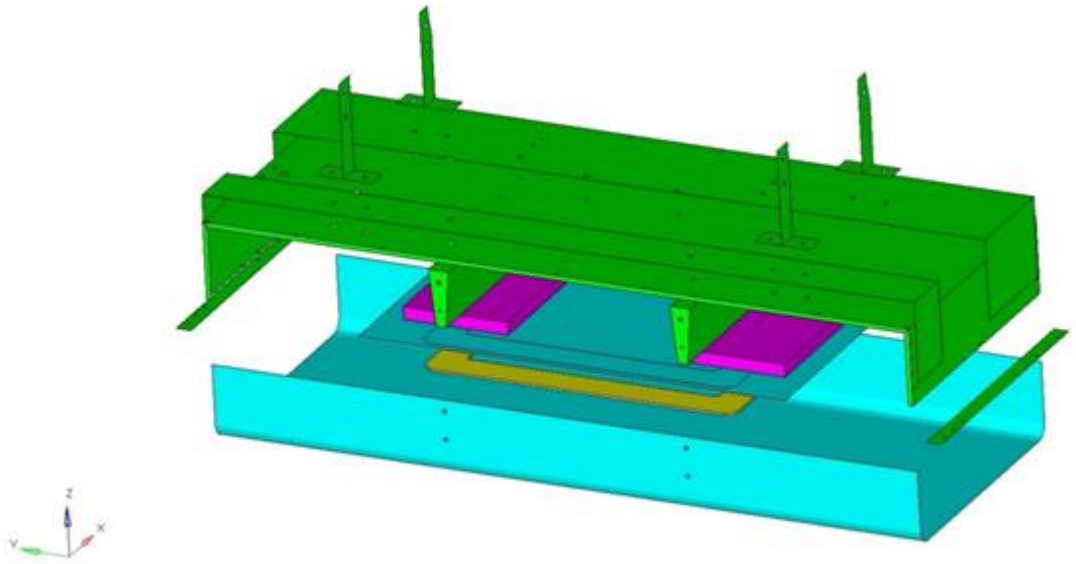

Figure 30: Material distribution in the model.

3. The third and final consideration is about the electric and fan boxes (shown in Figure 31 in red circles). They have been substituted with the RBE3 elements with a concentrated mass in their master nodes (see previous chapters). They assume the following values:

 = 6.85 kg

 = 1.75 kg

There were several holes missing on the main rail of the underbody, where the attachment brackets of the receiving structure are connected (see Figure 32 – yellow squares).

Those holes have been modelled in order to attach the receiving structure and a washer has been added to the holes with a relevant behaviour.

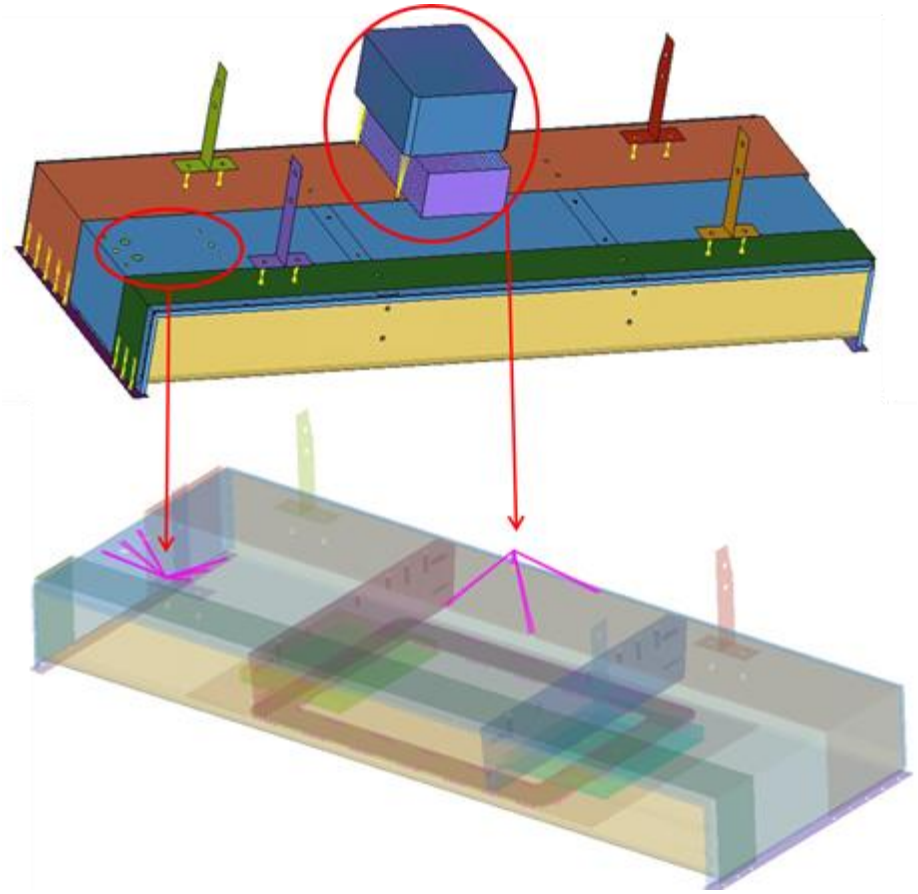

Figure 31: Electric fan boxes.

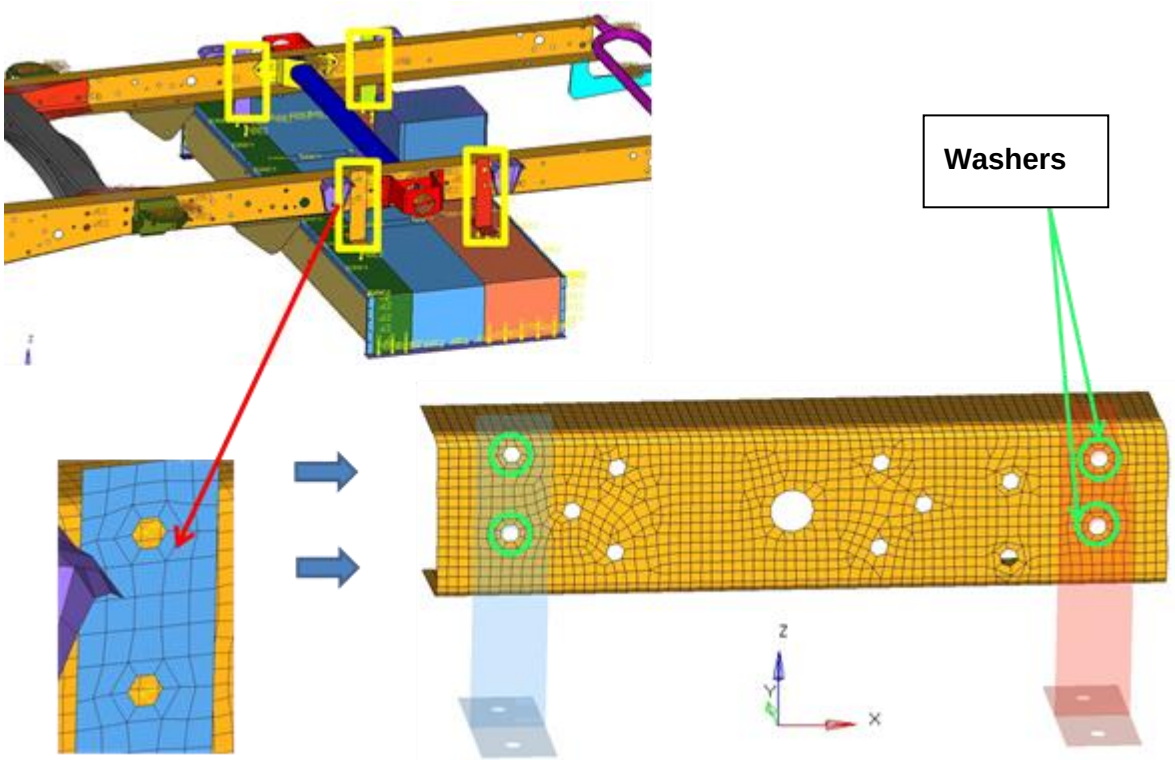

Figure 32: Attaching holes and washer creation.

For boundary conditions, no information was available, so a practical assumption was made: the model is considered simply, supported on four points, in which the suspension system is attached to the underbody. Only DOFs from 1 to 3 have been constrained, in order to simulate the capability of the underbody to rotate, with respect to the suspension system (see Figure 33).

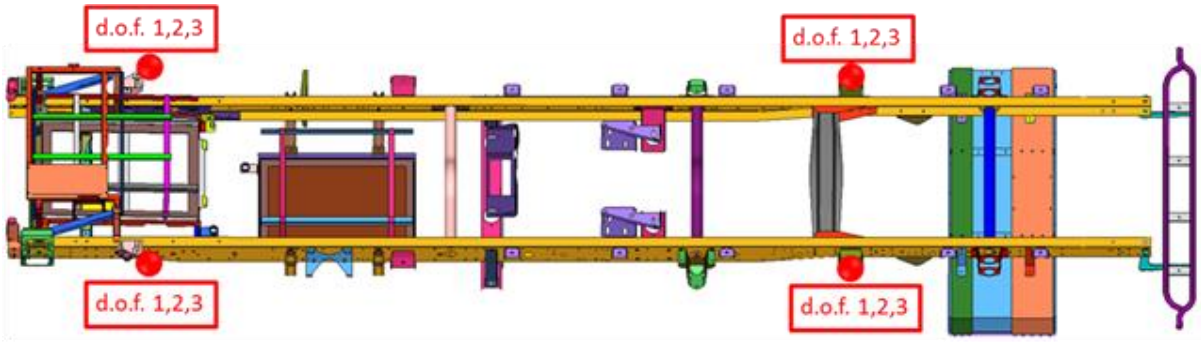

Figure 33: Boundary Conditions.

2.3.10 Modal analysis results

The first analysis carried out on the model is a modal analysis: a Lanczos method [2] was used to find the system's eigenvalues (see also page 23). The Lanczos algorithm is an iterative algorithm, that is an adaptation of power methods, to find the most useful eigenvalues and eigenvectors of an nth order linear system with a limited number of operations, m, where m is much smaller than n.

In the following (from Figure 34 to Figure 39) the first modes involving the charging box are shown. The modes that also involve the underbody are skipped in the post processing phase.

The modes of the receiving structure are mainly related to the external case, excluding internal components; a non-symmetric behaviour is shown in higher order modes (see Figure 37, Figure 38 and Figure 39) due to the suspended mass on the left side of the box.

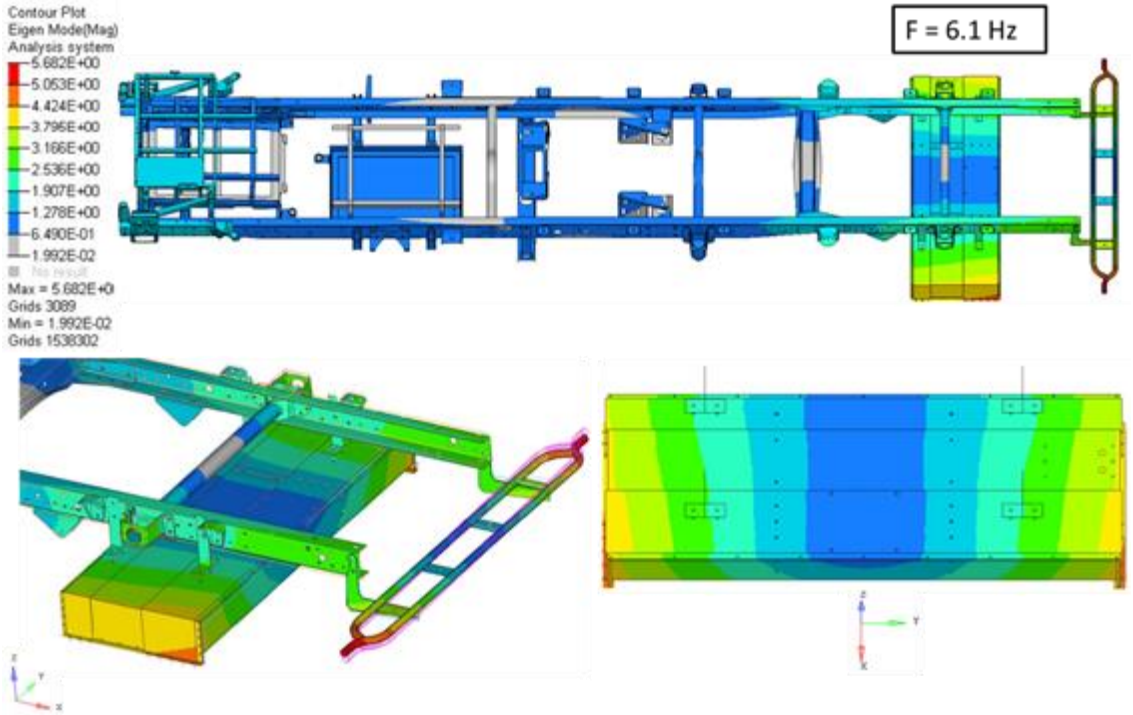

Figure 34: Modal Analysis at F = 6.1 Hz.

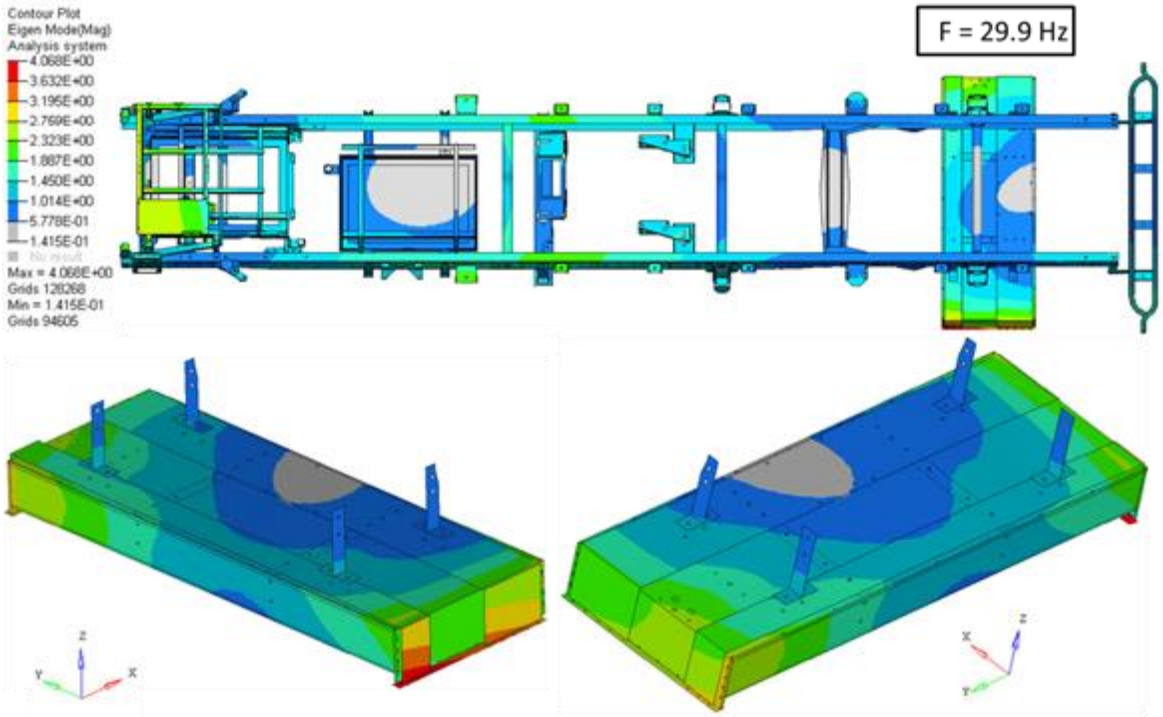

Figure 35: Modal Analysis at F = 29.9 Hz.

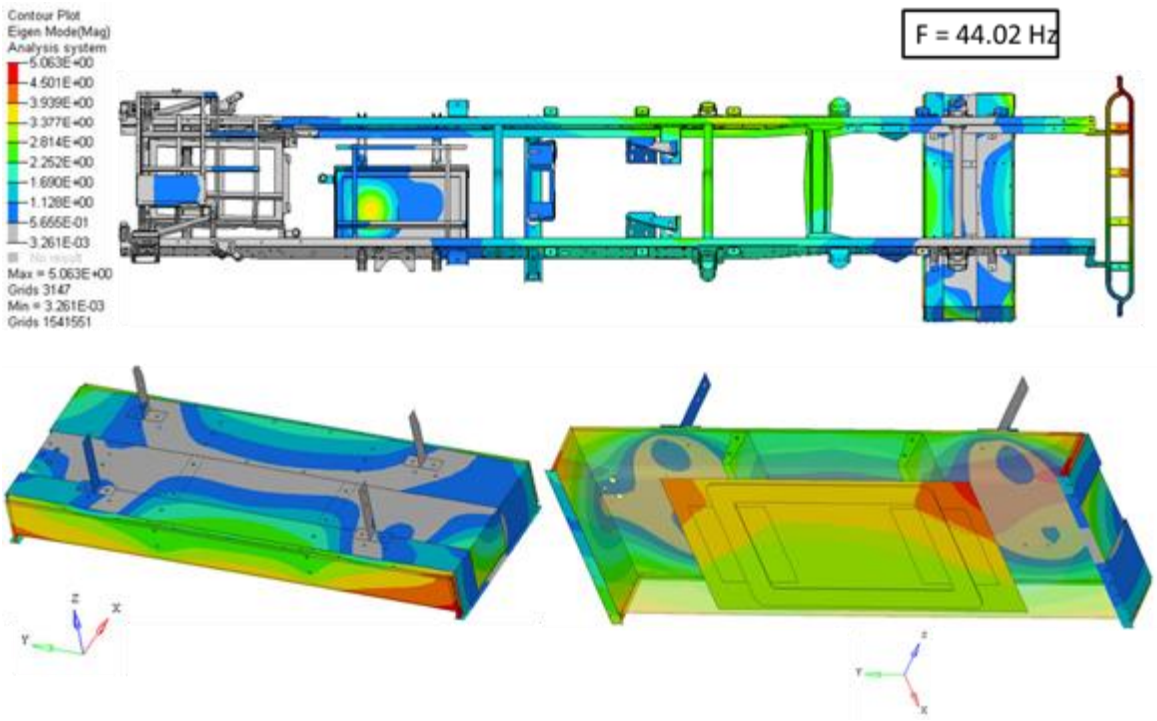

Figure 36: Modal Analysis at F = 44.02 Hz.

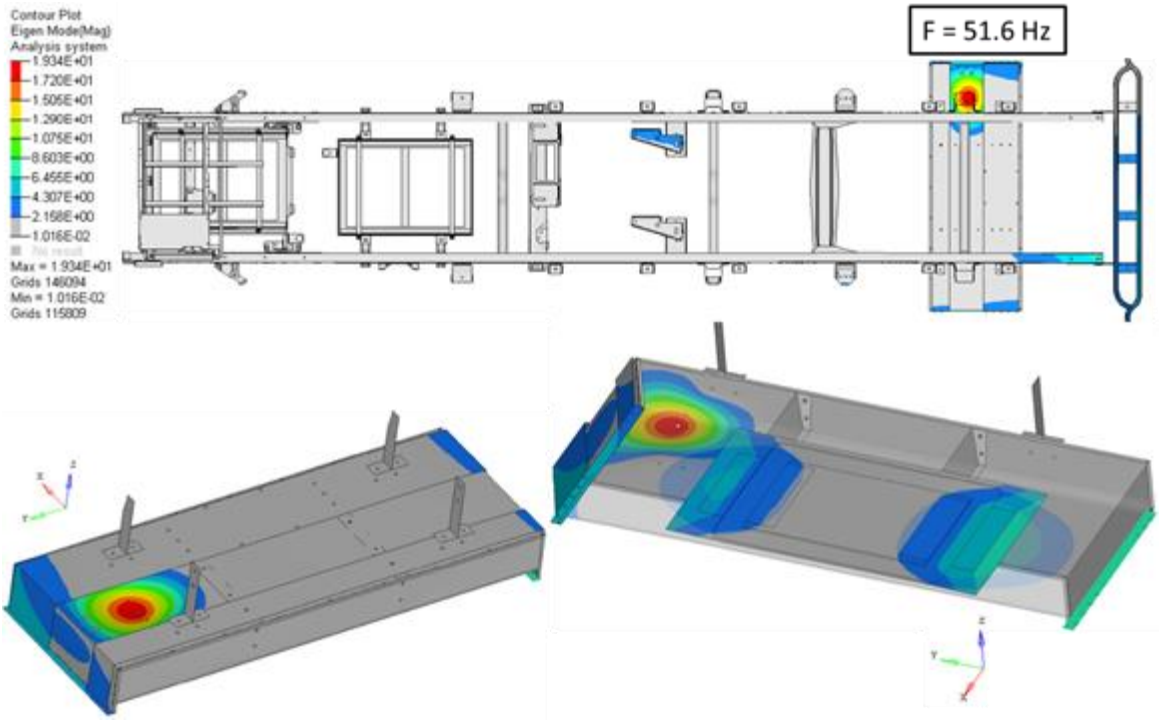

Figure 37: Modal Analysis at F = 51.6 Hz.

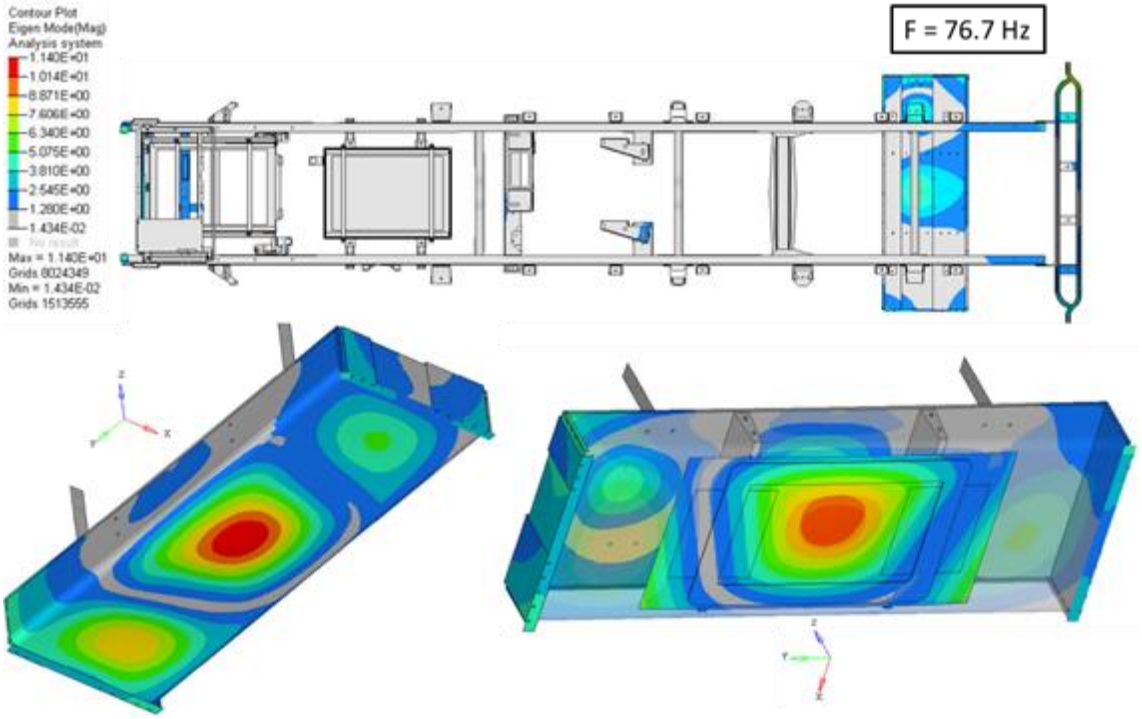

Figure 38: Modal Analysis at F = 76.7 Hz.

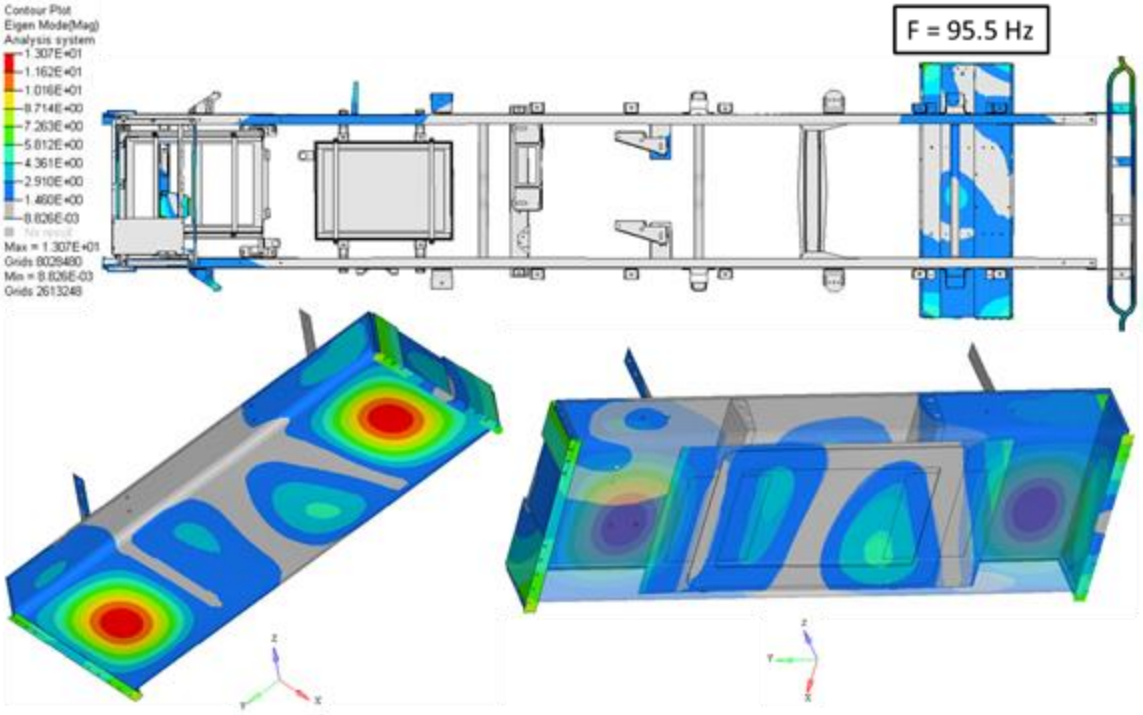

Figure 39: Modal Analysis at F = 95.5 Hz.

2.3.11 STATIC analysis results

The static analysis was performed on the load cases discussed in previous chapters (2.3.7–2.3.9) and involved normal usage conditions (1g gravity load) and accidents (front or side impact). The results are described below.

In the 1g load case, no plastic deformations are expected and the component presents a linear behaviour. Figure 40 and Figure 41 show the results of static analysis, in terms of stresses and displacement respectively, in the case of 1g gravity load applied in –Z direction.

The same behaviour (of the 1g load) is detected in a 3g field, used to simulate a bump condition and we can consider the receiving structure's behaviour still in a linear field.

The front impact load case is simulated applying a 25g gravity field along +x direction. The simulation is done using a linear code, so no plasticity or non-linearity in material behaviour is taken into account. The final result is a slight overestimation of sigma in component.

Figure 42 and Figure 43 show the results of static analysis, in terms of stresses and displacement respectively, in the case of 25g gravity load applied in X direction.

From the load case, there is clearly a failure of the brackets attaching the charging box to the underbody: the expected behaviour is a failure of all the brackets and a detachment of the receiving structure from the underbody.

Gravity (1 g in -Z direction)

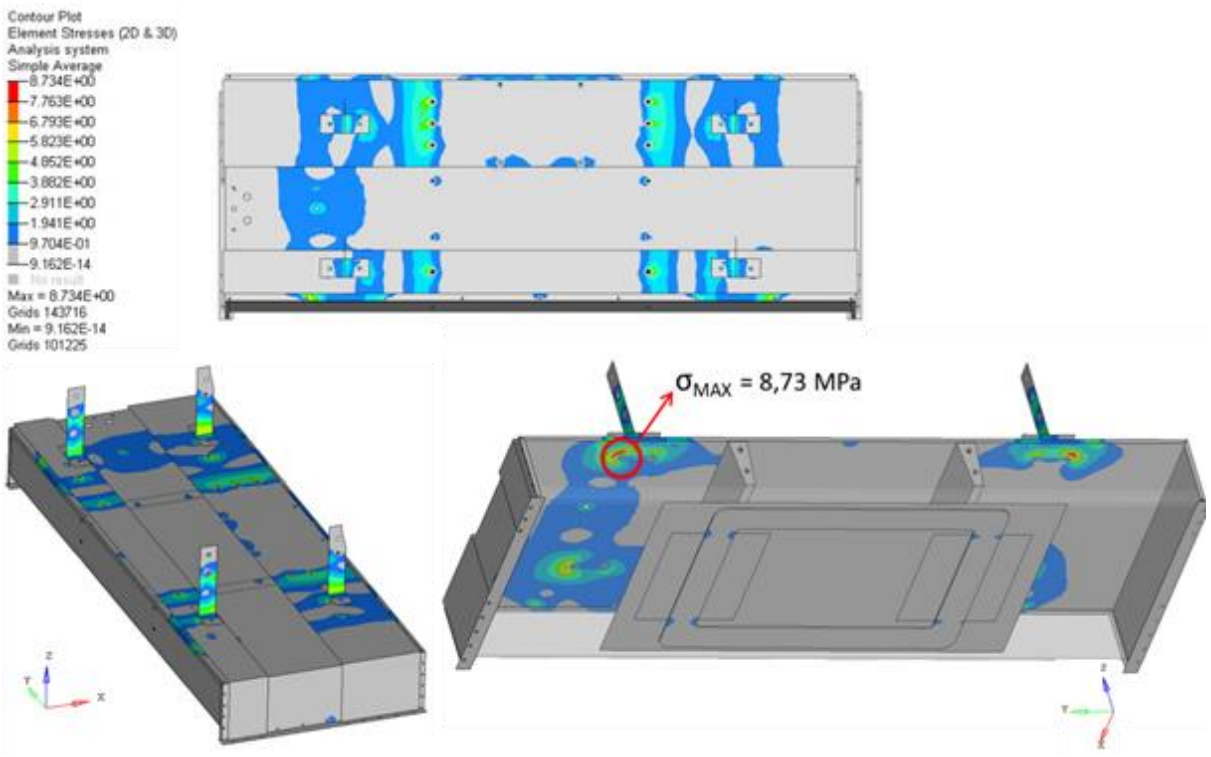

Figure 40: Static Analysis – Stresses (1g in –Z direction).

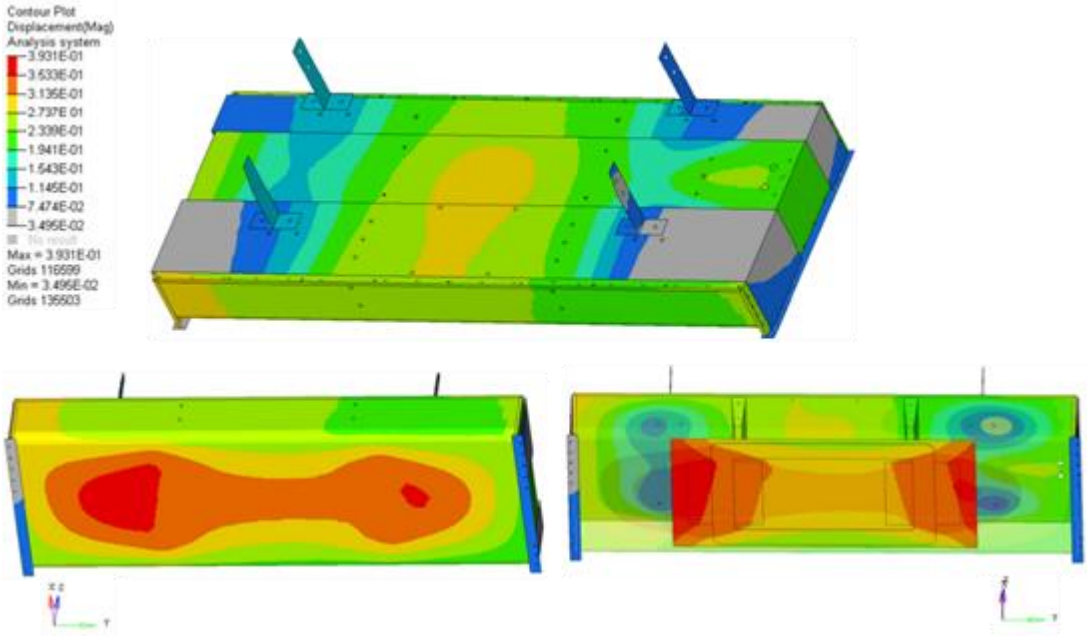

Figure 41: Static Analysis – Displacements (1g in –Z direction).

Front Impact (25 g in X direction)

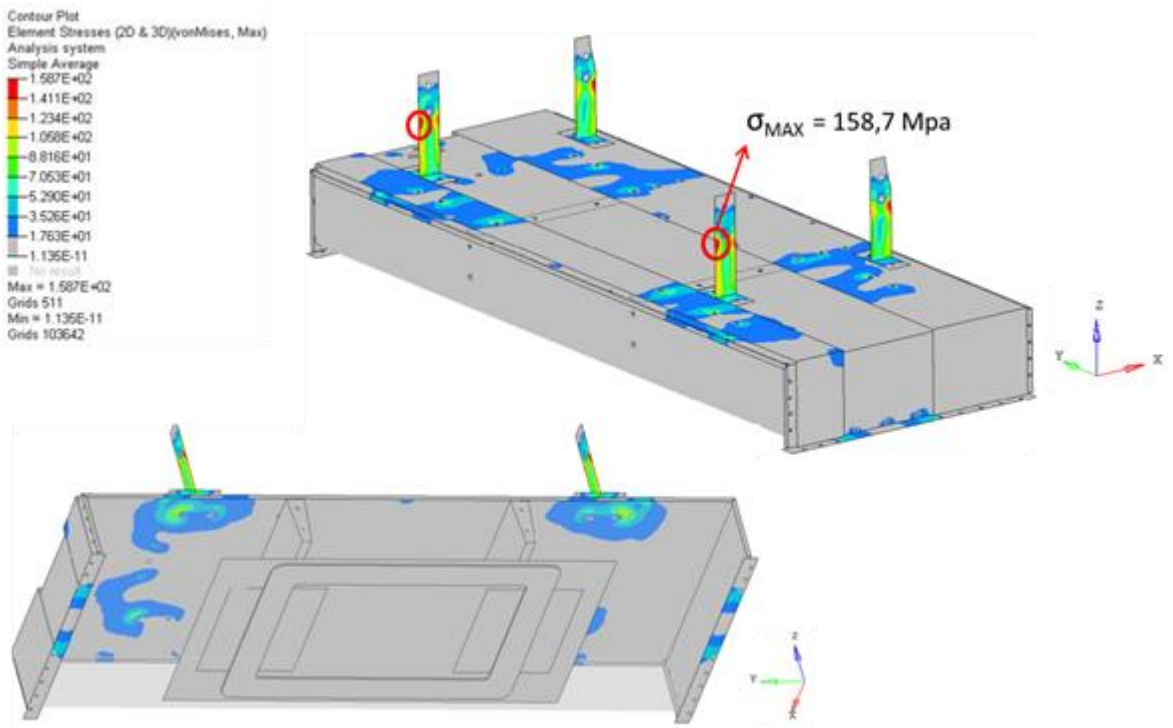

Figure 42: Static Analysis – Stresses (25g in X direction).

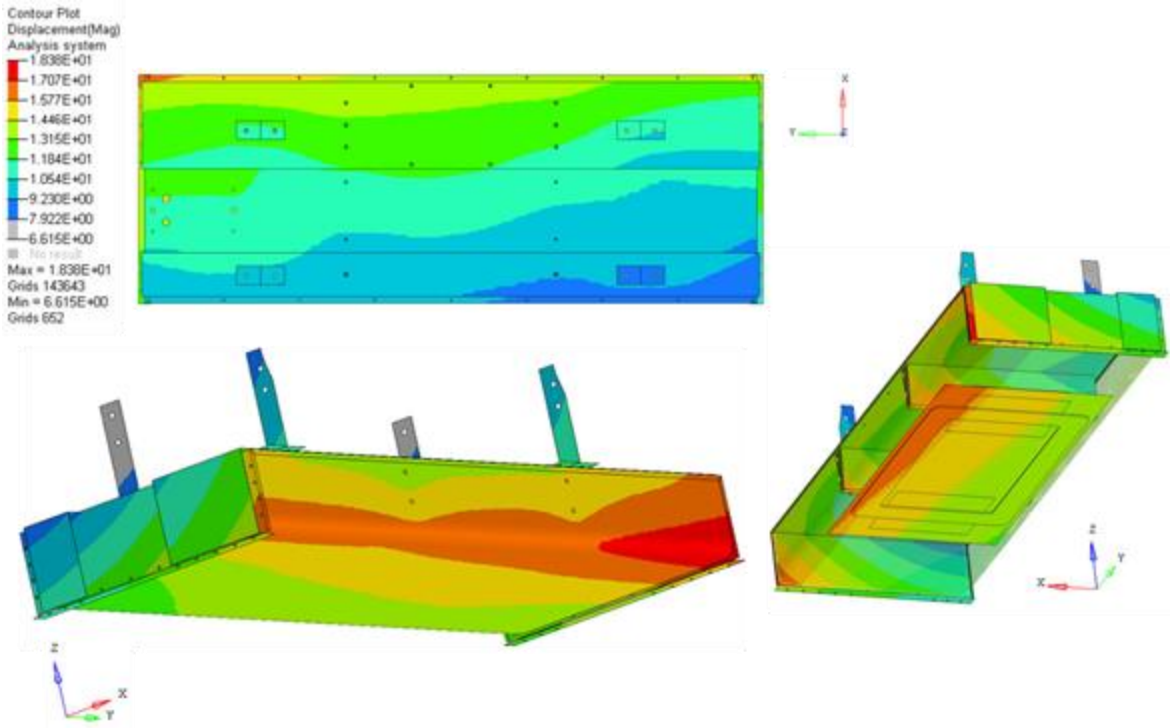

Figure 43: Static Analysis – Stresses (25g in X direction).

A second impact condition was simulated applying two components, 25g along X direction and 1g along –Z direction: as expected in linear calculation, the results are simply a linear combination of single load cases. (See results in Figure 44).

Front Impact (25 g in X direction plus gravity 1g in -Z)

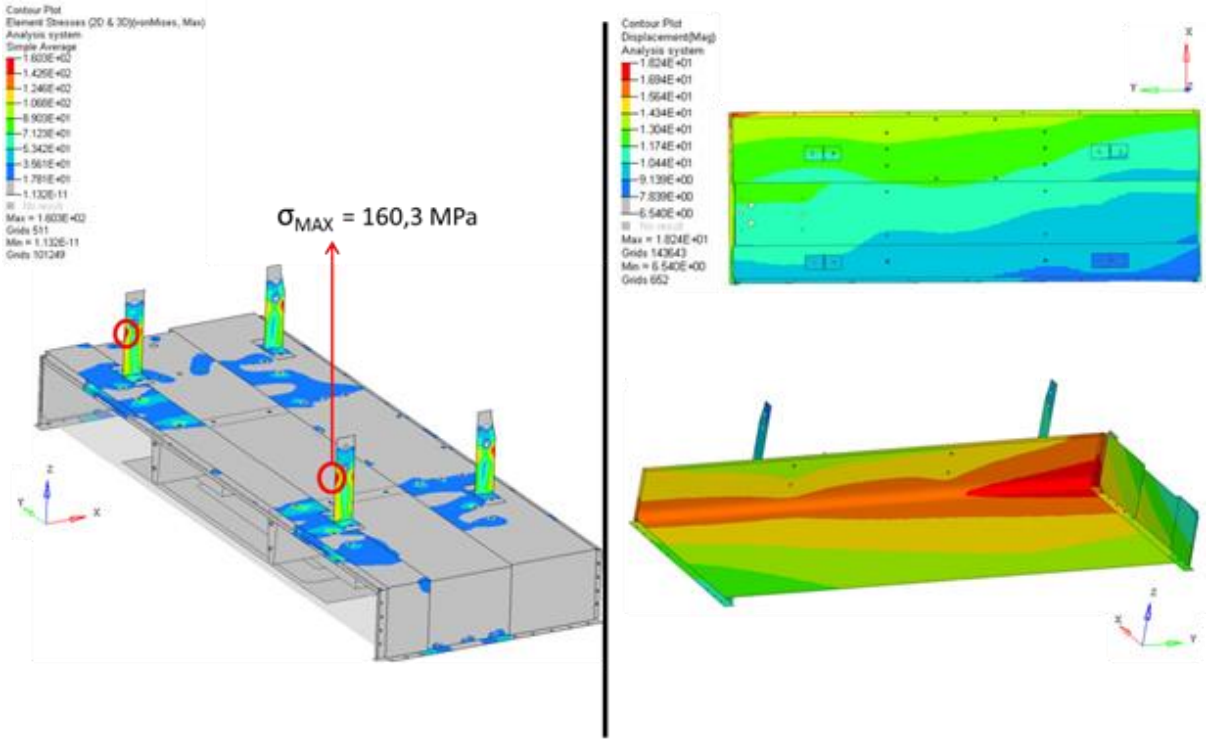

Figure 44: Static Analysis – Stresses and Displacements (25g in X + 1g in –Z).

Note: Front Impact (25 g in X) only: σMAX = 158,7 Mpa.

The third case shows the behaviour during a side impact (25 g along Y direction): as in the front side impact the failure components are the attaching brackets, with an overestimation of sigma. In this case the side impact and the gravity load case are combined to obtain a complex load case. The principle of superposition of effects is still valid.

The results obtained from this third case are shown in Figure 45 and Figure 46, in terms of stresses and displacements, while Figure 47 shows the results obtained in the case of Side Impact, with 25g in Y direction plus gravity 1g in –Z direction.

Side Impact (25 g in Y direction)

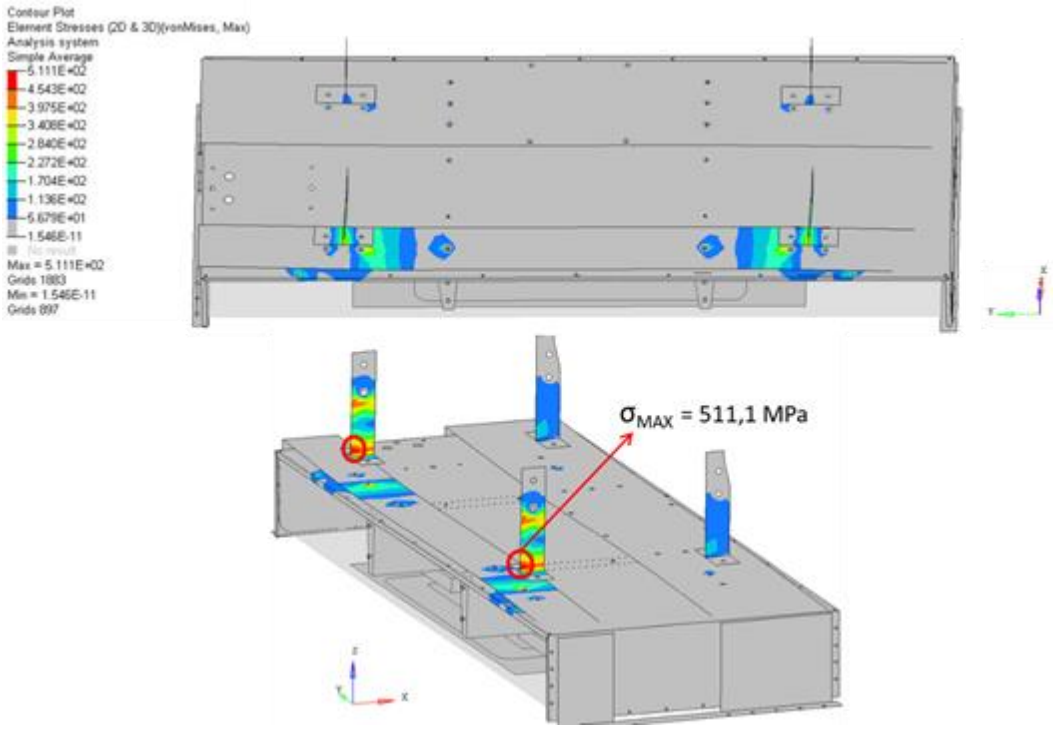

Figure 45: Static Analysis – Stresses (25g in Y direction).

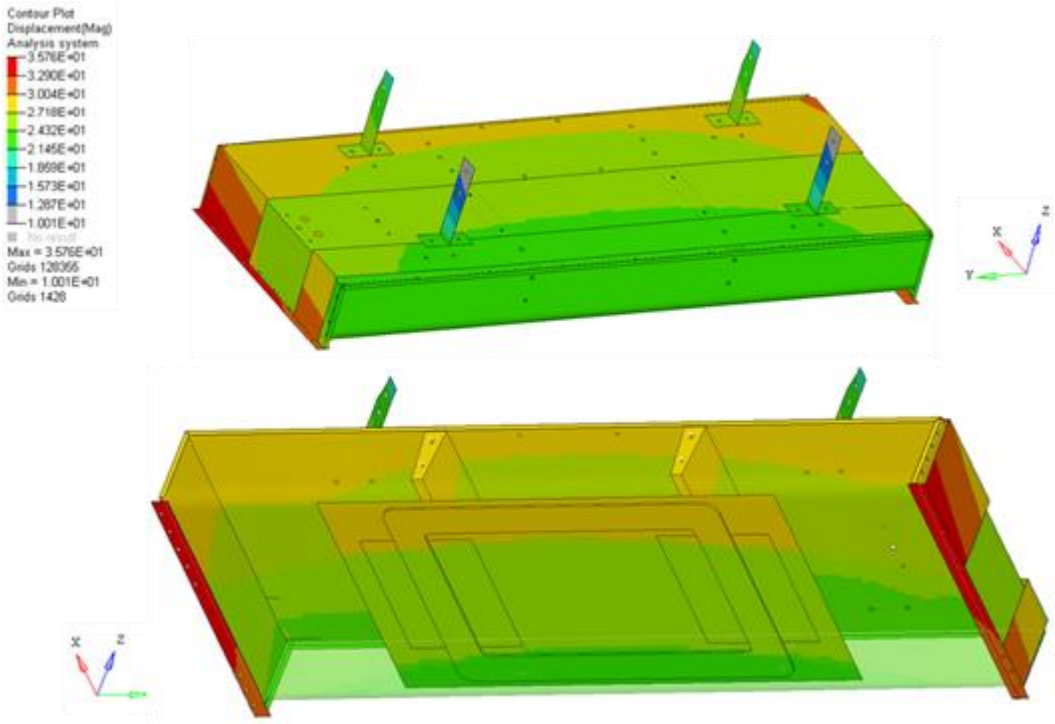

Figure 46: Static Analysis – Displacements (25g in Y direction).

Side Impact (25 g in Y direction plus gravity 1g in -Z)

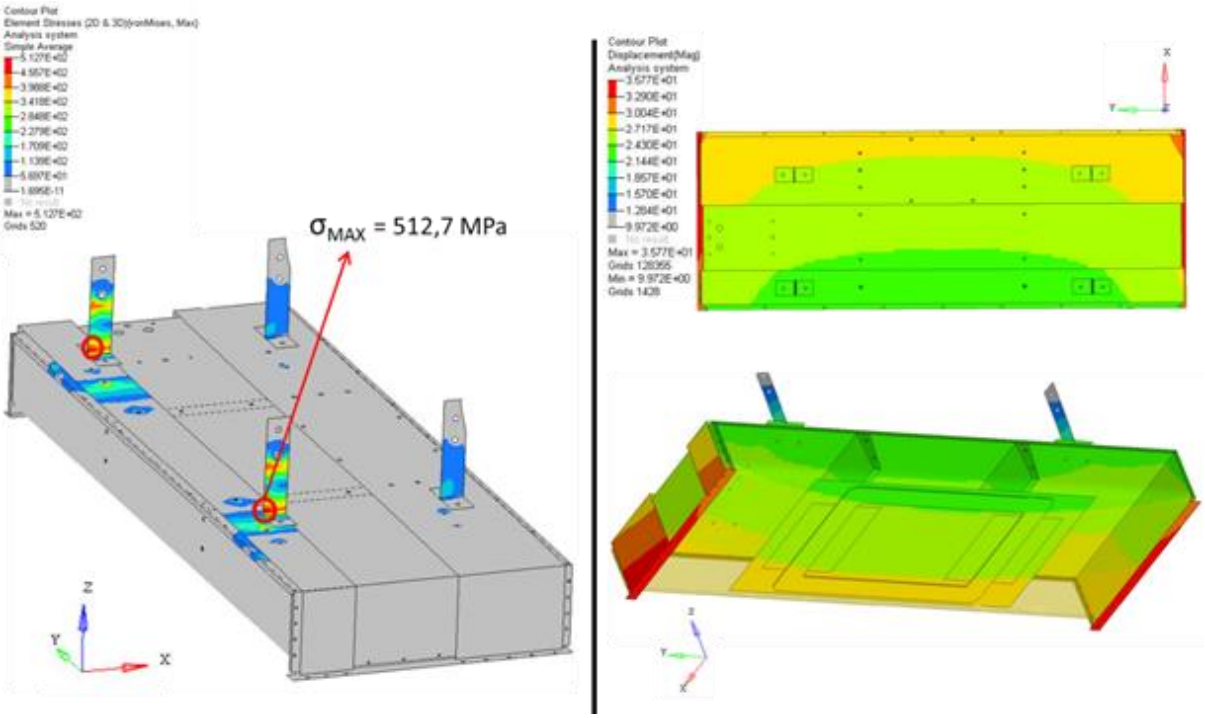

Figure 47: Static Analysis – Stresses and Displacements.

Note: Side Impact (25 g in Y) only: σMAX = 511,1 Mpa.

Figure 48 shows a summary of the maximum sigma measured on the charging box and the position for all the load cases analysed (results shown from Figure 40 to Figure 47).

LOADCASE	σ_{MAX} (MPa)	Component (Position)
Gravity:	8,73	Box cover (1)
Bump (3G in Z direction):	26,2	Box cover (1)
25G in X direction:	158,7	Attachment bracket (2)
25G in X plus 1G in (-Z) direction:	160,3	Attachment bracket (2)
25G in Y direction:	511,1	Attachment bracket (2)
25G in Y plus 1G in (-Z) direction:	512,7	Attachment bracket (2)

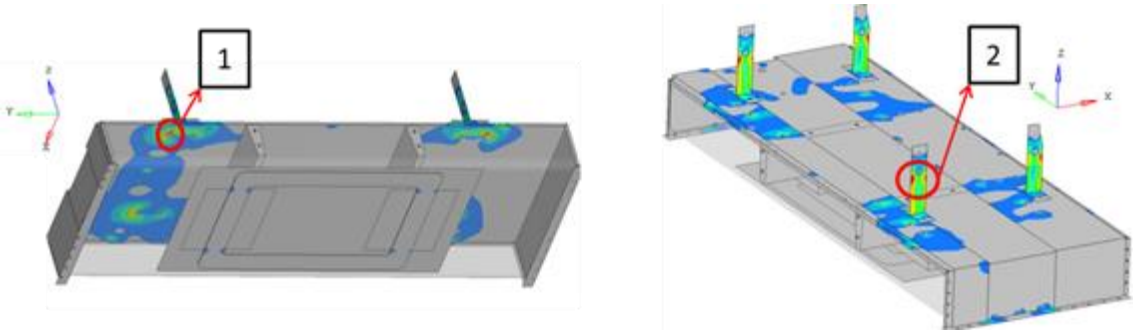

Figure 48: Static Analysis: - maximum stress results summary.

2.4 Conclusions and remarks

The performed evaluations lead to the conclusion that there were no structural problems with the system in normal vehicle operation conditions.

All analysis performed with the loading of 25 g, should simulate the influence of the front and side impacts. Due to the fact that they were evaluated using the linear approach, it is expected that these results are the worst-case.

Analysis with 25 g in X and Y direction, with added 1 g in -Z direction, presents a state where gravity acts during the impact acceleration simultaneously with the lateral acceleration due to the impact. As can be seen in the results, the differences in stress distribution, as well as in deformations, are minimal compared to load cases with 25 g of impact only.

Considering the current FE model and boundary conditions, the maximum value of stress has been reached in the following subcase:

Side Impact (25 g in Y direction plus gravity 1g in -Z), σMAX = 512,7 MPa .

Taking into account the conservative case that we are analysing, it is to be expected that during the accident, the most likely area for failure to occur is the attachment bracket of the charging box to the underbody of the vehicle (see Figure 49).

It has been found that the suspended system is feasible, but, as it was reasonable to expect, the fastening could be critical, in case of accident. In order to optimise the receiving structure it could be useful to re-design the shape of the brackets, for example with a widened profile, or increased thickness.

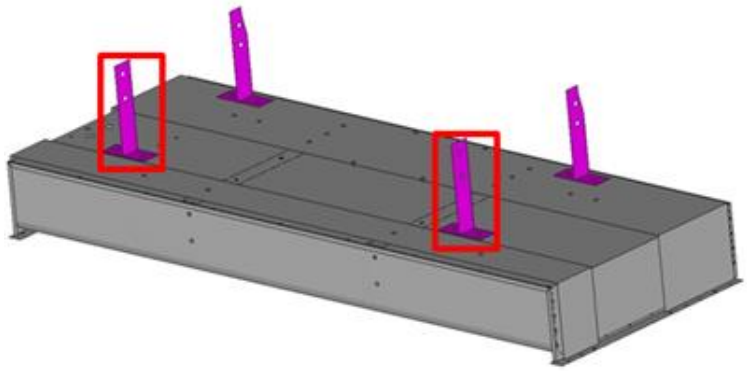

Figure 49: Static Analysis – Stresses and Displacements.

Another aspect for possible improvements is the choice of material for the parts currently made of Lexan. Lexan has been used here because it was particularly suitable for the prototype's requirements, not only from the point of view of technical performance, but also in aesthetic terms, being a demonstrator. The choice of materials must be revised from a manufacturing point of view.

The most critical point of architecture definition, in term of components, materials and assembly, is the need to satisfy electromagnetic, thermal and mechanical requirements by means of the best compromise solution, for a shielding with additional structural and thermal functions; the case has to be completely hermetic.

Furthermore, it would be very advantageous to obtain a significant weight reduction of the system, for example by means of integration between the receiving system and structure.

2.5 Safety and operational concerns considered for VEDECOM prototype cars

2.5.1 General safety provisions for Qualcomm Halo integrated car components.

Given the prototype nature of the components supplied by Qualcomm Halo and the subcontracting conditions of cooperation with VEDECOM, some general considerations can be addressed in this document, however, not all safety conditions are addressed at this stage; a fully developed product will address all the safety and operational conditions.

2.5.2 General safety provisions for the prototypes supplied by RSA

As a commercial vehicle, the Kangoo Z.E. has specific regular provisions regarding electric safety (http://iuv.sdis86.net/wp-content/uploads/2015/07/RENAULT_KANGOO_2012.pdf). These general provisions include a safety fuse protecting the battery (Service-plug). However, additional safety provisions were issued to VEDECOM due to additional power transfer system that is on the vehicle; these safety measures were:

- Initial checks prior to car use (cooling liquid)
- Sequence of activation of LV additional switches specific warnings.
- Two emergency stop buttons have been implemented to stop the vehicle safely (one from inside and the other from outside with radio command).
- A third emergency stop button has been integrated in the architecture to warn Qualcomm Halo system to stop charging in case of LV loss.
- Any serious warning sent by the vehicle BMS is relayed by VEDECOM supervisor to Qualcomm Halo EVCC in order to terminate power transfer.
- The Kangoo has not been designed to receive power from an external source such as a wireless power transfer system, which has its own EM emissions that OEM must meet, specific OEM (confidential) specifications were provided to Qualcomm in order to make sure that the chargers are designed to meet OEM requirements.

Additional operational considerations:

A series of laboratory tests has been conducted with the vehicle on the test bench with HV connected to an external power source delivering 20 kW in various conditions of speed (up to 90 km/h) in order to assess the vehicles capability to receive power from an external source in various driving conditions. A number of tests have been carried out where the chargers provided severe power switching sequences in conjunction with regenerative braking to test the batteries capability to accept charge (limited to BMS settings). These extensive tests pointed out the vehicle is capable of accepting 20 kW power in various driving conditions and the power generated by regenerative braking without any safety and operational warning by the BMS.

Notes:

1). Additional description of VEDECOM car prototype can be found in D46.1.

2). No significant issues were encountered regarding the mechanical integration of the different Qualcomm Halo car components structural robustness.

2.6 Safety and operational concerns considered for future prototype cars/experiments

Current commercial EVs are designed recoup energy during braking and store safely in the battery (regenerative braking). External source such as wireless power systems have high power transients where the charge into battery varies significantly. Wireless power transfer solution could also have high radiated EM emissions and harmonics. Extensive tests are to be conducted at Satory test site in order to characterize potential effect on car protection relays and other safety car systems in a broad range of frequencies.

The charge system can produce conducted emissions (harmonics on charge current due to charge system) with an impact on the car BMS. Radiated emissions (EM field) can also have an impact on electronic components and humans. It is necessary ensure that these emissions are below the levels specified by OEMs, guidelines and standards.

Concerning passive safety aspects, no structural concern was reported as such pointed out on the Italian prototype. However, it is clear that the additional components of Qualcomm Halo on-board system will raise additional concerns in a crash, in particular a rear collision on prototype 2, where the converter is located at the back of the car.

A magnetic shielding could have an impact on the ground clearance. The ground clearance must be compatible with specifications and standards.

The system must be able to cope with at least 1kW heat produced by the system; and the cooling systems should be designed to ensure that heat can safely be emitted.

Future design of wireless power transfer system should integrate non nominal extensive analysis use cases (such as excess power from the charging station, loss of 12V, protection against overcurrent etc.). Specific safety measures/warnings should be thoroughly studied (as for the autonomous vehicle). Note that the solution should automatically protect itself against overcurrent or loss of 12V system due to the protections measures taken during design.

Adding a secondary coil exposed to strong magnetic field elevated to HV 400 V, is adding another electrical risk of loss of electric insulation of HV circuit (due to mechanical impact by metallic objects like metallic bar , screw projection etc.). A risk would be to connect the HV to the mass of the vehicle for example due to aging. Further studies have to be carried out.

3 ON-ROAD EQUIPMENT ARCHITECTURE

3.1 Introduction

This chapter describes the outcomes of Task 3.5.2 of D3.5.1, “Architecture Definition” as stated in the DoW.

Note that in this section we will refer to “on-road” infrastructure as being the sum of all equipment between the AC power source and the interface to the vehicle. For those parts of any solution which are buried under the road surface, we will refer to “in-road” equipment, for example the charging coils of a wireless solution.

Task 3.5.2 defines on-road dynamic power transfer architecture. The architecture of each solution is tailored to meet the specifications and capabilities of the test site that it will be tested on. This section adopts the following layout:

- Overall high level system architecture;
- In-road infrastructure architecture;
- Road side infrastructure architecture.

Figure 50 shows the dependencies on Deliverable D3.5.1. The results from this report feed into Deliverables D3.6.1 to D3.6.4 in order to design a prototype system for each solution provider.

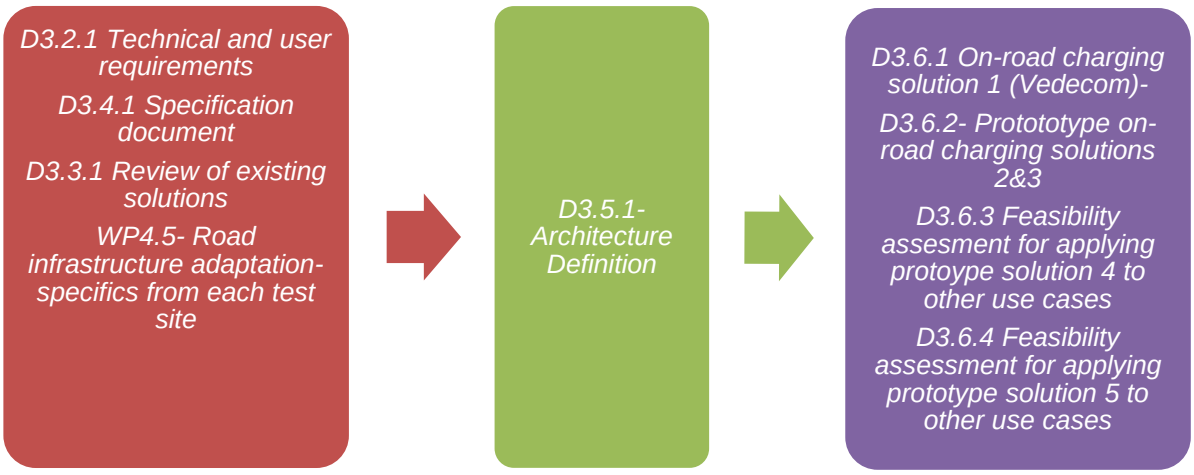

Figure 50: D3.5.1 dependencies.

A full description of the task is given below, as in the DoW.

A system architecture can be defined as “…the conceptual model that defines the structure, behaviour, and more views of a system” (Wikipedia). The System Architecture primarily

concentrates on the internal interfaces between the system's components or subsystems, and on the interface(s) between the system and its external environment. System architecture includes:

- System elements;
- Interfaces;
- Processes;
- Constraints;
- Behaviours.

This task only considers the on-road infrastructure, (shown encircled in red in Figure 51 for a wireless solution) of a power transfer system. The boundary of this work is between a three phase supply into the roadside equipment and the road surface.

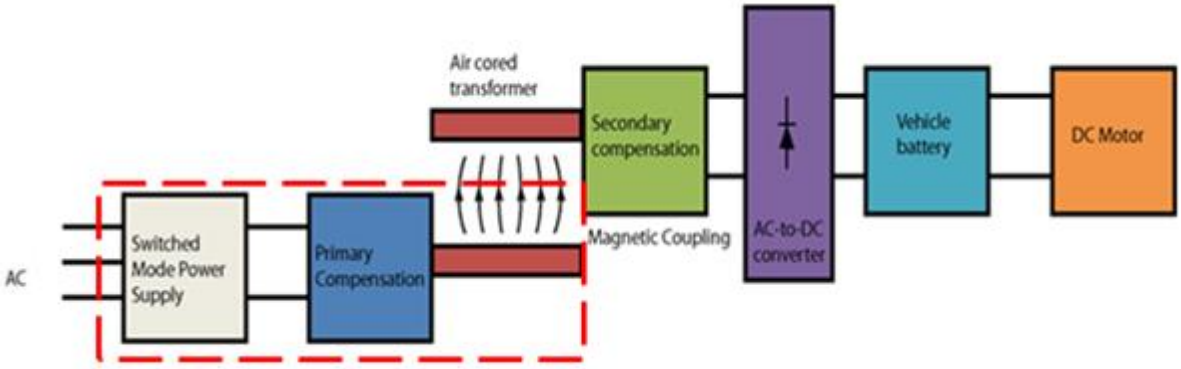

Figure 51: High-level example of an Inductive Power Transfer system layout.

Figure 52 shows the basic architecture of the whole system, including Grid side, Road side and Vehicle side, and their basic connections, addressed in this document, while in Figure 53 there is the scheme of the system with Road architecture based on Qualcomm Solution, including one DC/AC 85 kHz converter for several coils.

More details on the on-road infrastructure are described in the following sections.

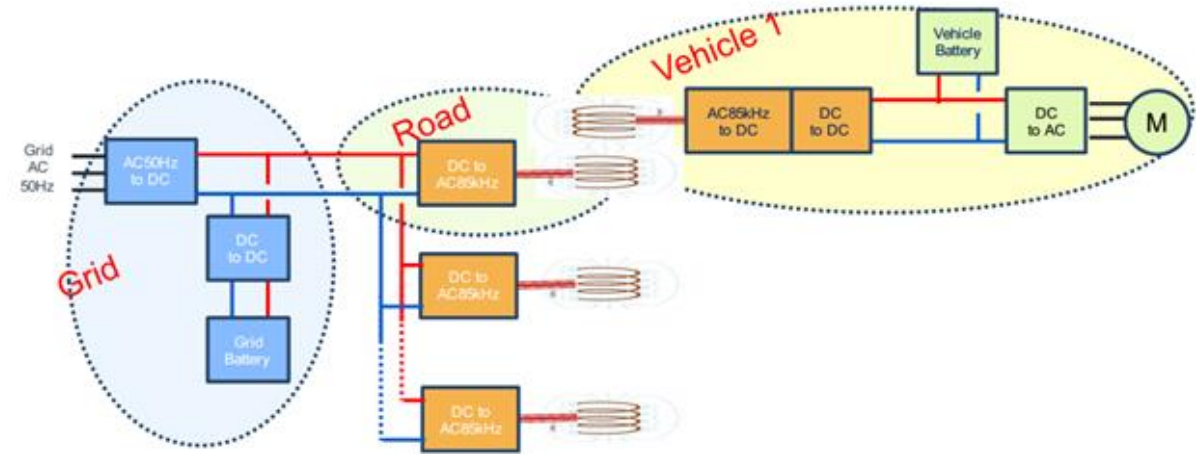

Figure 52: Basic architecture.

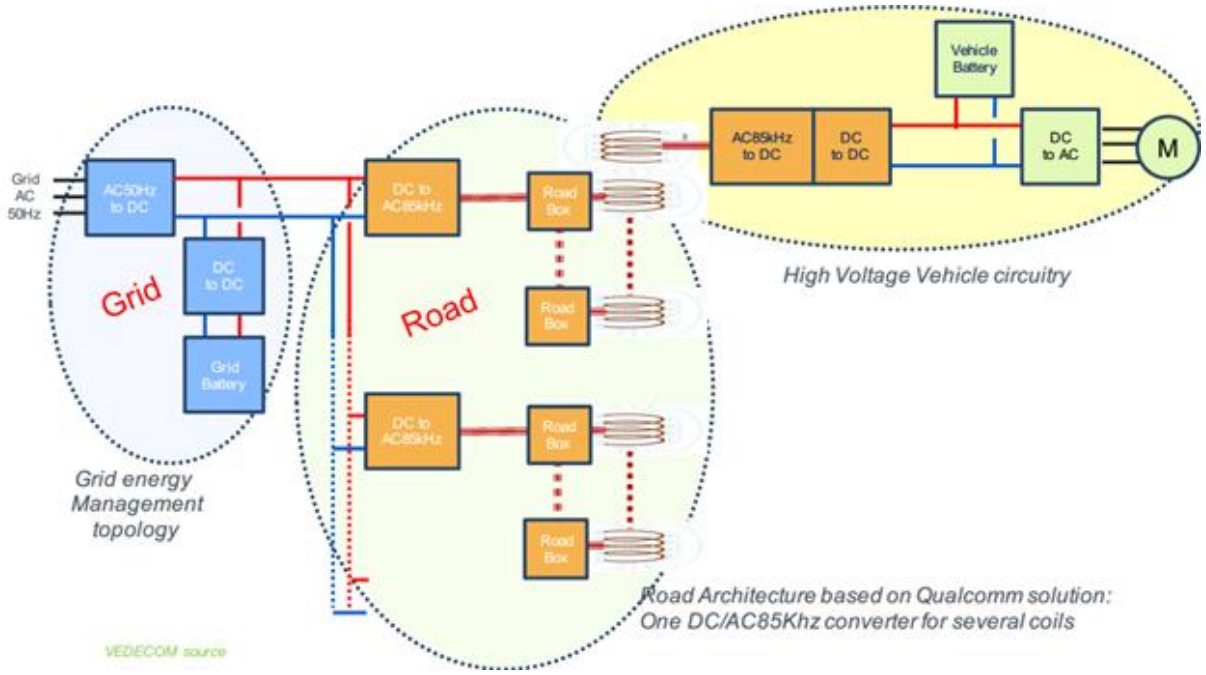

Figure 53: Road architecture based on Qualcomm Solution.

The high level system architecture defines the system layout as a whole, which includes in-road infrastructure (or overhead for some solutions), road side equipment, sensors and connections (see Figure 54). The high level system architecture includes the block diagram of the solution as well as detailed schematic drawings of the solution as whole. The schematics diagrams include the locations of the in-road power transfer equipment with reference to road lanes and pavement layers, and locations of the road side equipment schematics are shown with respect to the road boundaries. A substation can power one or more road side equipment and a road side equipment can power one or more segment and finally a segment could consist of one or more coils; the number of road side equipment, segments and coils depends on the solution providers design.

Figure 54: Sample high level architecture.

The system architecture includes the connection between the power transfer coil and the distribution network substation, so it should include any road side equipment that is connected to that substation connection point, the segments connected to each piece of road side equipment, and the power-transfer coils within a segment. The system architecture should include physical dimensions as well as electrical parameters at each main connection point and any safety measures. The high level system architecture should also consider the pavement and surrounding areas. In-road infrastructure architecture describes the in-road power transfer module and its location within the pavement structure through the use of schematic diagrams. This includes connections to power grids and subsystems, i.e. primary and secondary coils, cooling systems, unit sensors etc.

In-road infrastructure can be considered at two levels:

- Segment level- where each in-road segment consists of one or more power transfer coils grouped together and supplied from a single connection to the road side equipment. The number of coils in a segment varies between different suppliers, as does the length of each segment.
- Component level- which describes the connections between each in-road components and the road side system, such as rectifiers, inverters, monitoring equipment, cooling, cabinets, communication links, control and protection equipment, sensors, ferromagnetic material etc. It includes system dimensions and positions of the equipment within the modules or cabinets.

The road side infrastructure architecture defines the parameters of the equipment which provides the interface between the in-road equipment and the grid system. This includes equipment dimensions, location of the road side infrastructure with regard to the road and defines the connection diagram between grid, road side equipment and in-road infrastructure.

3.2 Methodology

To gain an oversight of architectures used for dynamic power transfer systems, we review the systems used in previous trials as well as existing systems deployed in current installations and trials.

Following this, we review methods of installation, primarily of in-road systems as these have a direct bearing on the integrity of the road structure. Where regulations are referred to, these will concentrate on the UK. It is expected that details may differ in other countries, but the main points of the architecture are not expected to change substantially between jurisdictions.

Finally we consider the architecture of the solutions proposed for both the Italian and French test sites in this project, and briefly consider the architectures of the conductive systems to be used in the theoretical studies. From the above considerations, a generic architecture is proposed.

3.3 Review of existing and previous projects

This section reviews the previous infrastructure and already existing infrastructure for on-road power transfer systems. This review does not include the architecture of systems being investigated in FABRIC as these will be discussed in more detail in subsequent sections. The review investigates the following wireless systems:

- Bombardier Primove;
- University of California PATH (Road powered electric vehicle);
- KAIST OLEV (Korea Advanced Institute of Science and Technology).
- Flanders DRIVE.

As well as the following conductive systems:

- Slide-in Electric Road System;
- Elways;
- Siemens eHighway.

Note that while the PATH system was installed many years ago, the basic technology is the same as is being proposed in various current systems, and hence any lessons which can be learned from the installation are still relevant.

3.3.1 PRIMOVE

The following information regarding the Bombardier Primove system has been extracted from the Swedish ICT report [3] unless otherwise stated.

3.3.1.1 In-road equipment

Primove uses power transfer segments where each segment containing the primary windings is 20 m long and is powered by 20 kHz AC using the Wayside Power Converter (WPC) inverters. The WPC inverters receive a 750V direct current from rectifier substations which are connected to the medium voltage power grid at regular intervals (see Figure 55 and Figure 56).

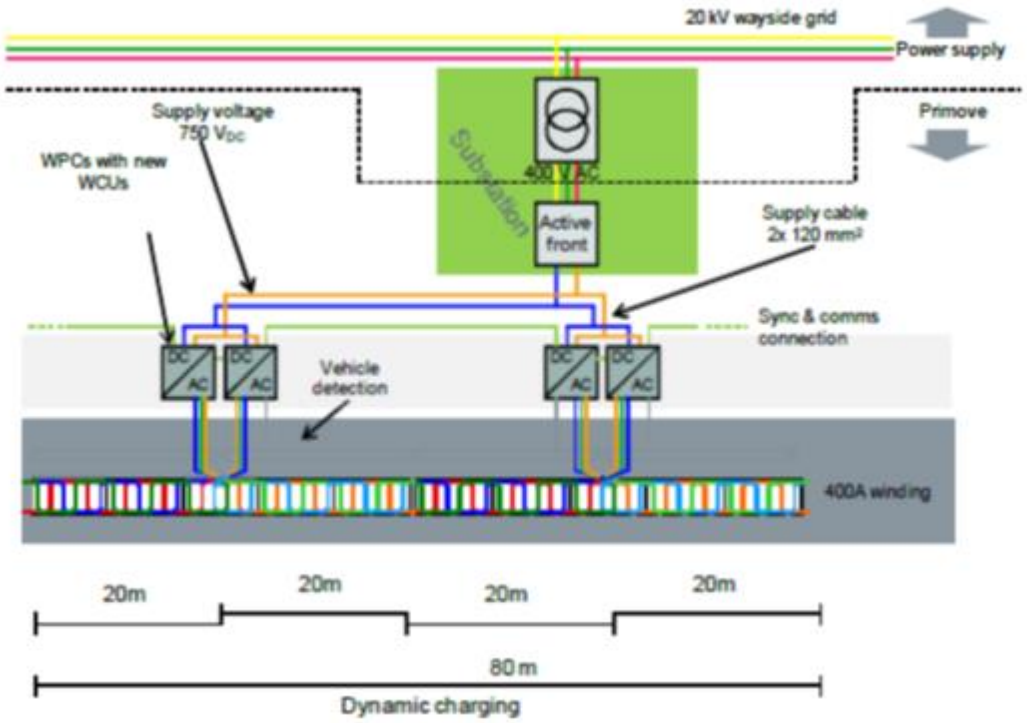

Figure 55: Primove track setup.

Approaching the electrified section, the vehicle is notified by the transponder installed on the vehicle. The transmitter on the vehicle communicates with the Vehicle Detection and Segment Control (VDSC) system on the roadway and, in cases where the clearance to supply power has been given by the driver, the WPC energises the segment.

The VDSC transmission is halted if another vehicle is closer than 20 m to the front of the vehicle and, in the case of a truck, 10 m to the rear or if the speed is below 50 km/h.

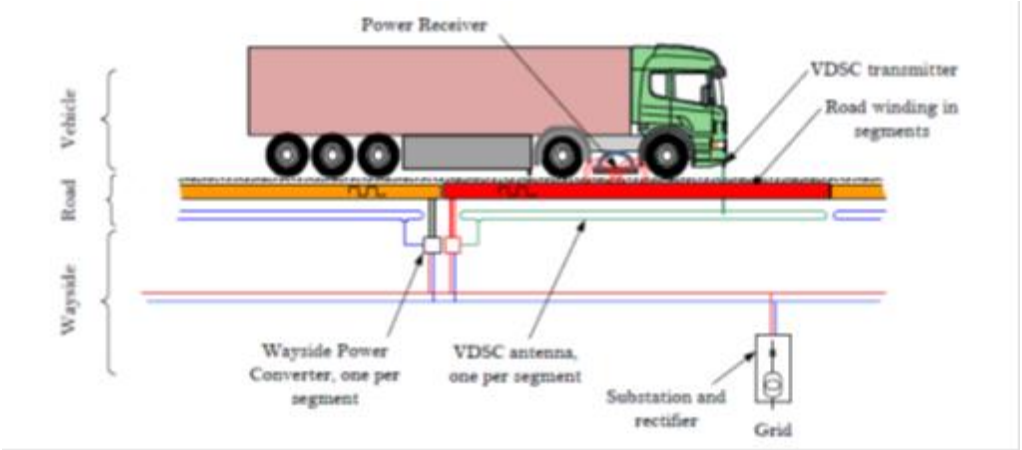

Figure 56: Primove Highway architecture.

Built-in protection is installed in order to intervene in case the system is damaged and the wayside equipment is arranged in such a way that emergency personnel can switch it off.

3.3.1.2 Roadside (wayside) Infrastructure

The wayside power inverters, which are connected to the primary windings, are small, air-cooled units with a “minimum number of passive components and a maximum of software control”. They include the VDSC antenna which receives the clearance code from the vehicle and manages the information with the central controller, switching on as directed, monitoring the energy consumption, and reporting it. The WPCs provide a constant current of 400 A per phase, and they are able to detect a cable breakage and shut it off. They receive DC power from the rectifier substations connected to the 30 kV MV power grid which in turn is connected to the 130 kV HV distribution grid.

The Victoria ICT report mainly studies the operation of the wireless power transfer system. Even though four 20 m segments (80 m power transfer loops/coils) were installed in the test facility, the construction and installation details of in-road and road side equipment have not been reported.

3.3.2 PATH (Program for Advanced Transit and Highways)

In the framework of the PATH Program of the University of California, a test track for testing the concept of power electric vehicles using an inductive coupling system was built at the Richmond Field Station of the University of California, Berkeley [4]. The track length was 210 m and the two electrified segments were 60 m long (Figure 57). The research investigated both dynamic and static charging. Only the dynamic facility is reported on here.

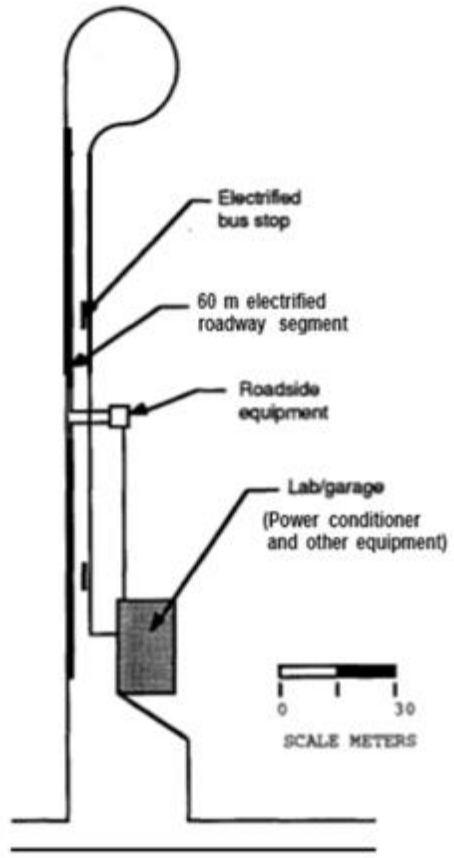

Figure 57: Test track layout.

3.3.2.1 In-road Infrastructure Architecture

Segment Level

The modules embedded in the road were made with tape-wound C-cores and laminated iron pole pieces held in an epoxy-sand matrix (Figure 58). They were about 2.8 m long and 0.5 m wide and weighed about 400 kg or about 900 pounds. Two modules were placed side by side to form the roadway inductor. The roadway was surfaced with a 5 mm slurry seal. It is noted that the use of slurry seal as a surfacing material is not normal road building practice, and was probably due to the small air gap this early technology required.

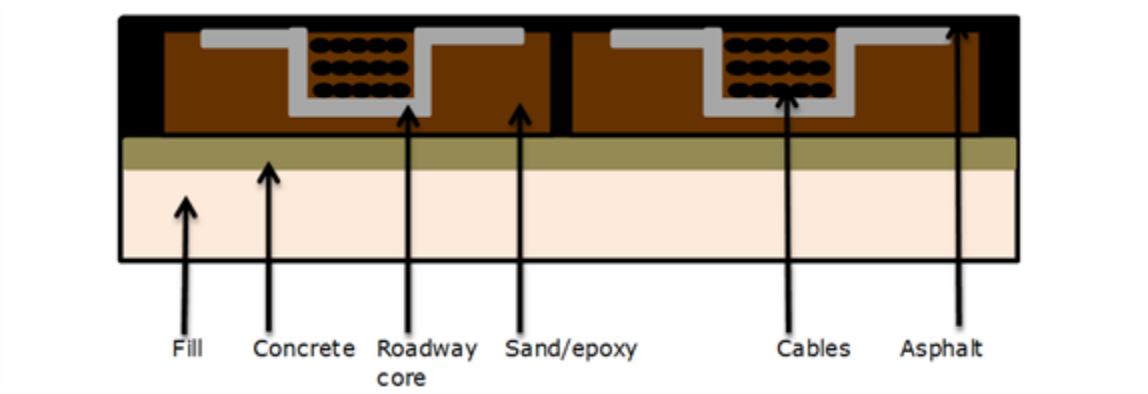

Figure 58: Roadway and pickup cross section.

Component level

Roadway Inductor

The roadway inductor comprised the inductor modules and the conductors.

The inductor modules measured 2.8 m x 51 cm x 11 cm and weighed over 400 kg, of which 191 kg were due to the silicon-iron laminations, while 218 kg were in the epoxy/sand mixture protecting and supporting the laminations.

Mechanical design of modules

The core modules were flat on the bottom and had provisions for lifting and supporting them from above. The core modules were built in a mould lined with fiberglass mat and the loose pole face laminations were loaded in by hand. Once the C-core was placed in, the entire assembly was filled with the sand/epoxy filler and an additional layer of fiberglass mat.

A slot in the roadway core module was included, designed to accept either cable or bus bar conductors.

Conductors

Aluminium cables were chosen as material for the secondary and the roadway conductor, since it has the same resistivity of the copper, but it is cheaper and lighter (the last characteristic in particular is an important advantage for the pickup).

Terminations/Crisscross

A vault at the end of each section allowed connections to be made between adjacent sections or between the segments and the power cabinet at the roadside. This was largely included for flexibility during testing, and is unlikely to be required in operational installations.

Mechanical Design of Roadway Inductor

Pairs of 3 m long modules (co-located side by side) were installed in trenches under about 1.3 cm of covering material. Expansion joints, made of 1.2 cm thick polyurethane foam, filled the lateral gap while the longitudinal gap was filled with the same grout that was poured below the module. The modules containing the conductors were placed into a mixture of sand and polyester. The eight PVC detector loops were buried in the subgrade and the roadway was finally covered in a 3 mm thick slurry seal.

Construction Method

The project had three phases: design and planning, roadway construction and trench excavation, and installation of the modules and conductors.

The surveying, excavation, and removal of the old pavement took one week to complete. Simultaneously the construction of the concrete troughs and vaults was carried out. In total, approximately seven weeks were needed to complete the construction.

3.3.2.2 Road side Infrastructure architecture

The power distribution system included a power conditioner, transmission lines, and wayside equipment (compensation capacitors, capacitor cooling system, junction box, and instrumentation), plus additional equipment associated with the segment switching system, high current solid-state switches and vehicle detection hardware.

A rectifier/inverter unit that received a 3-phase power at 460 V and 60 Hz and that could supply up to 200 kW at 2000 A at frequencies in the range 180 – 400 Hz was located next to the track. For the tests performed, 1200 A at 400 Hz had been used. Considering these high values for the current and frequency, more conductors were run in parallel to avoid the skin effect. Their positions were selected in order for them to have the same inductance and therefore the same current flow. The current was routed to the roadside equipment (Figure 57), which in turn could power one or both the segments in the track.

The positions of the cables were carefully selected to ensure all parallel paths had nearly identical inductances and carry essentially equal currents. The output from the power conditioner went to a patch panel, where the current could be directed to the indoor test stand or to the equipment pad at the centre of the track. From the equipment pad, current flowed to one or both of the segments of the test track.

In the power cabinet, a cooling system pumped ethylene glycol through the capacitors and switches to prevent their overheating. Safety switches on the capacitors triggered by overheating were connected to an emergency cut-off switch for the power conditioner.

Dynamic Segment Switching and Communication System Concept

A control system that allowed the segment to emit power only if there is a vehicle over it was devised.

Beneath the surface, at three points along the test track, preformed inductive loops (of the same kind used for monitoring the traffic) were installed. Some of these were dedicated to the detection of the position of the vehicle to give the commands for switching the segments on when the vehicle was over it and off in absence of the vehicle. Directional Logic Units were used for determining the direction of travel.

3.3.3 KAIST OLEV

The KAIST (Korea Advanced Institute of Science and Technology) On-Line Electric Vehicle (OLEV) system is a dynamic wireless power transfer technology which is already in use on bus routes in Korea. Like most wireless systems, it makes use of resonant inductive coupling to transfer the power between the primary and secondary coils.

The 20 m primary winding segments are embedded 40 mm under the surface. Similarly the VDSC antenna loops are installed as a module to allow paving over it. All windings, antennae, starpoint junctions, and connector leads are installed prior to the final paving step. Where utilities run under the road, a layer of aluminium is laid between the winding and the utilities as a shield between the WPT and utilities equipment.

3.3.3.1 In-road Infrastructure

There are two possible methods of construction:

1. Trench based construction
2. Full lane width construction.

Trench based construction involves creating a trench in the existing highway, installing the system (whether in situ or pre-cast), backfilling and laying an asphalt surfacing layer. Figure 59 presents a schematic of the cross-section of the trench based system, whilst Figure 60 shows an example of trench based construction (in-situ and prefabricated) of a KAIST dynamic power transfer system in a flexible pavement.

A trench of 0.8 m width is excavated to full depth of the bound layer, from the centre of the road. Once the foundation is prepared, the installation of the systems is undertaken, either in-situ built or using pre-cast built modules. These systems are then connected to the roadside equipment before being covered in concrete and overlaid with an asphalt layer.

Whilst the option of cutting a trench in the road is likely to be the quickest and cheapest of the options, the introduction of an concrete section within the pavement would almost certainly lead to reflective cracking at the surface at or near to the wheel paths, as well as cracking of the transverse joints where the power supply is taken in from roadside cabinets. The reflective cracking could potentially be reduced and / or delayed through the use of a SAMI or grid layers between the system and the asphalt layers.

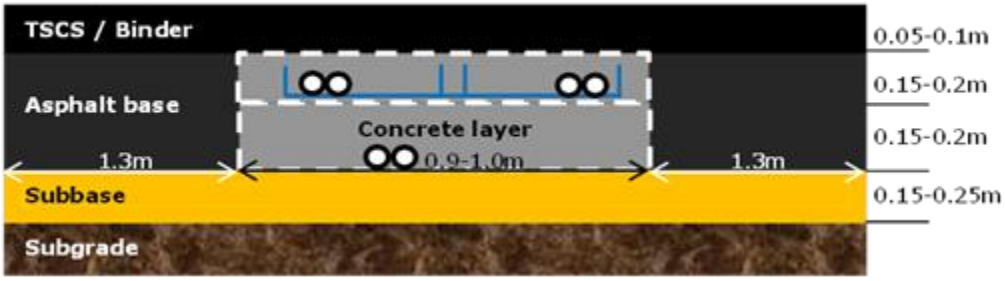

Figure 59: Schematic cross section of KAIST system using trench construction.

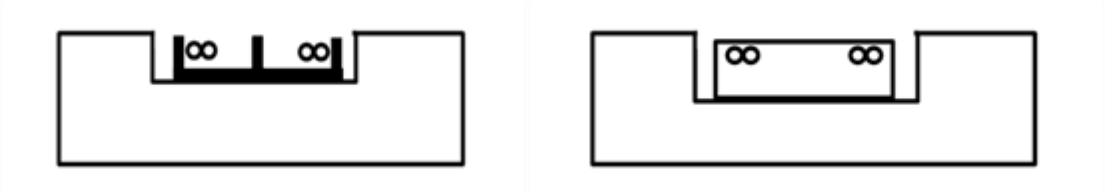

Figure 60: Trench construction of KAIST system: (left) In-situ construction (right) Pre-fabricated system.

Unlike placing the WPT system within a trench, full lane width reconstruction would involve removing the full depth of bound layers from lane 1, and either constructing in-situ or using pre-cast units, followed by construction of a concrete pavement around the units, followed by asphalt surfacing.

Whilst this is a more time consuming and expensive construction exercise than the trenching option outlined above, it has the advantage of locating longitudinal construction joints at the edge of the lane. The number of transverse joints would be the same and would extend across the full lane width. However, it is thought that any on-going maintenance requirement may be less with full lane width construction.

An alternative to the full lane reconstruction outlined above would be to plane out the full lane width of asphalt, but rather than reconstructing the entire lane on site, it would be replaced with a full lane width prefabricated section containing the entire system. This could possibly be finished with asphalt surfacing as above, or by having a porous concrete surfacing already placed on the prefabricated sections. The significant advantages of this approach, compared with on-site construction, would be an accelerated construction period and factory construction quality.

3.3.3.2 Road side infrastructure

The power inverter at the road side receives a 3-phase current at 380 V or 440 V at 60 Hz and gives as output, a constant current of 200 A at 20 kHz. The power is then transferred to the precast ground modules. The power capacity of the power inverter is between 100 kW and 200 kW, but it can be scaled-up depending on requirements [5]. A sketch of the system is shown in Figure 61.

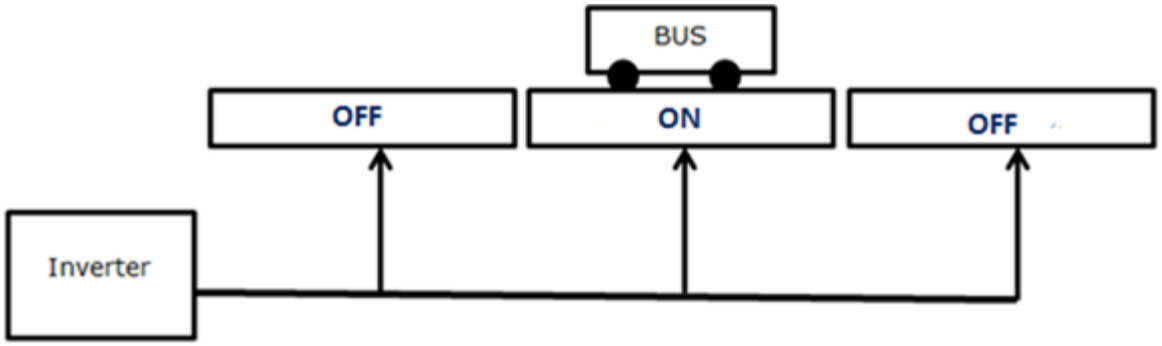

Figure 61: Schematic overview of the OLEV system.

3.3.4 Flanders' DRIVE

In 2010 Bombardier joined the "Inductive Charging of Electric Vehicles" project in collaboration with the Flanders' DRIVE consortium (Flanders' DRIVE, 2013). The goal of the project, concluded in 2013, was to study the feasibility of inductive charging systems for electric vehicles, both in dynamic and stationary conditions.

3.3.4.1 In-road Infrastructure Architecture

Power transfer systems were installed in two sections of road, one covered with concrete and the other with asphalt. Different segment lengths were installed (see Figure 62), namely:

Concrete: 124 m, 1 x 4 m, 1 x 8 m, 7 x 16 m segments

Asphalt: 16 m, 4 x 4 m segments

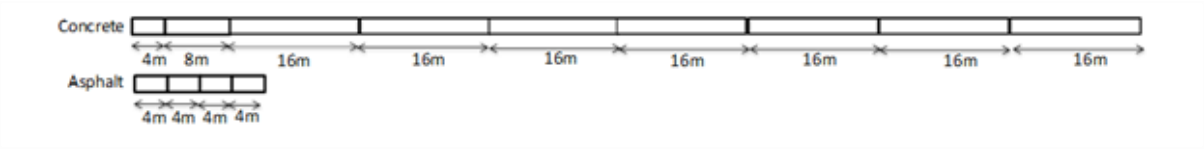

Figure 62: Test track segmentation.

The inductive emitters were contained in adjacent modules embedded in the road (see Figure 63). A shield was placed below the modules in order to isolate from other cables which may be present in the road and to support the generated magnetic field. Metal elements were not used as the magnetic field could have heated them.

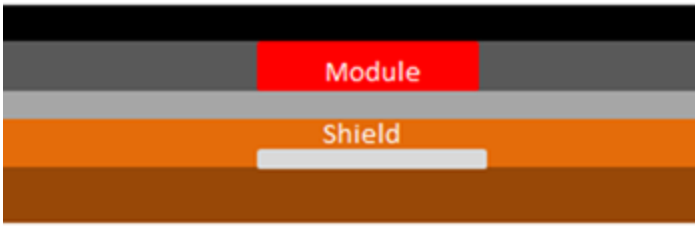

Figure 63: Road layers.

The concrete based in-road system comprised modules containing the windings and anchored to the pavement through a special glass-fibre. Similarly for asphalt roads the windings were embedded into the asphalt. During the asphalt laying procedure it was necessary to pay particular attention to those components sensitive to high temperatures and that could suffer from the compaction process.

During the first tests performed with the concrete road, the wayside electronics were placed in such a way that allowed easy access. Once they proved their reliability, they were installed in the ground on the roadside for the second part of the tests.

3.3.4.2 Road side Infrastructure Architecture

The substation on the roadside received 10 kVAC from a mid-level supply; the voltage was reduced to 400 VAC, rectified so that the inverters powering the primary coils were fed with 750 VDC (see Figure 64).

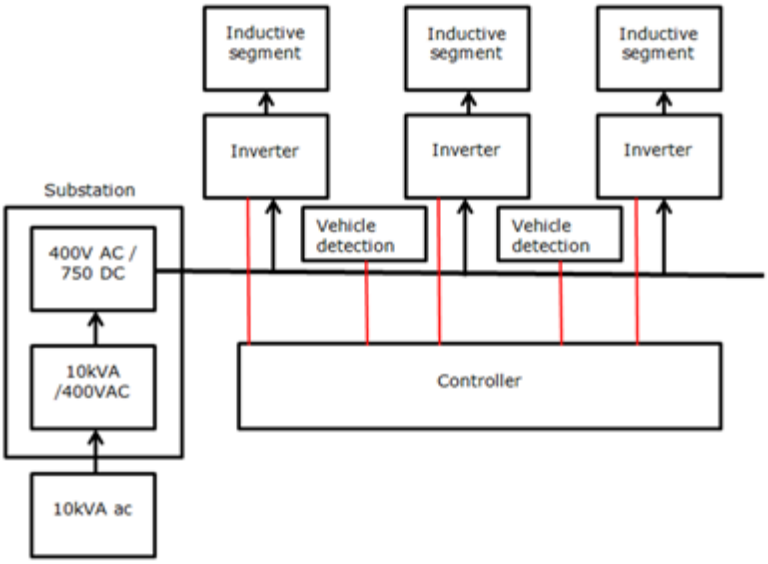

Figure 64: Roadside system architecture.

Each inductive segment was equipped with a vehicle detection system and both this and the inverter were controlled by a proprietary controller.

3.3.5 Slide-in Electric Road System – Conductive

The conductive ERS is based on the Aesthetic Power Supply (APS) technology developed by Alstom for the tramway in Bordeaux city. The embedded system is made by a segmented road rail and power boxes manholes. The power is transferred through a pick-up arm installed beneath the vehicle (Figure 65).

Figure 65: Conductive ERS.

3.3.5.1 In-road Infrastructure Architecture

The segments into the road are activated when a suitably equipped vehicle is running over them with speed between 60 km/h and 100 km/h. In Figure 66 the concept of the speed detection system is shown. Only the segments in close proximity of the running vehicle are energised.

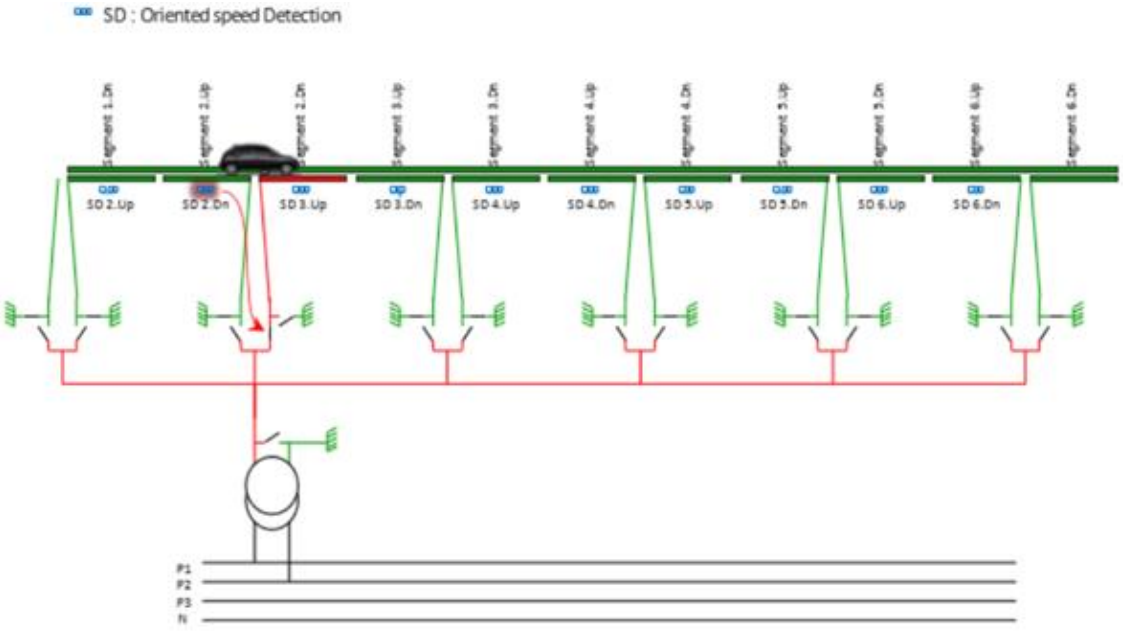

Figure 66: Illustration of the speed detection system.

The length of the conductive segments is determined by safety considerations. These are based on the minimum time a person needs to clear the way in front of an oncoming vehicle, which is one second. During this time a vehicle travelling at 60 km/h covers 17 m distance (the “Danger zone” in Figure 67), that can be electrified because in any case it is not safe for a pedestrian to stay in that range from the forward moving vehicle. Adding 2 m for the space between the front of the vehicle and the collector shoe, we obtain a length for the segment of 19 m.

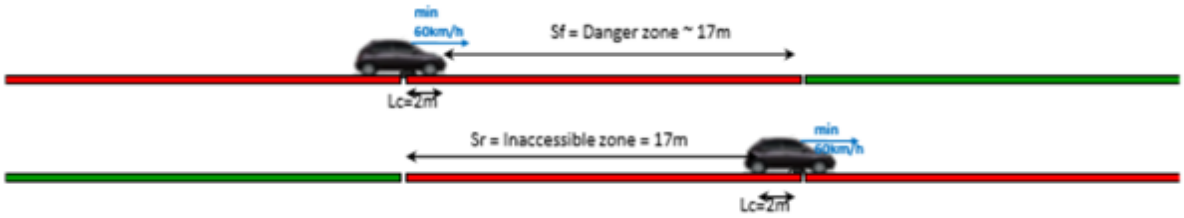

Figure 67: Safe segment length.

The power rails are installed as a pair of side-by-side conductors, one delivering the “live” voltage and the other held at or near earth potential to provide a return path and hence complete the electrical circuit. The two conductors can be seen in Figure 65. Figure 68 shows a cross-section through one of the conductor rails for the APS. Note however that an updated version improved for road integration is under development.

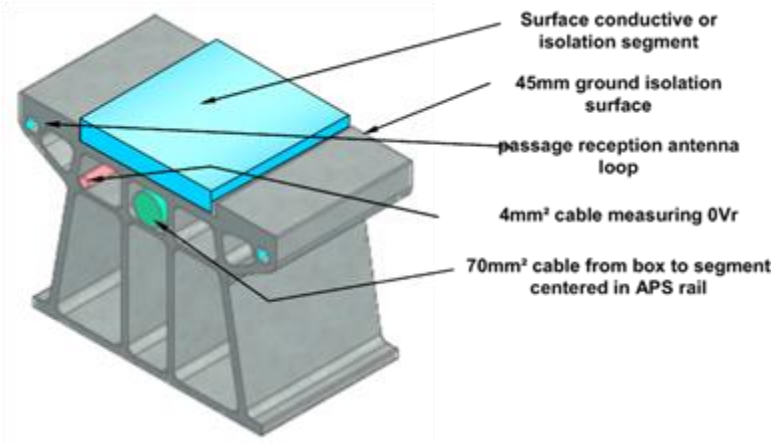

Figure 68: Cross section of the APS rail.

3.3.5.2 Road side Infrastructure Architecture

The connection to the regional 130-kV power grid is presented in Chapter 4 of this report. The 30-kV distribution grid is also shown there.

Figure 66 shows in more detail how the 750 VDC substations are connected to the road system. Between the substations, along each direction, there are twenty-two power boxes, controlled by dual APS cabinets, and two 210 mm2 copper cables, one for the 750 VDC and one for the 0 VDC return current. These cables could potentially be formed by 3 x 70 mm2 cables in parallel. Each power box feeds two road segments, as can be seen in Figure 69.

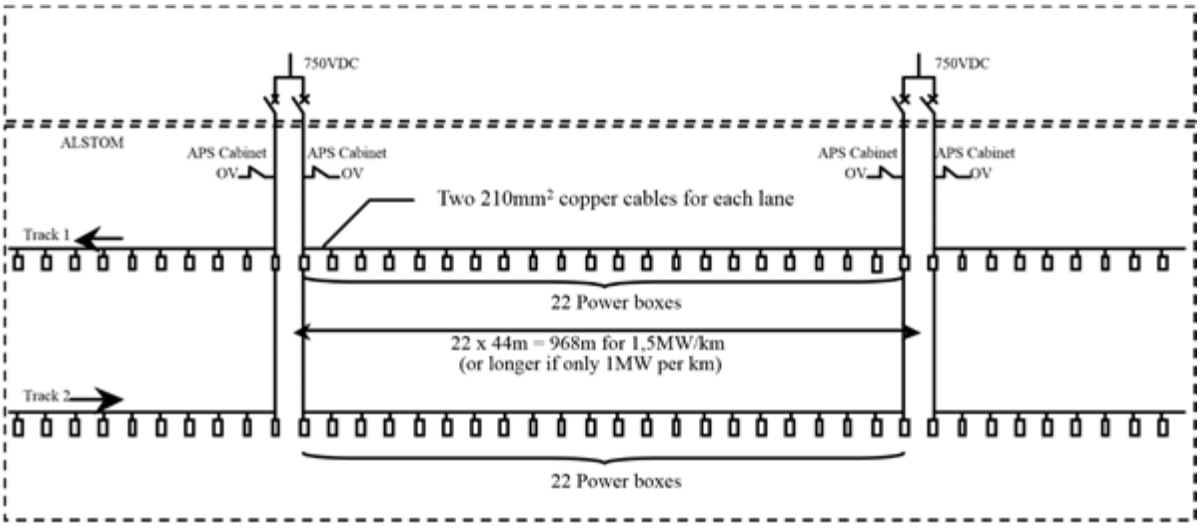

Figure 69: Road side architecture for the Alstom ERS.

A power box energises a segment and connects it to the 0 V. It has different switching and supply devices as shown in Figure 70. For example, it contains an electronic unit for the managing of the safety line with the other power boxes; a communication unit for continuously informing the substation about the box status. If the signal does not reach the substation, a short-circuit is closed in order to protect the whole section.

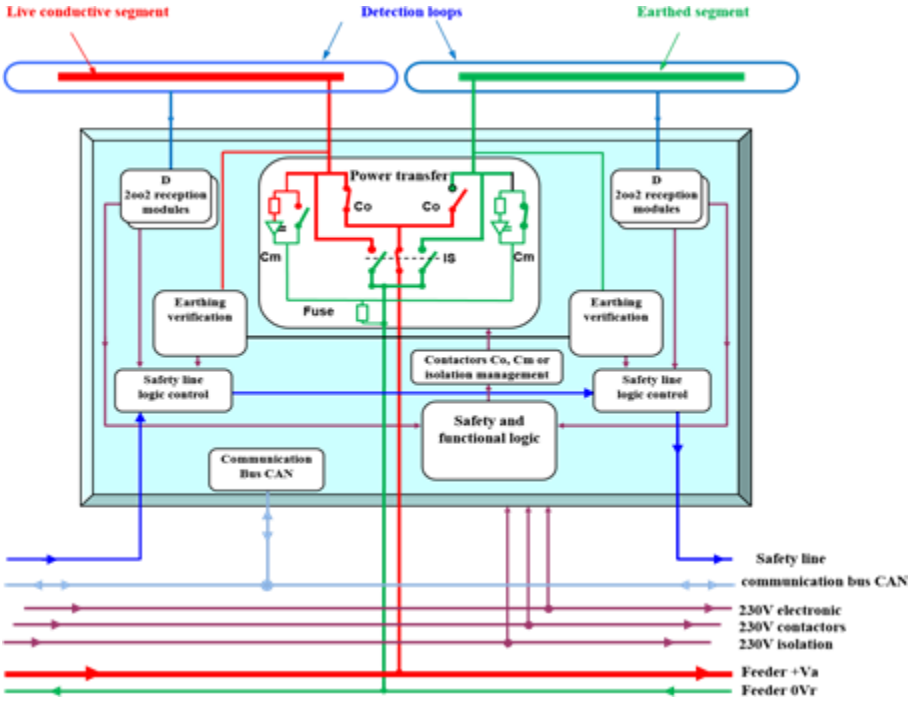

Figure 70: Power box.

3.3.6 ELWAYS - Conductive

Elways developed a conductive system for charging dynamically. At the time of writing, this is still being developed and must be considered as a prototype. The system consists of a sliding arm beneath the vehicle on which a contact is installed on the lower end. This receives the power from a rail deployed in the road (Figure 72), and transmits it to the battery or directly to the electric motor (Figure 71).

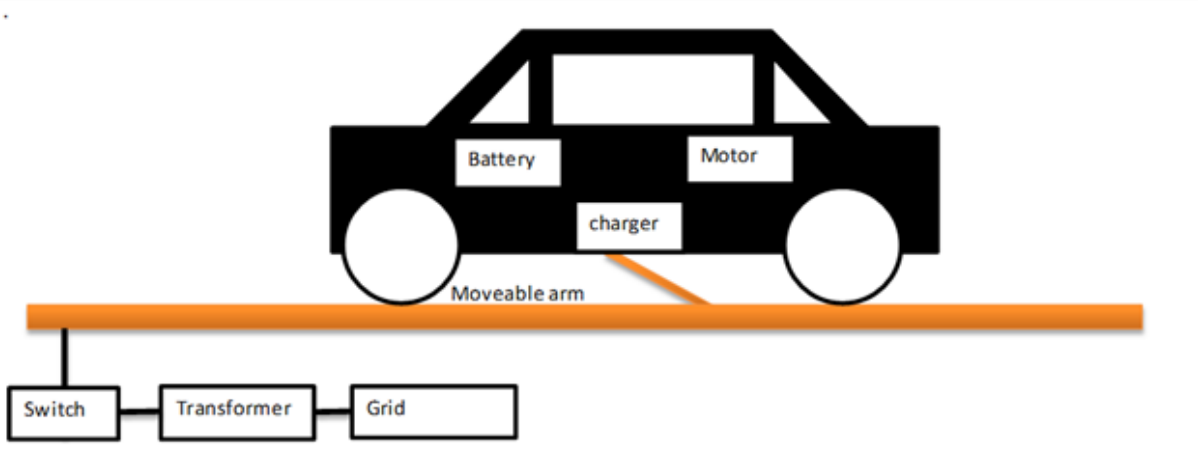

Figure 71: ELWAYS conductive dynamic system.

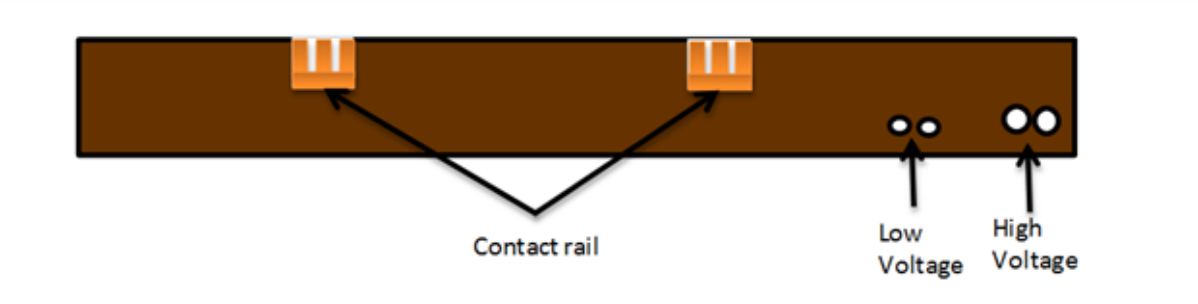

Figure 72: Cross section of the in-road system.

The voltage from the grid is reduced in two steps before feeding the vehicle. The different sections of the on-road system are connected to the side-road equipment through buried low voltage cables (Figure 73).

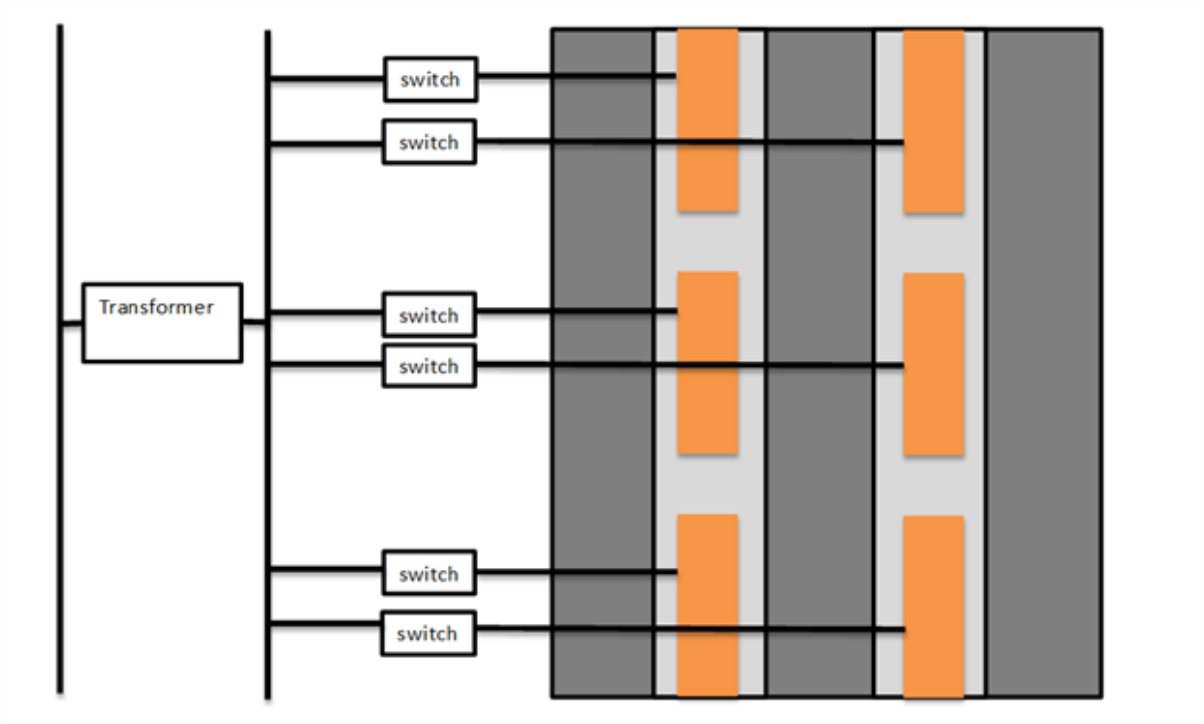

Figure 73: Simplified outline of the electric connections between the in-road and the roadside equipment.

As many roads are located in sparsely populated areas, a parallel high voltage cable may need to be considered as the power requirements of electric vehicles are such that frequent in feeds from the electric grid may be required.

As with the ERS system described in the previous section, the section of the rail is energised only when a vehicle is passing over it and for speeds above a certain threshold. Consideration has been given to equipping the track with an electrical heating that could be enabled when the temperatures were particularly low and the traffic flow not sufficient to melt the ice.

The friction of the track's surface is approximately equal to the one of the asphalt, in order to be safe for bicycles and motorcycles.

On-board equipment

The system currently in development includes solutions for keeping the track free from foreign objects, including a cleansing device installed in front of the contact, and a radar to detect the presence of objects that could damage the on-vehicle equipment. Should this occur, the system would lift up the arm.

Rail detection and pickup arm guidance systems are still in development.

3.3.7 Siemens eHighway - Conductive

Overhead conductive systems have been successfully employed on rail systems throughout the world. For road vehicles however; the twin difficulties of the lateral positional uncertainty and a requirement for a return conductor (trains use their rails for this) mean that overhead systems have been confined to low-speed trolley-bus systems in towns and cities.

The eHighway system is based on rail-like overhead conductive charging where the power is provided to the vehicle through cables and pantographs, but using twin conductors. Since the overhead line must be at a certain height, the system has been considered for large vehicles, like trucks (Figure 74).

Figure 74: Siemens eHighway technology tested in Germany.

3.3.7.1 Road side Infrastructure Architecture

The technology has been tested in Sweden, where the regulations demand a distance of 40-50 m between the poles carrying the overhead low voltage cables (750 V or 1500 V), which must be at least at 5 m from the ground; under bridges the catenary system can be located at 4.2 m or 4.8 m for high voltage.

The overhead line is a two-pole system and is fed from a container substation. The one used at the testing site (Figure 74) is equipped with a medium-voltage DC switching system, a power transformer, a rectifier 12-diode array and a controlled inverter, which is used for the feedback of the energy generated by the vehicles' regenerative braking.

3.4 VEDECOM/Qualcomm French Test site architecture

The French test site is located in Satory, near Versailles. The test facility is equipped with a substation that can provide up to 200kVA power. The French site will be used to test VEDECOM/Qualcomm in-road power transfer infrastructure system (see Figure 75 to Figure 78).

Figure 75: French Test site facilities

Figure 76: Overview of FABRIC track with 100 m charge zone (in blue).

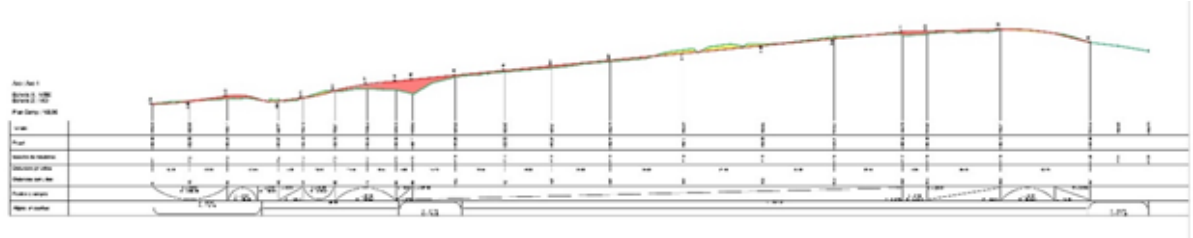

Figure 77: FABRIC track ground profile (height difference insignificant).

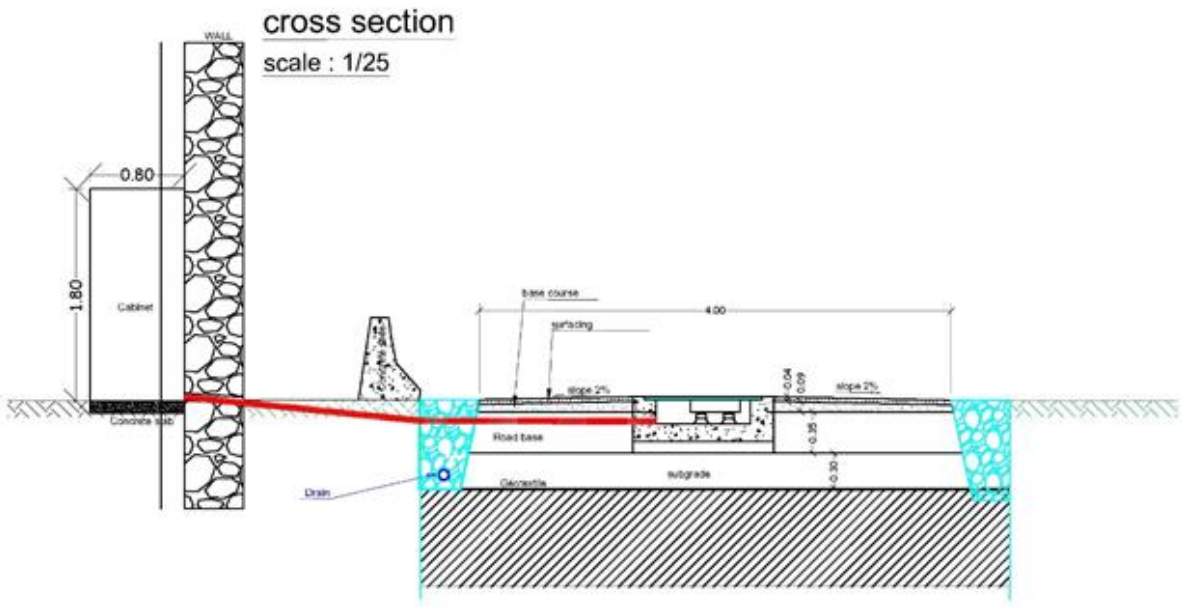

Figure 78: Cross section of the experimental road showing road side cabinet and in-road equipment.

In Table 3 the main parameters of the road layer in the French test site are reported.

Table 3: French test site parameters.

Test Site road layers	Unit	Comment
Thin surface layer depth :	4 cm	Asphalt concrete
Binder course depth	9 cm	Road base asphalt
Base course depth	35 cm	Treated base gravel
Subgrade	30 cm	Substratum (deep natural soil) Further to the excavation (80 cm deep), a test has been conducted on the natural soil which was found (following the French standards NF P94-117-1, “essai à la plaque”). That floor meets the lift required for the road type defined for the experimental track (class T3 according to applicable standard in France (NFP 98082)

3.4.1 High Level System Architecture

The Qualcomm Halo™ system to be installed at the VEDECOM test site in Satory (“Qualcomm System”) will operate at full power up to 60 km/h (16.6m/s). Power transfer may be tested at higher speeds if the test site road geometry allows. Each segment is rated at 25kW with power transfer per vehicle rated at 20kW. Multiple vehicles can receive power from a single segment at the same time but at a reduced power level. Figure 79 shows the test site layout for the Qualcomm System, each segment (in blue) consists of 14 “BAN

modules" (in orange), and each segment is connected to the same 400VAC feeder supply. It should be noted that the BAN modules are physically discrete with each module separately installed. The length of electrified test track is approximately 100 m, with 56 BAN modules.

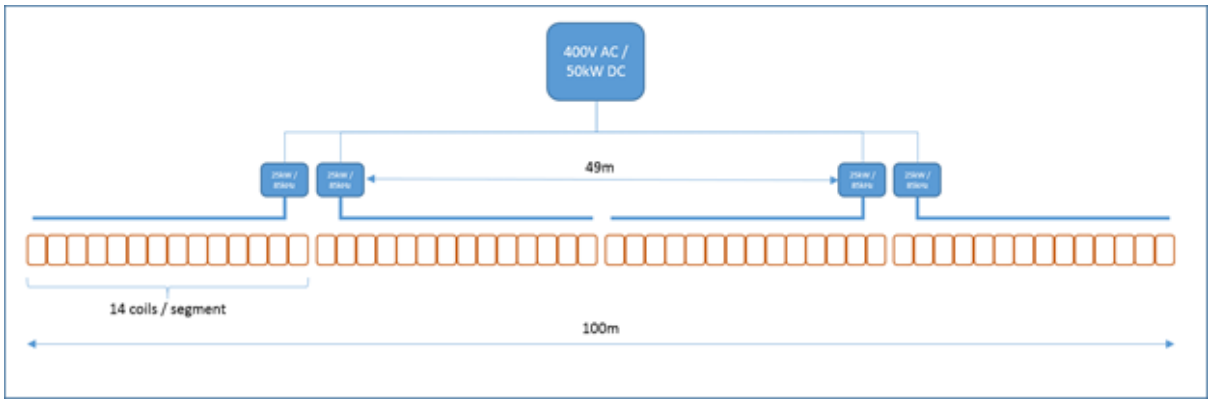

Figure 79: Test track layout for Qualcomm System

Table 4 shows the segment parameters for the Qualcomm systems; as segment is approximately 25 metres and whole test site consists of four segments.

Table 4: Qualcomm system architecture

Parameter	Unit	Comment
Distance between feeder transformers		Dependent upon cost-benefit analysis for specific installations.
Distance between road side equipment	Approx. 50 m	Two units located adjacent to each other approximately every 50 m.
Number of roadside equipment per feeder transformer	4	Dependent upon cost-benefit analysis for specific installations. One transformer will feed 4 units at Satory.
Length of a segment	Approx. 25 m	A segment is the set of loops or coils that is connected to a single road side equipment
Width of a segment	Approx. 0.45 m	
Depth of a segment	Approx. 0.15 m	
Gaps between segments (metres)	Approx. 0.02 m	
Number of loops or coils per segment	14	BAN modules per segment, not loops or coils

Parameter	Unit	Comment
Weight	Approx. 30 kg	Per BAN module
Positioning in the road	Centre of lane	The system is designed such that the vehicle coil is mounted, and the road coils are nominally, on the vehicle centreline. Note that the coil is off centre, 10 cm to the right of the trench at Satory. The road and vehicle centreline should also be offset 10 cm to the right of the trench for full alignment.
Length of a coil/loop	Approx. 1.71 m	Dimensions of BAN module
Width of a coil/loop	Approx. 0.45 m	Dimensions of BAN module
Depth of a coil/loop	Approx. 0.15 m	Dimensions of BAN module
Gap between coils/loops (m)	Approx. 0.02 m	Gap between BAN modules
weight	30 kg	BAN module weight
Distance below surface level	35 mm	To top surface of BAN module
Air gap	115±25 mm	Bottom of vehicle pad to ground surface level

3.4.2 Electrical system layout on Satory experimental road

Figure 80 shows a view of the Satory test site with positioning of different converters. AC (50 Hz)/DC is located in the “labo bunker”, DC/AC (85 kHz) are located along the track in the double cabinets. Each cabinet is equipped with elementary converter of 25 kW power.

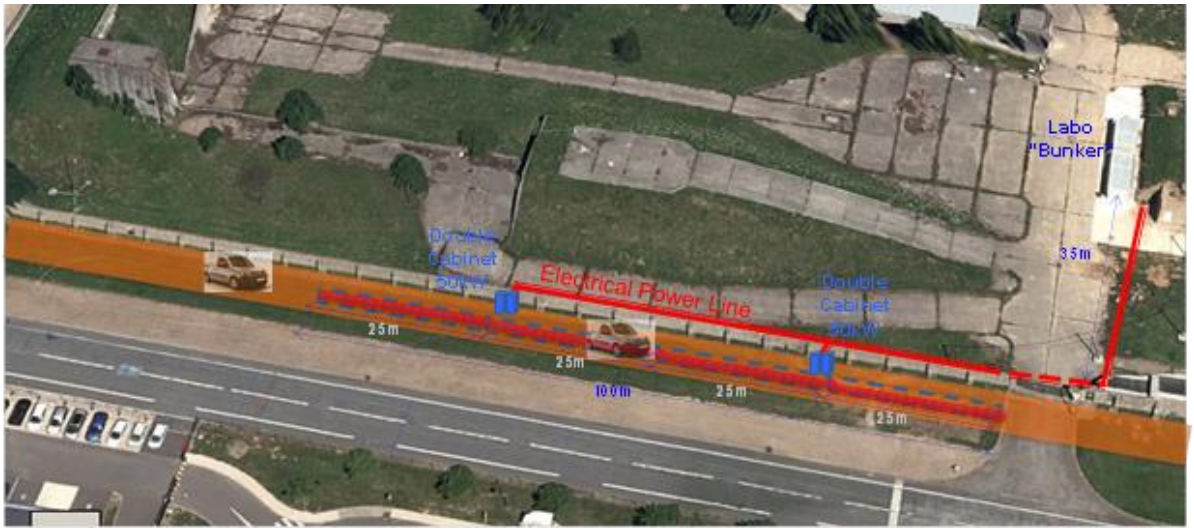

Figure 80: Photograph of the Satory test site

3.4.3 In-road Infrastructure

Segment level

Figure 81 and Figure 82 shows the drainage works; the drainage runs throughout the road and wireless chargers. The wiring and conduits between road side equipment and in-road infrastructure runs under the drainage pipes.

Table 5: Segment level drawings

Requirement	Response
In-road built schematics (overhead, cross section, side)	See Figures 5,6,7
Location of the shielding	No shielding in BAN module
Magnetic flux levels from centre line	Not available
Connectors between segments	Backbone cable per segment routed through conduit from roadside cabinet. Inductive power connection to BAN modules under road.
Provision of drainage	See Figure 78, Figure 79 and Figure 80

Figure 81: Schematic overview of the complete drainage system to water storm

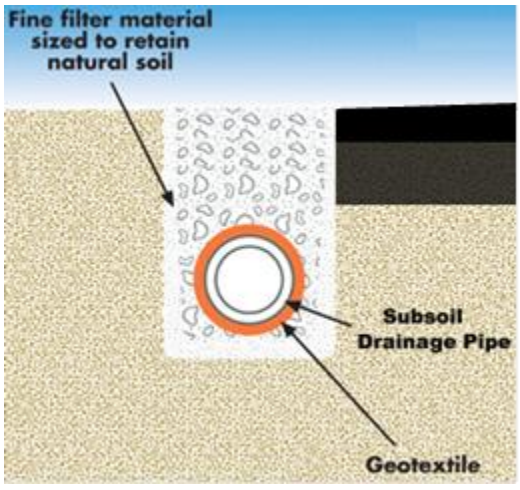

Figure 82: Schematic cross section of the longitudinal drainage system (on wall side)

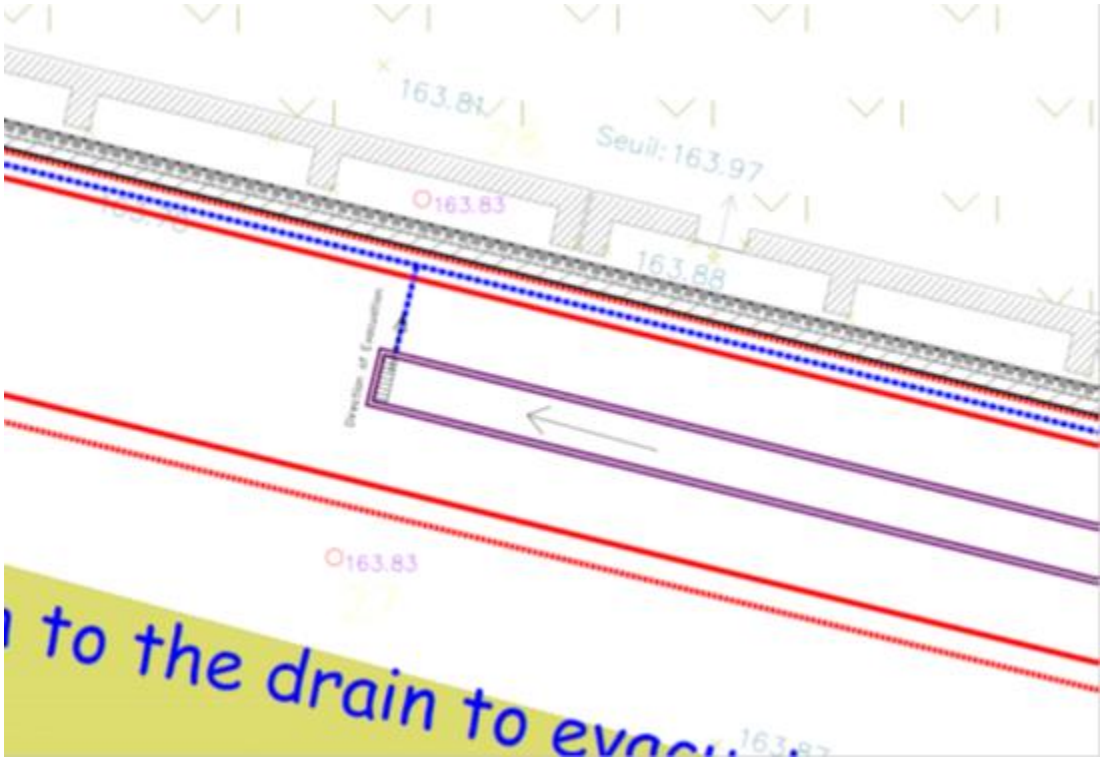

Figure 83: Schematic overview of the drainage system of the trench

Component level

Table 6 shows the parameters for in-road infrastructure.

Table 6: Component level parameters

Requirement	Response
Location of inductor coil/loops	Not available
Location of power cables	Backbone cable laid longitudinally under road adjacent to power transfer coils
Location of vehicle detector sensors	Detection is inherent to system. No additional sensors.
Prefabricated or built in?	Prefabricated BAN modules
Coils/loops thermal expansion	Conservative gaps and conduit sizes have been designed to minimise any thermal expansion concerns.

3.4.4 Road Side Infrastructure

Figure 84: FABRIC test track.Figure 84 shows the French test site layout. Figure 85 and Figure 86 show the location of the in-road equipment and the location of the road side equipment. The road side cabinets receive the power from 200 kVA power substation.

Road side infrastructure	Unit
Road side equipment height	Not available
Road side equipment width	Not available
Road side equipment depth	Not available
Weight	Not available
Total number of road side units	2 cabinets located approximately every 50 m
Maximum allowable distance between roadside and in road infrastructure	Less than 5 m

Figure 84: FABRIC test track.

Figure 85: FABRIC on-road section.

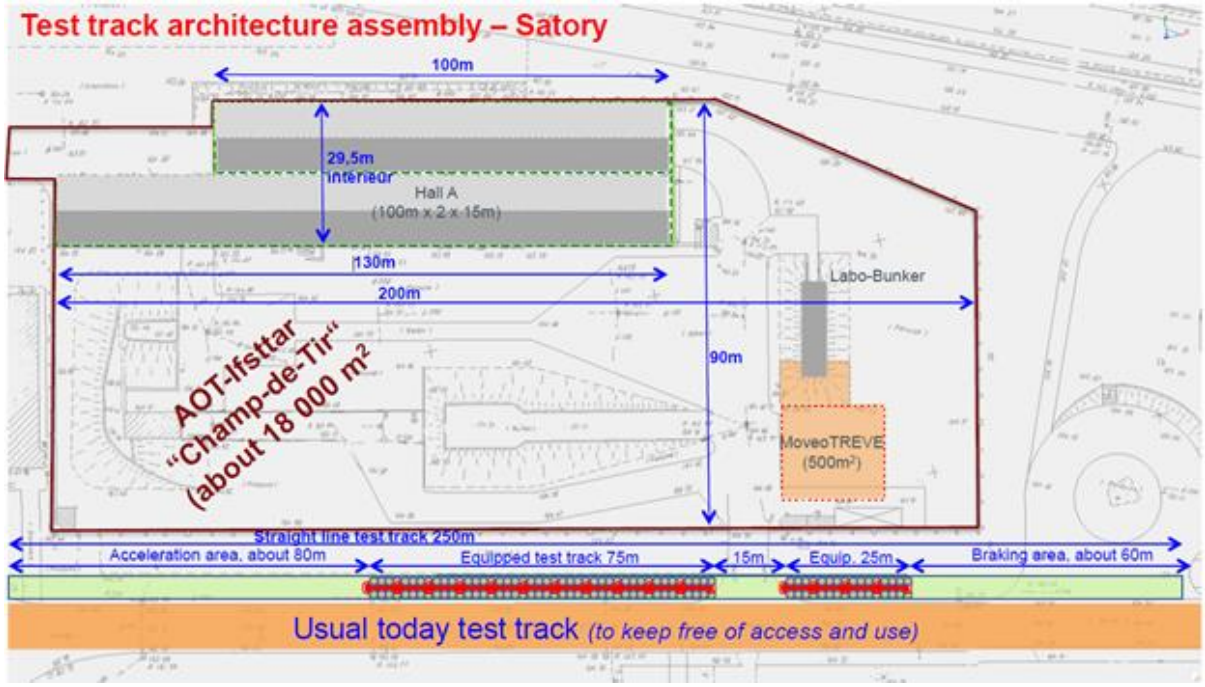

Figure 86: FABRIC on-road section schematic.

3.5 Safety and operational concerns considered for VEDECOM infrastructure

One starting point of the "subcontracting collaboration" with Qualcomm Halo was to agree and specify as clearly as possible the interfaces between the wireless power transfer charging system (infrastructure part). The important aspect was to consider was:

- Horizontal positioning

- Height levelling and adjustability
- Ferrous-free environment
- Easy access to the coil subsystem (BAN in Qualcomm Halo terminology) and power and control electronics (see Qualcomm Figure) ensuring magnetic resonance at fixed frequency and proper synchronization with the car in motion.

The Qualcomm in-road infrastructure was accessible; after six months of testing, the accessibility to the embedded subsystems has proved to be a great asset since many adjustment/repair actions were necessitated to fix or optimize the functionality of the system. The subsystems are waterproofed (IP 66), however, it was not designed to be buried in hot asphalt. This was judged to be unrealistic since the beginning of the project.

The adjustable height and horizontal location of the coils through plastic adjustable pillars has been very useful to set the BAN at the optimal height (maximizing efficiency for nominal power transfer of 20 kW).

The absence of ferrous material in the road was essential to guarantee proper functioning of the transfer system. Indeed, any presence of ferrous material has an impact on the resonance of the circuit, which significantly affects the functionality of the system (as experienced on the Italian test site with different kind of asphalt). Since the asphalt is not yet a controlled material with regards to presence of ferrous elements, the first approach to bury in asphalt these expensive prototype systems could have been unsuccessful.

3.6 Further Safety and operational concerns to be considered for future road infrastructure architecture

The power electronics, control systems and communication subsystems are located in the road side cabinets in order to minimise the size of the equipment which will have to be integrated in the road. Integrating the BAN subsystem (coils) into asphalt with durability objectives, would certainly be interesting. Positioning of the coils (height and horizontality); the road surface gets eroded by a few cm every year. The conditions of nominal functioning would certainly be affected. Therefore, the airgap should have a tolerance to ensure efficient power transfer due to changes in surface layer depth

One can assume future highway concept will be fully adaptable, automated and resilient as described in sources such as forever open roads (http://www.foreveropenroad.eu/?m=11). From this source, the future adaptable road should be based on a pre-fabricated/modular system that can gradually be implemented across Europe’s motorway, rural and urban road networks.

These fully automated roads will also incorporate a fully integrated information, monitoring and control system; communicating between road users, vehicles and operators. Wireless dynamic charging could be integrated amongst all these new functionalities.

From these prospective views, one should assume asphalt layer of at least 5 cm will still always be needed for noise and friction reasons. The coils should therefore be integrated in the middle of the road below the asphalt so that the distance between the road surface and the secondary coil remains about at 10 cm (reasonable). The upper surface of the coils should be (flush mounted) adjusted with the upper surface of the (concrete) modular road

whose structure shouldn't contain ferrous material at least 20 cm away from the surface of the blocks.

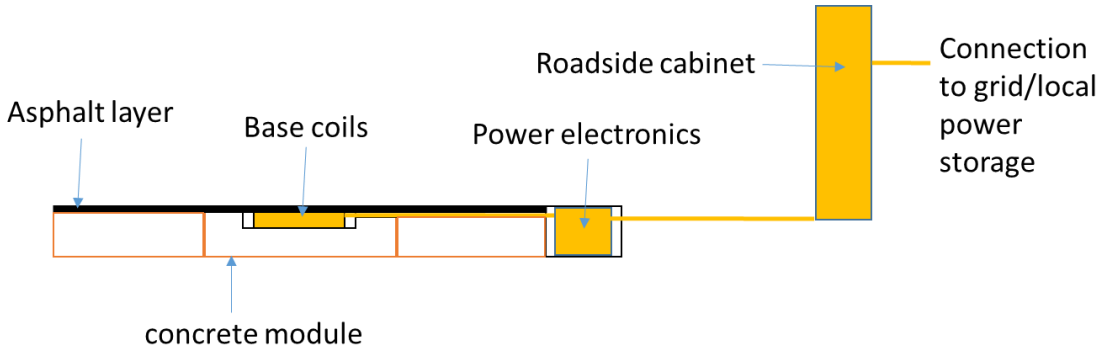

Figure 87: Possible concept for future dedicated lanes for wireless charging (deported power electronics)

The power electronics are located on the road side cabinets for good accessibility reasons and also not to overload the subsurface layer of the road with equipment.

The next phase in the prototype development is to take Bombardier's approach and study durability of the infrastructure; these studies can be carried out in a durability test facilities like IFSTTAR's in Nantes (http://35ans-manege.ifsttar.fr/pgm.php). This phase would eventually lead to an industrial concept validation.

One important aspect for in-road power transfer solutions is to install the in-road infrastructure quickly and efficiently as possible. This could mean designing a new machinery that can install these new system quickly and efficiently (similar to ALSTOM non-ballast railway systems http://www.railway-technical.com/track.shtml).

Finally, the installation of such complex new infrastructure would require the coordination of many administrative bodies (not less than 6 bodies have been identified in France as a first overview) such as:

- La Direction Générale des Entreprises (DGE) (http://www.entreprises.gouv.fr/dge)
- Direction générale des infrastructures, des transports et de la mer (DGITM) (http://www.developpement-durable.gouv.fr/direction-generale-des-infrastructures-des-transports-et-mer-dgitm)
- La Direction de la sécurité et de la circulation routières (DSCR) (http://www.securite-routiere.gouv.fr/la-securite-routiere/qui-sommes-nous/la-delegation-a-la-securite-et-a-la-circulation-routieres)
- Direction générale de l'énergie et du climat (DGEC). (http://www.developpement-durable.gouv.fr/direction-generale-lenergie-et-du-climat-dgec)
- Service Technique des Remontees Mecaniques et des Transports Guides (STRMTG)(http://www.strmtg.developpement-durable.gouv.fr/les-transports-guides-urbains-r28.html)
- CERTIFER (http://www.certifer.fr/)

3.7 Italian Test site architecture

The Test Site is a motor track, located in Susa Municipalities near the A32 motorway (Torino- Bardonecchia). The test track consists of 250 m, two lane pavement including uphill sections. The test track consists of two three-phase (400VAC, 32A) feeder points of a 600VDC power distribution that allow two vehicles to be charged at 22 kW simultaneously (see Figure 88 and Figure 89).

Figure 88: Italian test site facilities.

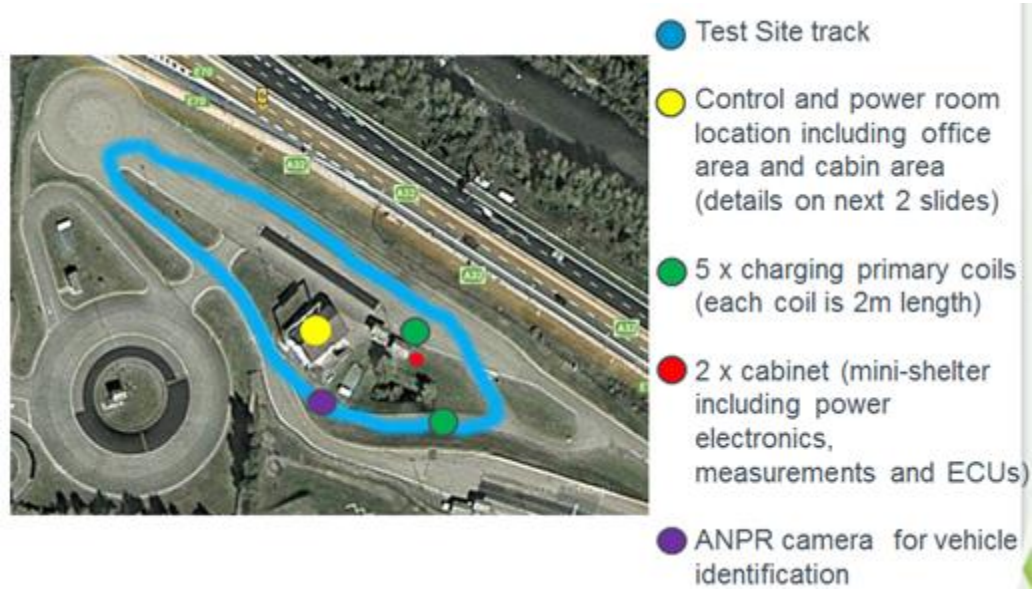

Figure 89: On-road charging test track.

It is envisaged that a switch board and electric power line as well as buried cables will be designed and installed in order to guarantee a plug & play approach for new technologies. The FABRIC test bed will be designed and constructed in accordance with safety guidelines and standards to provide two different infrastructures for electric cars and LDV dynamic charging.

Some features of the test site include:

- Traffic information capabilities;
- Management of electric vehicles;
- Vehicle detection;
- Evaluation equipment;
- Simulation of urban and extra-urban environment;
- Electric power supply: around 50kW.

The following pages provide more detail on the layout and infrastructure at the Italian test site.

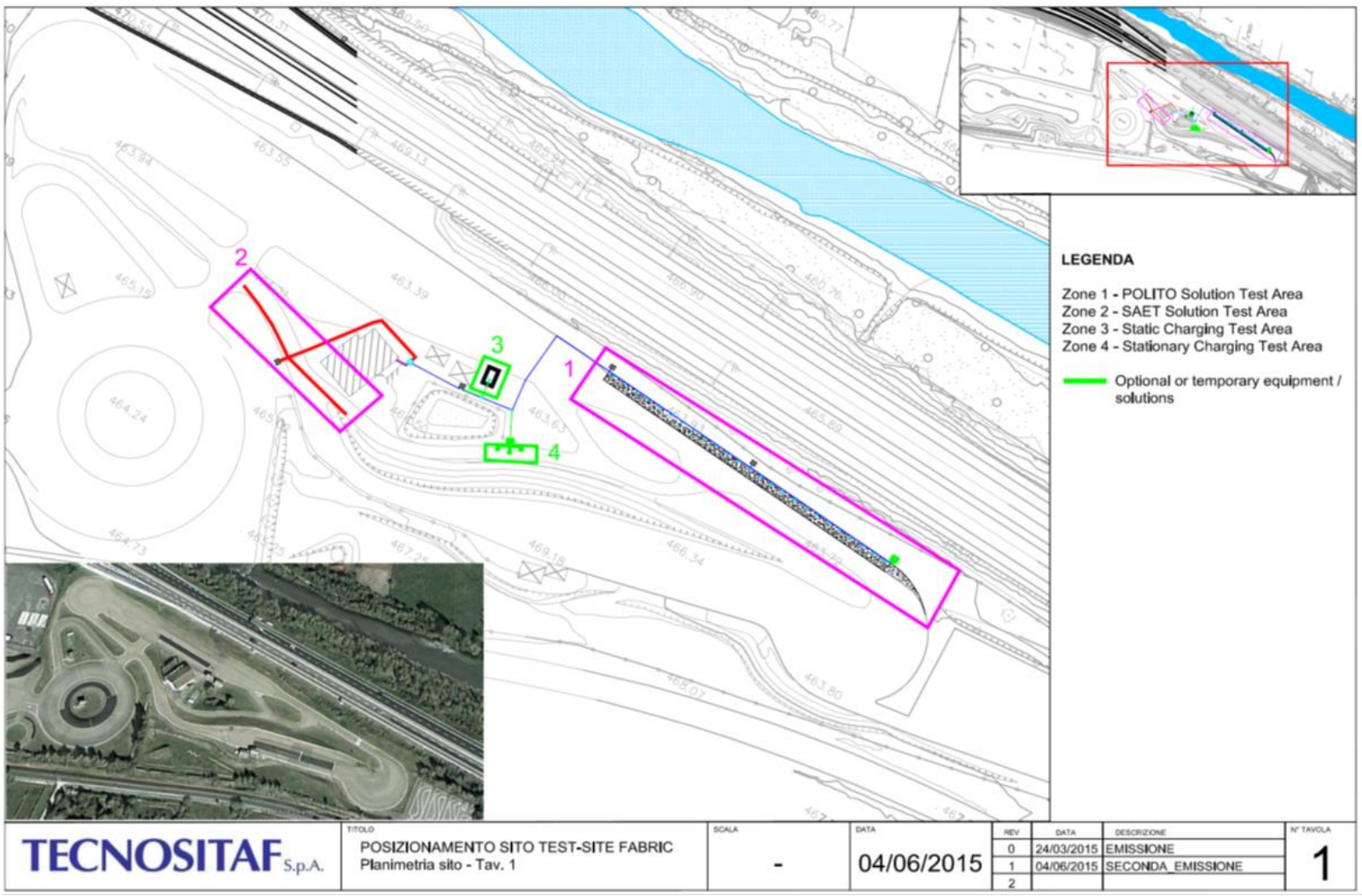

Figure 90: Proposed electrified section overview and possible road side equipment localization

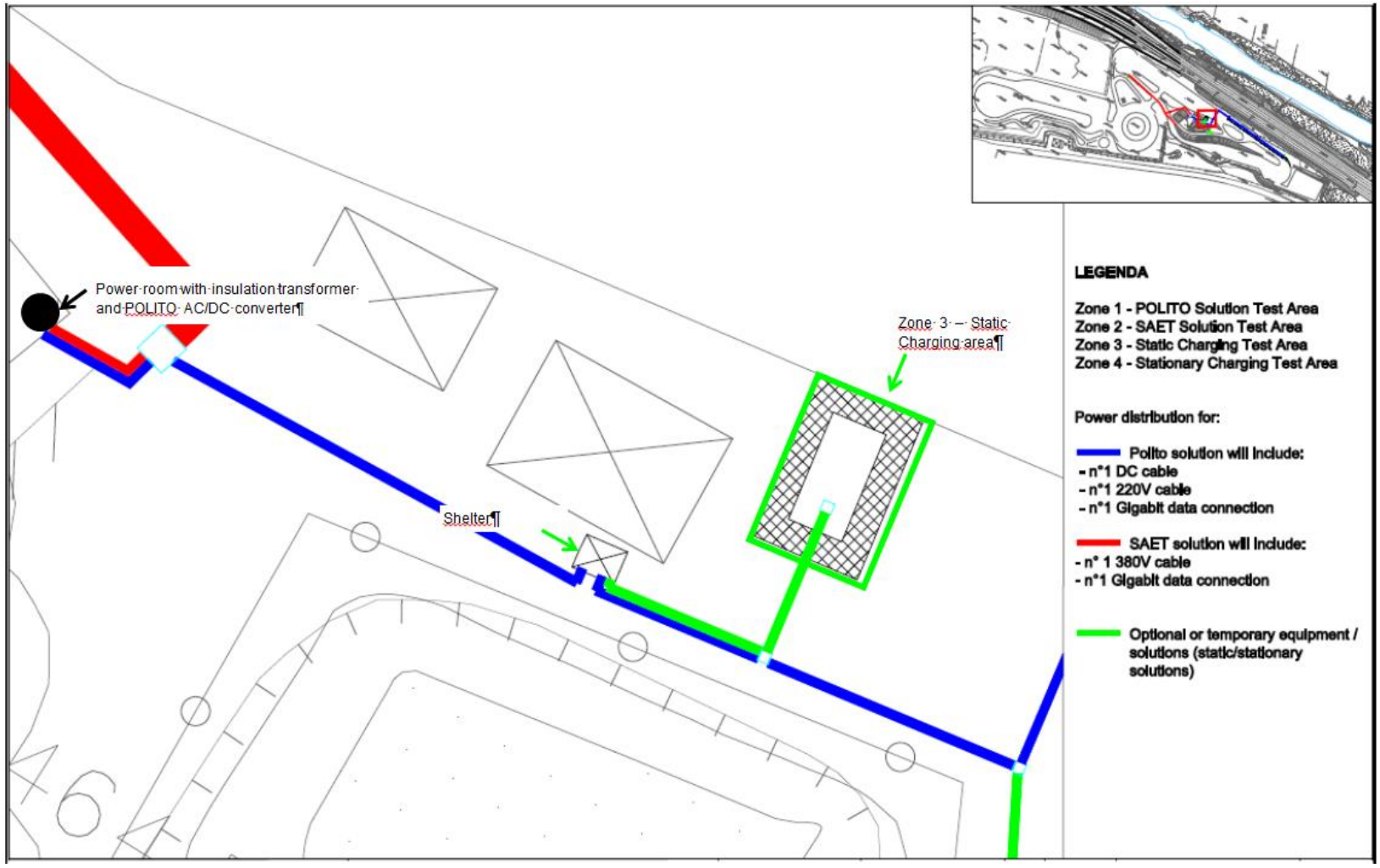

Figure 91: Power supply equipment location

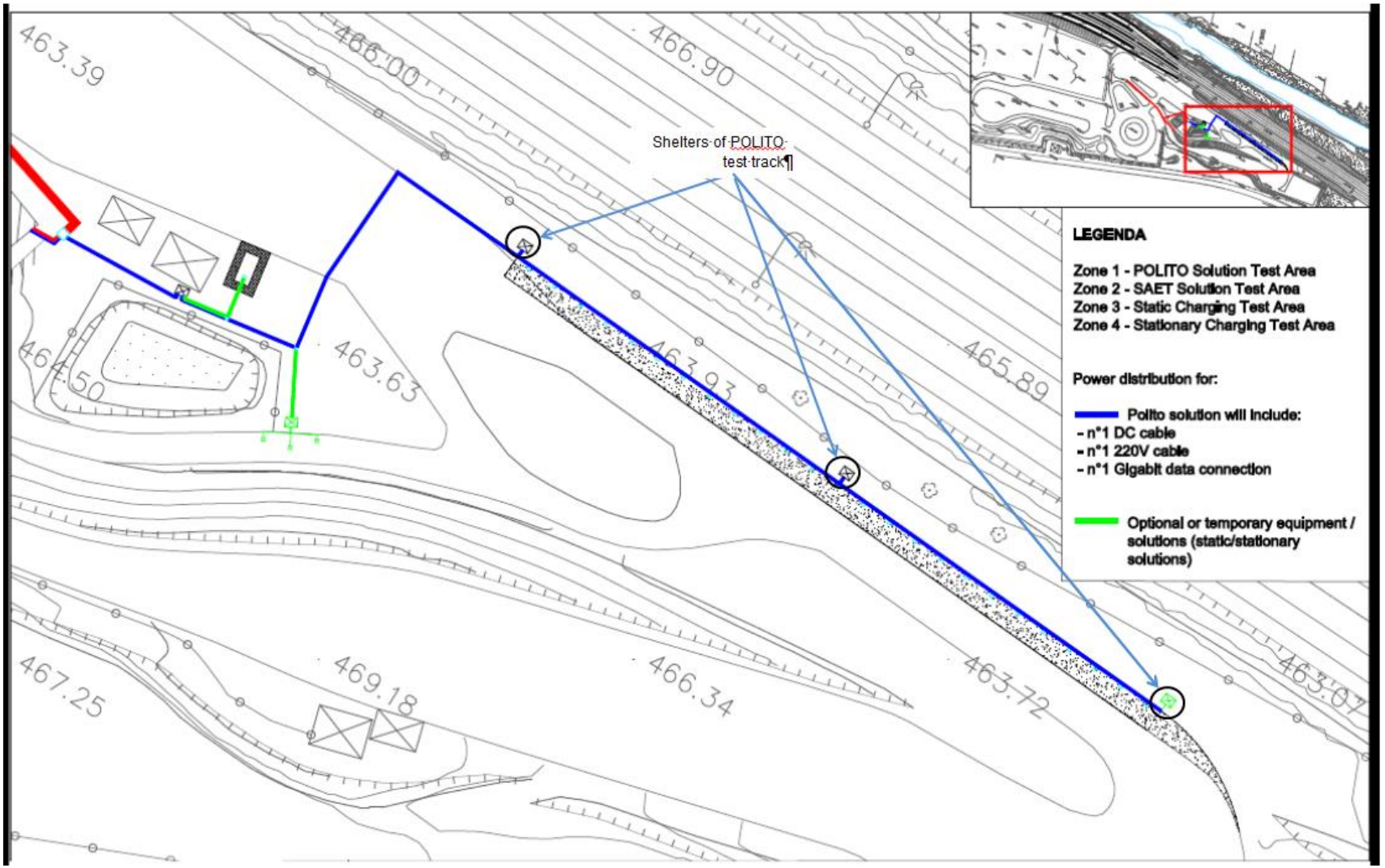

Figure 92: Polito solution charging area

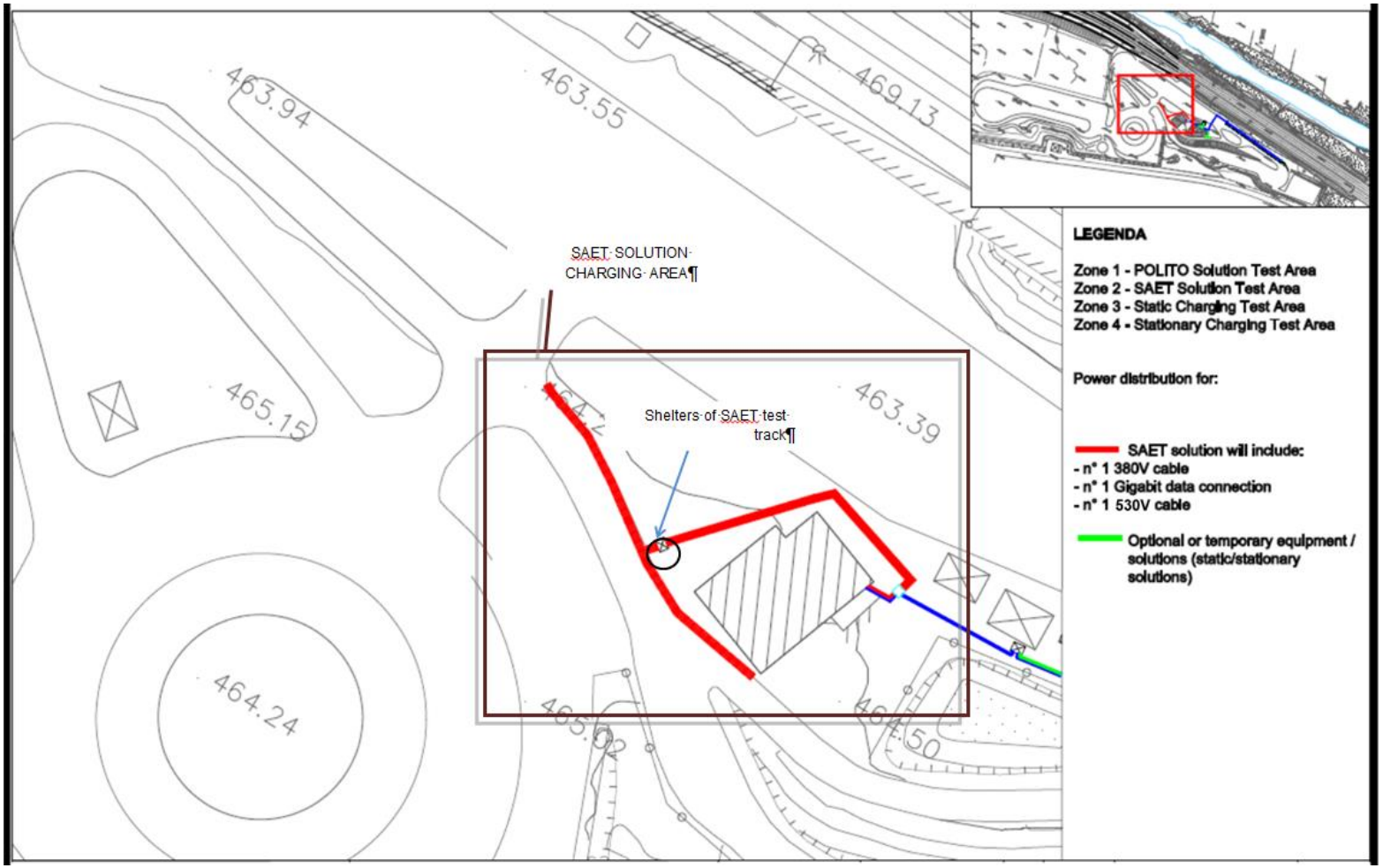

Figure 93: Saet solution charging area

Test site road layers (Tecnositaf)

Table 7: Italian site road layout

Test Site road layers	Unit
Road width	3.5 m to 7 m
Number of lanes	1 or 2
Test track length	100 m + 50 m
Speed	Max 70 km/h

The main features of the in-road equipment (Figure 94) are::

- Two tracks of 25 coils each;
- Each coil is approximately 2m long
- Distance between long coils more than 10 cm;
- Each coil and relative capacitor is set under 4cm of the level of the road;
- Each coil is supplied by a specific PE placed under the level of the road inside a plastic manhole and protected by a ip65 aluminium box;
- Each coil has its own Resonant Capacitor.

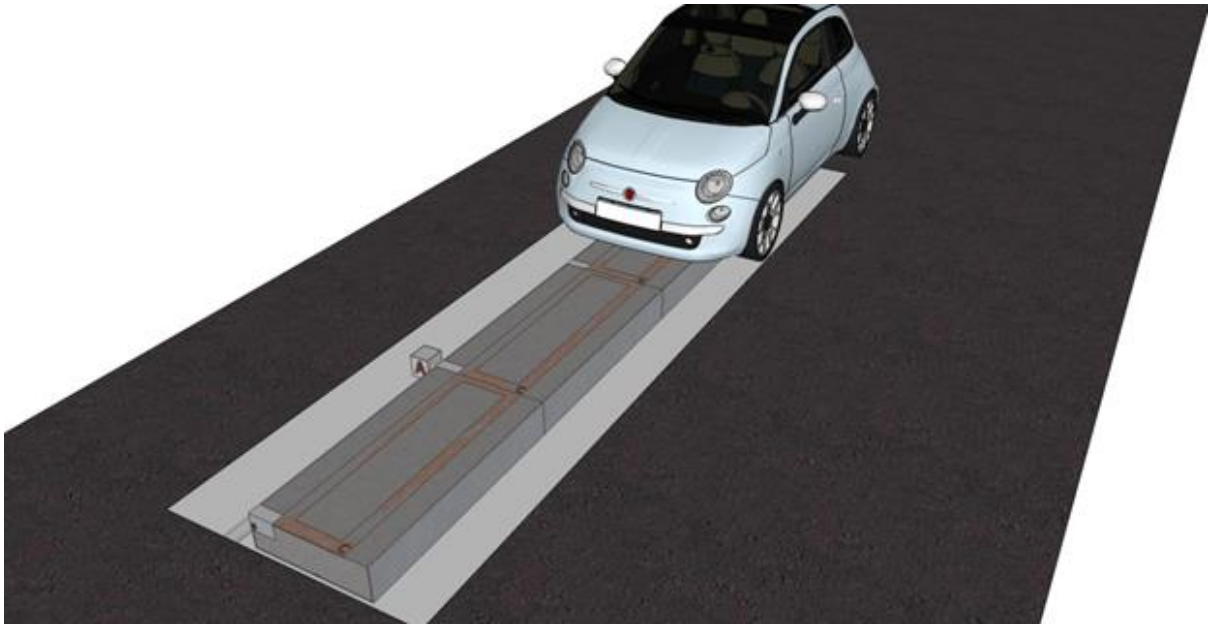

Figure 94: In-road charging at Italian test site

3.7.1 SAET Spa High Level System Architecture

The SAET SPA system is designed to operate at 80 km/h (22.2 m/s), and only one vehicle at one time can collect power from the segment, therefore the minimum time gap between two vehicles should be at least 1.125 seconds.

Figure 95 shows the test site layout for the SAET IPV (inductively powered vehicle) system. In this system, each segment (shown in red) is a loop coil (shown in orange), and each loop is connected to the 400VAC. A single feeder point provides power to a single segment which consists of 20 coils. The coil only switches on when there is a vehicle over it, so the feeder supplies power to approximately 2-3 coils at a time, each coil is rated at 40kW.

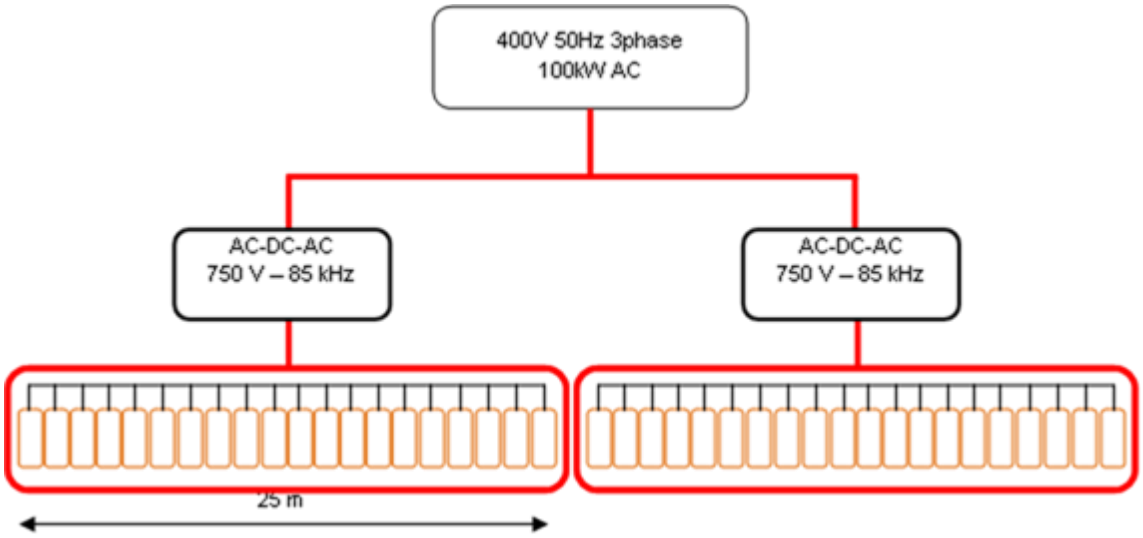

Figure 95: Test site layout for SAET SPA system.

The physical parameters for each segment and coils are presented in Table 8. The roadside equipment is housed in two cabinets; the physical dimension of a cabinet is 1 x 0.75 x 2 m (HxWxD).

The distance between the feeder transformer and the roadside inverter is approximately 100 m.

Table 8: CRF on-road solution parameters.

Parameter	Unit
Distance between road side equipment	25 m
Number of roadside equipment per feeder transformer	2
Width of a segment	1.3 m
Depth of a segment	0.05 m
Gaps between segments (metres)	0.25
Number of loops or coils per segment	20
Weight (kg)	30 kg for each coil (copper + aluminium + ferrite)
Positioning in the road	Centre of the carriageway
Length of a coil/loop	1 m
Width of a coil/loop	1.3 m (reduced with respect the previous 2 m)
Depth of a coil/loop	0.05 m
Gap between coils/loops (m)	0.25 m
Distance below surface level	5 cm
Air gap	20 cm

3.7.2 POLITO High Level System Architecture

The POLITO system is designed to optimally operate above 30 km/h. The solution consists of 2 branches of 25 coils individually fed by DC/HF converters. Each coil has a DC/HF converter and the distribution is at 600VDC. The feeder can be connected in parallel on the same cable (see Figure 96).

In addition, a supercapacitor solution will be provided to balance the possible load variations.

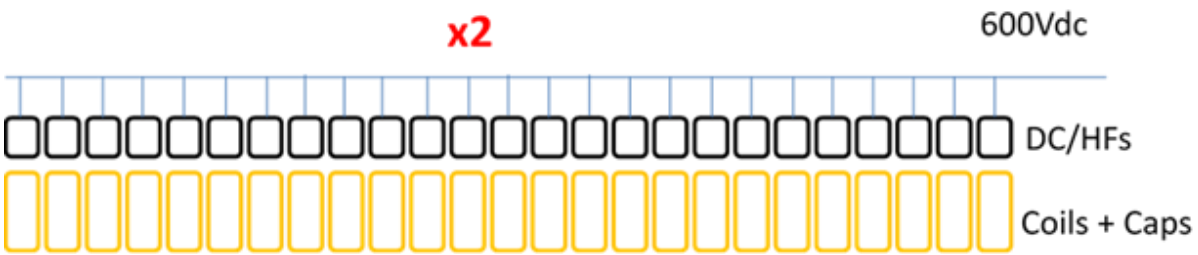

Figure 96: POLITO system test site layout.

The physical parameters for the segments and coils in POLITO on-road solution are presented in Table 9.

Table 9: POLITO on-road solution parameters.

Parameter	Unit
Length of a segment	50 m
Width of a segment	0.5 m
Depth of a segment	0.04 m
Gaps between segments (metres)	0.1 m
Number of loops or coils per segment	25
Positioning in the road	Central
Length of a coil/loop	2 m
Width of a coil/loop	0.1 m
Depth of a coil/loop	0.02 m
Gap between coils/loops (m)	0.1 m
Distance below surface level	4 cm
Air gap	20 cm

3.8 Scania High Level System Architecture

The Scania wireless power transfer system operates at vehicle speeds of 90 km/h (25 m/s). The system is installed at the Bombardier test site in Mannheim. The test track is 300 m long, consists of 4 segments of 20m wireless loops. Figure 97 shows the test site layout, each segment (shown in red) consists of one wireless loop (shown in orange), and each segment is connected to a 750VDC power supply. The 750VDC cable runs along the roadside and it connects to the power box every 40 m.

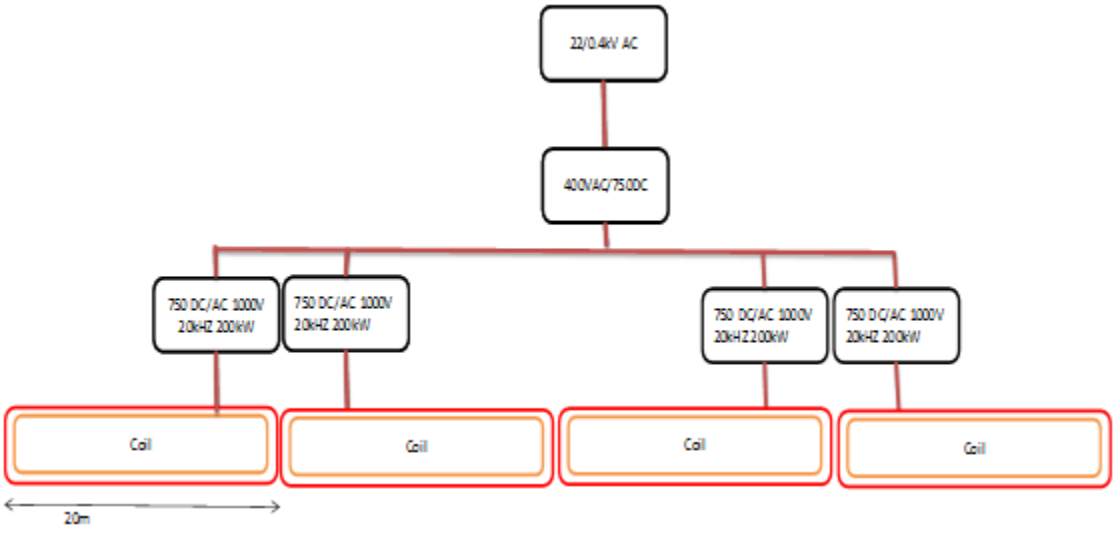

Figure 97: Scania test track system.

Figure 98 shows the connection layout in a full deployment scenario, where the system can be installed in the road at a large scale.

The proposed test track in Södertälje, Sweden, is 300 m long, consists of 4 segments of 20 m wireless loops.

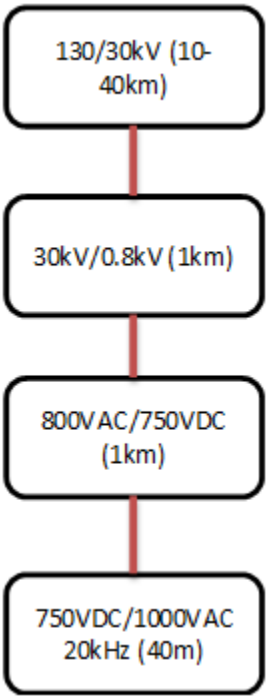

Figure 98: Full deployment layout for Scania system.

The physical parameters for the segments and coils are presented in Table 10.

Table 10: Scania on-road solution parameters.

Parameter	Unit
Distance between feeder transformers	
Distance between road side equipment	40 m
Number of roadside equipment per feeder transformer	4
Length of a segment	20 m
Width of a segment	0.8 m
Depth of a segment	
Gaps between segments (metres)	
Number of loops or coils per segment	1
Weight (kg)	
Positioning in the road	Central
Length of a coil/loop	20 m
Width of a coil/loop	1 m
Depth of a coil/loop	
Gap between coils/loops (m)	
Distance below surface level	4 cm
Air gap	25 cm

Note that the SCANIA system will not be tested in FABRIC, but as a project partner, results of previous trials involving the SCANIA system will be made available to the project team for comparison purposes.

3.9 Volvo ERS conductive system architecture

The Volvo's Electric Road System (ERS) transfers power from conductive in-flush rail to the vehicle via moveable arm. The minimum operation speed for the vehicle is 60 km/h (17m/s). Figure 99 shows the test site layout for the ERS. In this system each segment (shown in red) consists of one conductive rail (shown in orange) and each segment is connected to a 750VDC power supply. The 750VDC cable runs along the roadside and it connects to the power box every 44 m.

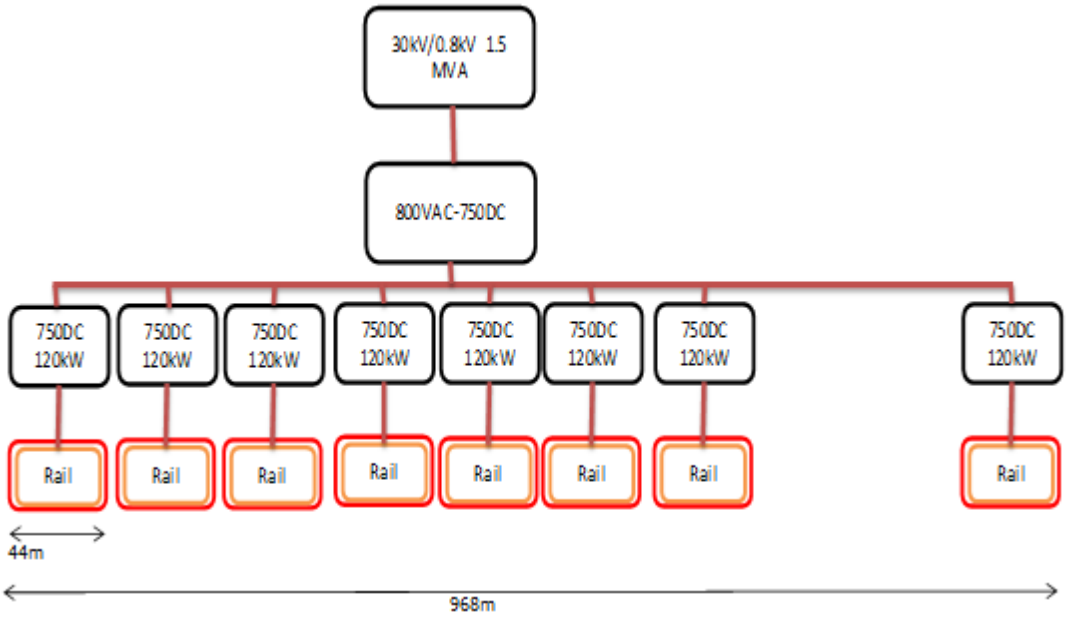

Figure 99: Test site layout for Volvo ERS.

Figure 100 shows the connection layout in full deployment scenario, where the system can be installed in the road in large take up levels. As shows the connection from the grid is from 132 kV feeder point at every 10-40km (dependent on demand). 30kV cable runs along the road side and every 968m, the voltage is transformed down and converted to 750VDC, this power supply runs along 968m connecting to the power transfer segment every 44 m.

Figure 100: Full deployment layout for ERS system.

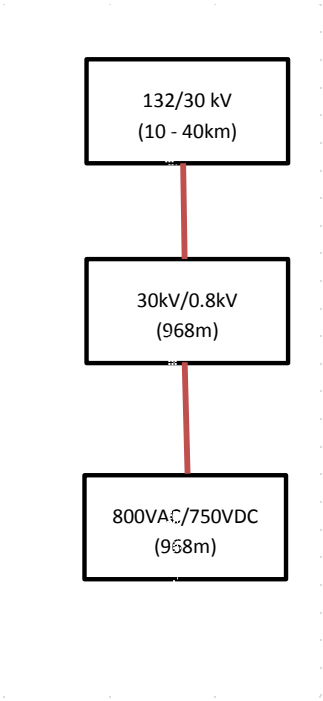

The physical parameters for the segments and coils are presented in Table 11.

Table 11: Volvo on-road solution parameters.

Parameter	Unit
Distance between feeder transformers	968
Distance between road side equipment	44 m
Number of roadside equipment per feeder transformer	22
Length of a segment	22 m
Width of a segment	
Depth of a segment	
Gaps between segments (metres)	
Number of loops or coils per segment	
Weight (kg)	
Positioning in the road	Central
Length of a coil/loop	
Width of a coil/loop	
Depth of a coil/loop	
Gap between coils/loops (m)	
weight	
Distance below surface level	
Air gap	

Note that the Volvo system will not be tested in FABRIC, but as a project partner, results of previous trials involving the Volvo system will be made available to the project team for comparison purposes.

3.10 Architecture Definition

3.10.1 Requirements

Grid

The current solutions are connected to three-phase 400V AC substation feeder points. However, the current solutions are primarily experimental and mainly used in controlled environments where the installation is used by a small number of vehicles. However, as the solutions become more commercial and installed at large scale other forms of connections must be considered due to the higher demand levels, stepping up from kW to MW range. . A similar approach to rail is proposed where the connection point is at MV (medium voltage) or

even HV (high voltage) feeders. This approach would also isolate the in-road power transfer infrastructure from the domestic supply.

Local electrical energy storage systems are proposed to be connected directly to the 750V DC line, in order to smooth power peaks and reduce power ratings of the feeding transformers and converters. This has already been demonstrated for light rail. The grid installation should adhere with all the standards and regulations required by regulators such as EMF, Residual Current Device (RCD), Electrostatic discharge (ESD) etc. Please see section 4 for grid installations.

Road side cabinets

The road side equipment can be installed above or underground depending on availability of space. In order to meet needs and requirements, the road side cabinets should be:

- Grouped together where possible;
- Sited well above flood level;
- Behind safety barriers where possible;
- At least 1 m between edge of the carriage way and cabinet.

The roadside cabinets should not obstruct the drivers' or pedestrians' view. The required distance behind safety barriers can be as much as 2 m for steel VRS, though if the VRS is concrete, the roadside equipment can be placed right up against it. In populated areas the road side equipment should allow for at least 1.2 m clearance on footpaths, up to 2 m in high pedestrian flow sections [6] [7].

It is also important to ensure that the roadside equipment's are electrically safe. Therefore roadside cabinets should comply with BS EN 12767, where the electrical connections are isolated during an impact. Therefore it is essential to use passively safe road side cabinets. Pull-out plugs or connectors that isolate during an impact can be used between inroad coils and road side equipment, so in a case of an accident the cables disconnect safely. The road side cabinets should be safely grounded.

In road equipment

On a busy motorway the time gap between two vehicles can be as low as 1.1 seconds, which at 80 km/h results in the distance between two vehicles being 20 m. The in-road power transfer system should only be active if there is a compliant vehicle over it. Therefore, an active segment should not be greater than 20 m and the power transfer system should switch off when the traffic speed is below a certain minimum. Active detection of vehicle positioning and spacing will allow longer segments, but will increase the incidence of segments needing to be disabled due to the presence of non-compliant vehicles over the charging equipment. The in-road equipment is normally positioned in the centre of the running lane.

However, at low speeds such as urban or congested driving; the 20 metre active coil could results in exposure of EMF to the public or other vehicles. Therefore; a segment could be up to 20 metre long but each segment should consist of smaller coils (ideally no longer than the length that ensures a car is over it every time is active) in order to make sure that the coil is only active if there is an approved vehicle over it. The in-road equipment should consist of

power transfer coil, detections sensors and necessary communication equipment. All the equipment where possible should be located at the road side in order to ensure easy repair and maintenance without having to strip off the parts of road and expose workforce to a live traffic. .

The length of the coils that can be activated is different from motorway conditions; the speeds in the city are very low and the gap between vehicles is smaller. Therefore, exposed active coils can pose a safety risk to surroundings; therefore the coils should be covered by a compatible vehicle when active. This will require shorter coils and locating secondary coil on the vehicle at the centre of the vehicle chassis rather than the front or the end. The length of an A-segment mini car can be approximately 3 m; this means that the primary coil must be 1/3 (1 metre) of vehicle length to ensure that primary coil is fully under a vehicle when active. Also, the inroad infrastructure is equipped with magnetic field shielding material to ensure that the magnetic field is only directed towards the secondary coil, this approach improves the efficiency of the power transfer and also reduces the EMF exposure to surrounding environment.

The coils should also be insulated from water and dust ingress therefore it might be necessary to encase or cover the coils with an insulating material. The insulation material should stop and dust or water getting in contact with the coil but at same time it should not have an effect on power transfer rate and electromagnetic induction; therefore any insulation material that is ferrous or interfere with the magnetic induction should not be used.

On-road Power Transfer Architecture

This section of the report presents an overall architecture for an on-road power transfer solution. Figure 101 shows the on-road power transfer architecture for Fabric solutions. There is no one architecture that describes all the on-road power transfer solution. At very high level there is a substation supplying power to roadside equipment; the roadside equipment converts grid power to the form that can be transferred by the equipment installed in the road and the equipment in the road senses the vehicle and transfer power when necessary. The location of some subsystems can change between in-road or road side depending on the solution providers; such as switches and compensation capacitor; these two could be either located on the roadside or in the road. The sensors that sense the vehicle and determine whether to switch on a coil is usually embedded with the coils; however these sensors can be a separate system such as cameras that are located on the roadside or above the road. Overall there is no one architecture to describe an on-road power transfer system and where each subsystem is located; with that said there are fundamental sub systems that all on-road power transfer systems have in common such as a substation, converters, compensation circuit, sensors, switches and power transfer coils/rail/wires.

The grid provides three phases 400VAC to a number of rectifiers and inverters, which converts AC to DC voltage and back to high frequency AC. The converters and control electronics are located at the roadside. The in road equipment consists of a number of coils that is connected to a roadside cabinet; one or more coils per segment can be switched on

at the same time depending on the solution design, power rating of the inverters and supply from the grid. The in-road equipment consists of coils, sensor and switches (switch can be located at the roadside depending on the system); the purpose is to minimise the amount of equipment to be buried in the road in order to avoid any excavation in case of repairs and maintenance.

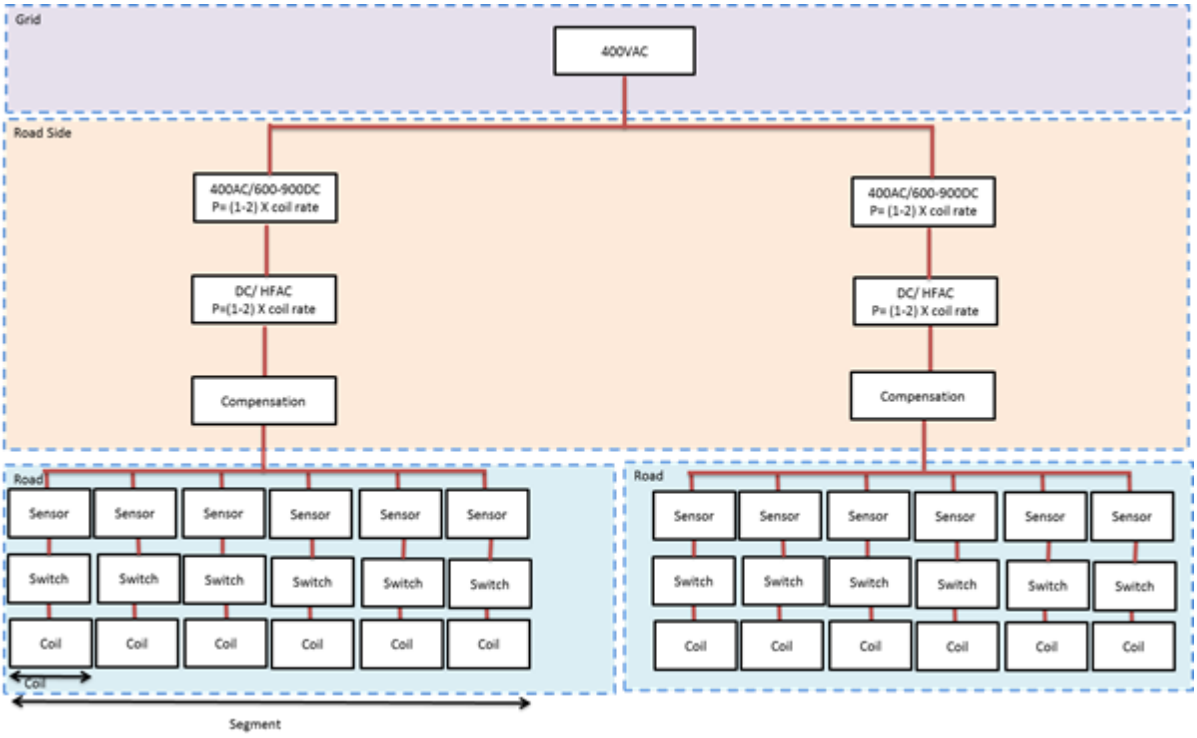

Figure 101: Power Transfer system Architecture

3.11 Installation

In this section we analyse the installation architecture for in-road wireless power transfer systems. Where regulations are referred to, these will concentrate on the UK. It is expected that details may differ in other countries, but the main points of the architecture are not expected to change substantially between jurisdictions.

3.11.1 Typical road construction

The road is made up of several layers (see Figure 102 in order to increase its longevity and improve the ride quality for the vehicles. These layers are:

- **Surface course**: Also known as wearing course, this is the top layer of the road surface. The surface course consists of asphalt, and it is designed to be water proof, durable, have high skid resistance and not to deform under the weight of the vehicles.
- **Binder course**: This is a load distribution layer of the pavement, helping to spread the load of traffic onto the base course evenly. It is designed to be stable and durable.
- **Base course**: Also known as the road base or base. This is the main load distribution layer of the road.

- **Granular base**: This base is a load bearing layer below pavement layers. It provides support and acts as a foundation.
- **Subgrade**: This is natural ground material that the road is built on.

The total thickness of the binder and base course can vary between 0.1 and 0.4 m. The binder course and base course are ideal locations to install in-road equipment.

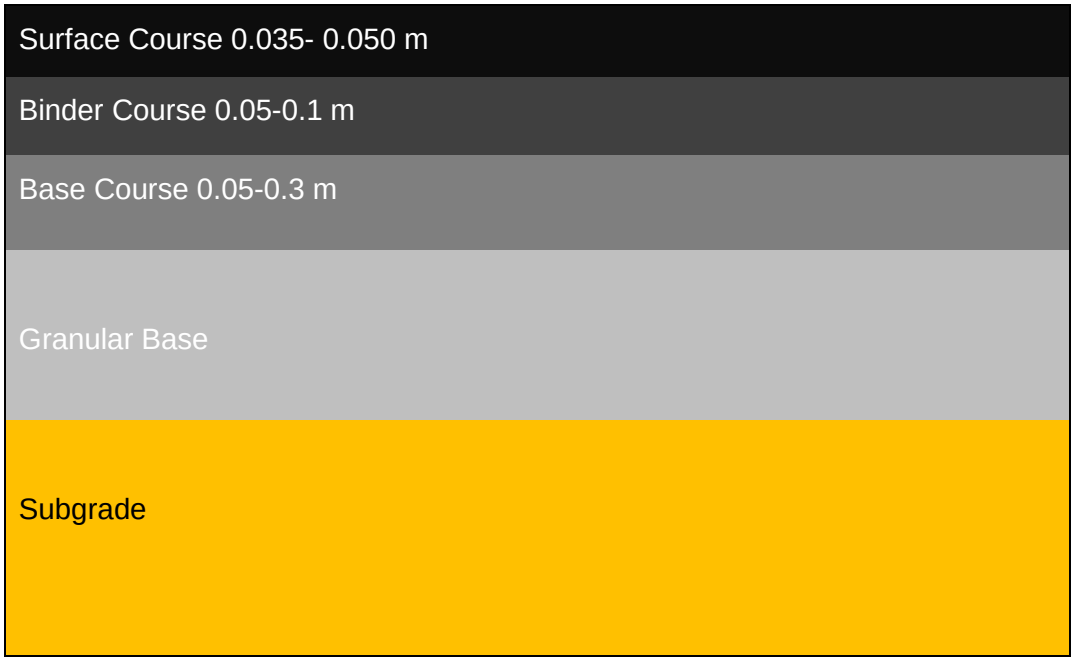

Figure 102: Pavement layer.

3.11.2 Layout

The two examples below show two very different road layouts. Due to the range of locations in which roads are built, many other layouts are possible, but these should be considered limiting cases of maximum available space and traffic speed, and minimum available space and traffic speed.

Primary roads, motorways and dual-carriageways

Figure 103 shows a typical motorway cross section in one direction. This particular example consists of four lanes plus a hard shoulder. The ideal location for in-road power transfer systems is lane 1, if a single lane is electrified. The roadside equipment cabinets can be installed on the verge, behind the vehicle restraint system (VRS); the distance between barrier and cabinet is dependent on a number of factors such as the speed of the traffic, strength or VMS, availability of the verge; a safe distance should be sufficient enough for the solution to be safe and practical; surveys will identify sufficient gap between VMS and road side equipment. The cable trough can be built between the edge of the hard shoulder and the beginning of the verge. [8]

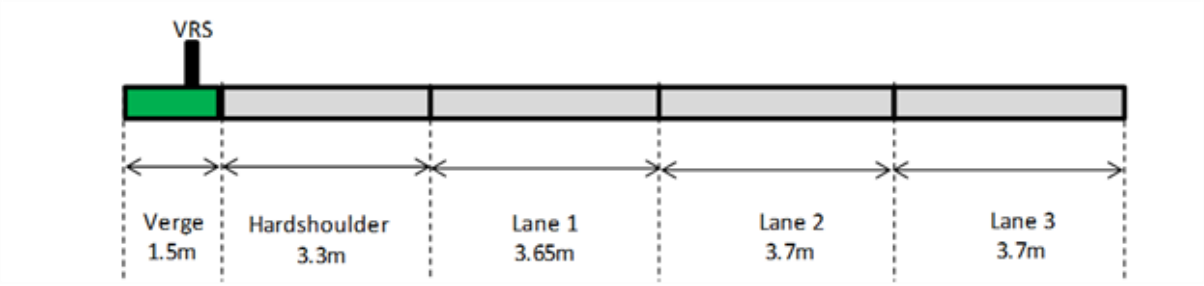

Figure 103: Motorway cross section.

Figure 104 shows an on-road power transfer system in the primary road. Red units show additional on-road power transfer infrastructure such as an in-road power transfer module, road side equipment, troughs and conduits. The on-road power transfer system is located below the surface course, in order to allow surface maintenance treatment or replacement; also to ensure the skid resistance of the road is unaffected by in-road equipment; this approach minimises the safety concerns for installing power transfer equipment in the road. Where possible, all roadside cables and connections should be placed under the bound. The trough is also used to provide a route between road side equipment and the distribution network transformer.

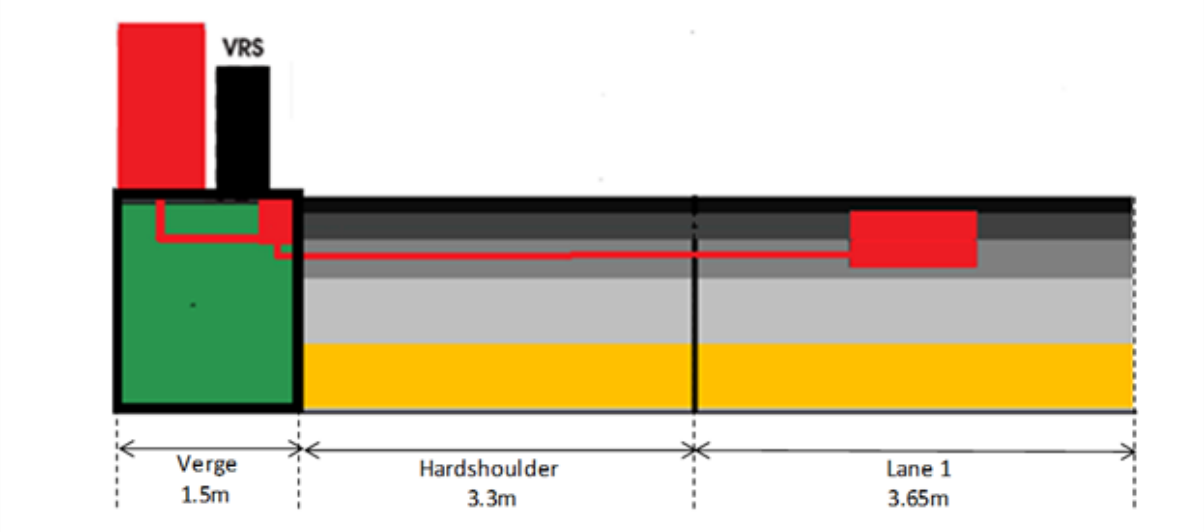

Figure 104: Motorway cross section with on-road power transfer system.

Figure 105 shows an on-road power transfer system joining two segments together. This:

- Reduces the number of toughing requirements;
- Allows two lots of road side equipment to be built on the same site;
- Increases the gap between road side equipment to two times the segment length.

The distance between in-road equipment and road side equipment is approximately 5.9 m. The gap between road side equipment can be as high as 40 m if each segment is connected

to the road side equipment. Note that the distance between roadside equipment and inroad equipment could have a significant impact on the design of the solution; manufacturers should ensure that cable distance is considered and measures are taken to ensure that the solution operates at rated power and required efficiency and it is safe.

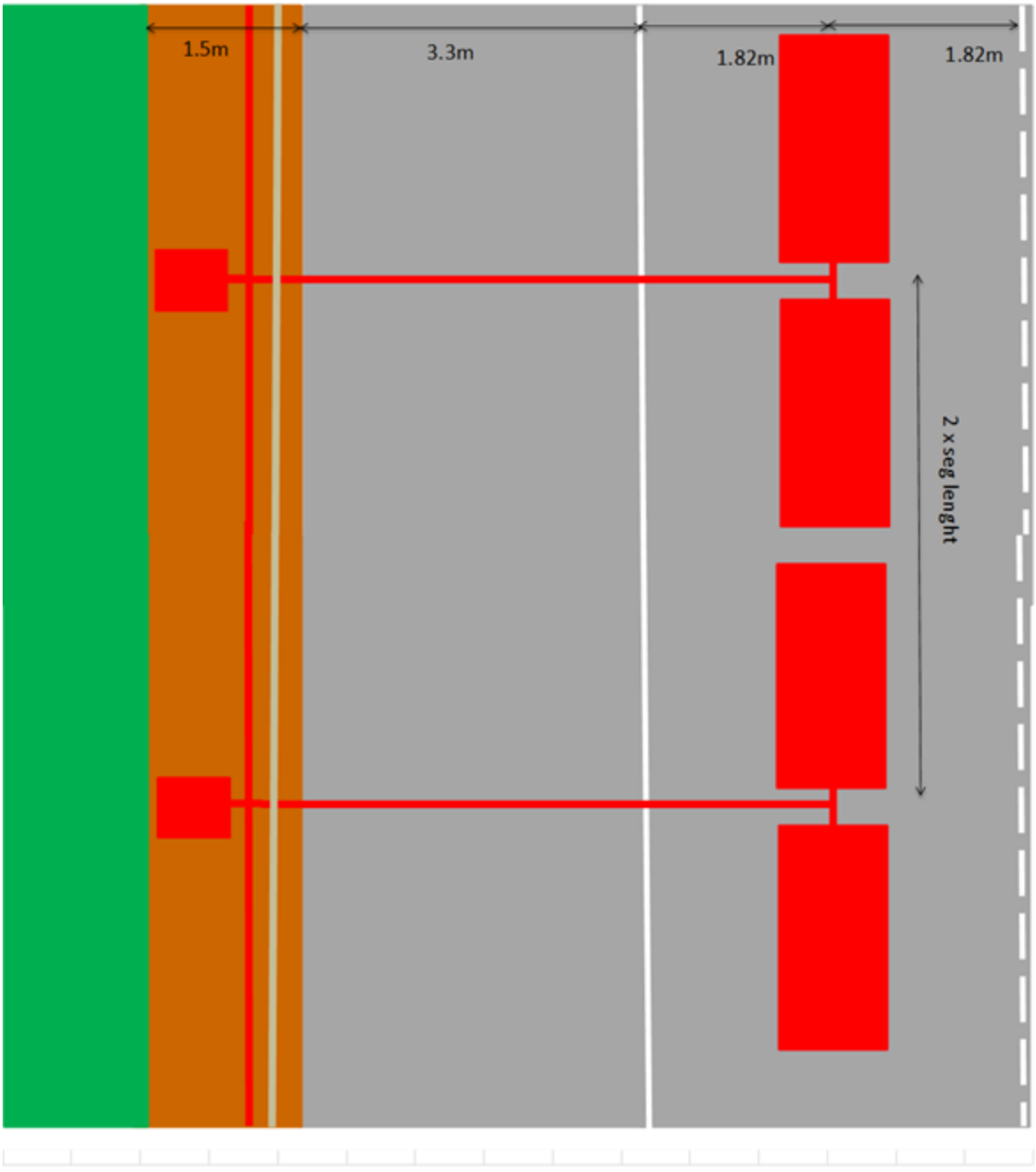

Figure 105: Overview of on-road power transfer system.

Urban roads

Figure 106 shows a sample urban two-way street layout. Where there is limited space available for road side equipment, it can be installed underground provided it does not interfere with existing utilities and drainage design [9].

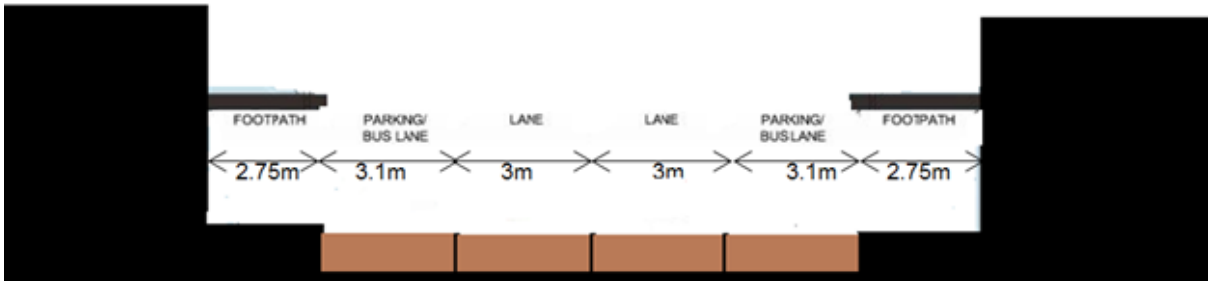

Figure 106: Urban street layout.

The installation of on-road power systems in built up areas may require alternative arrangement for road side equipment. Figure 107 shows the on-road power transfer system in built up areas. The road side equipment is under the kerb due to limited available space on the surface.

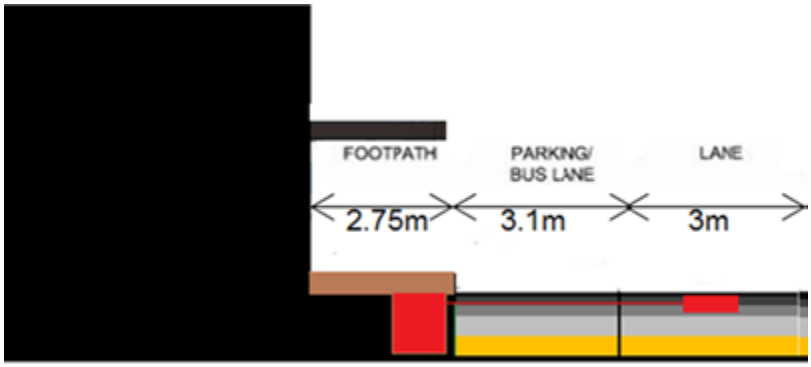

Figure 107: On-road power transfer system in urban areas.

Figure 108 shows the overview illustration, the distance between the road side equipment and in-road charger is 5.1 m assuming first lane is a bus or parking lane. However, if the first lane is open to the traffic, then the distance between the road side equipment and in-road equipment can be as low as 2.1 m.

The road side equipment can be installed over ground if:

- The minimum clearance for pedestrians is 1 m;
- The kerb width is greater than 2 m.

The cabinets may need to be redesigned to provide maximum clearance on the pedestrian path. It is ideal to use wider and shorter cabinets rather than square and / or tall cabinets in order to maximise the space for pedestrians and ensure good visibility. The tall cabinets could restrict visibility of drivers and pedestrians. Local government street furniture guides should be implemented.

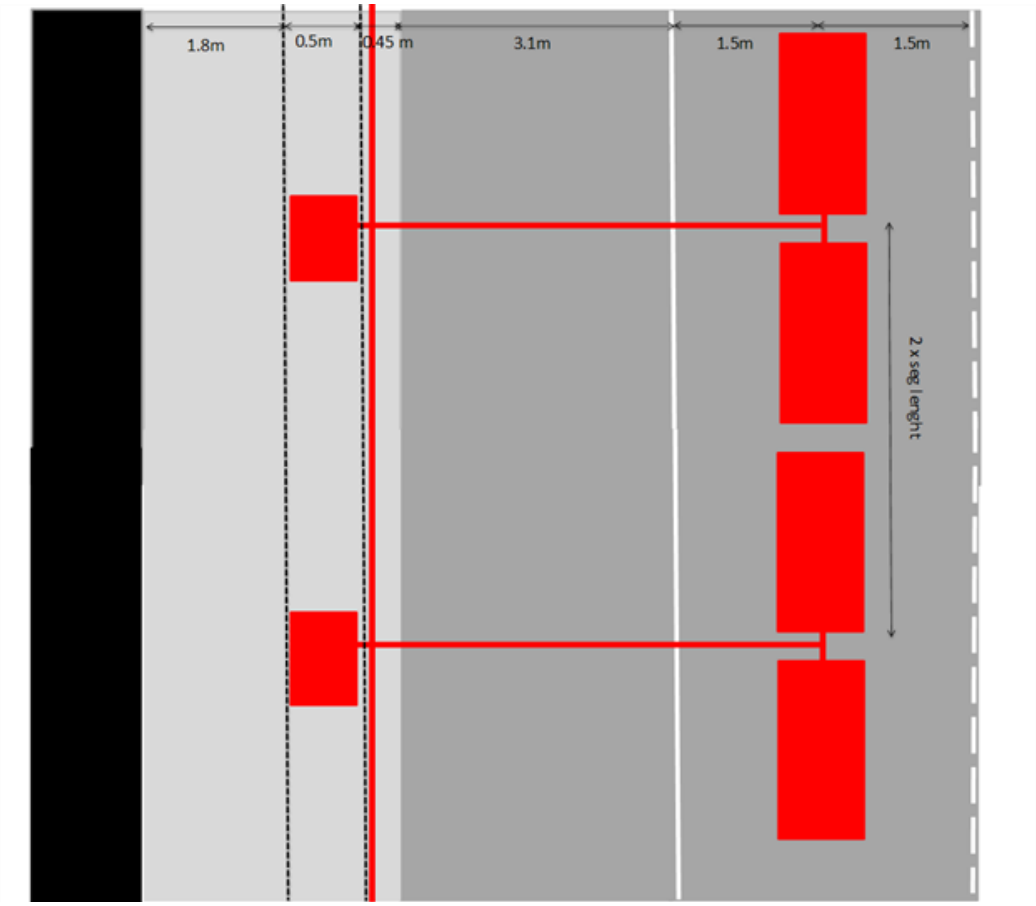

Figure 108: Overview of on-road power transfer system in built-up areas.

3.12 Conclusions

Figure 51 shows an example of a high-level architecture of an inductive power transfer system, though this architecture could be applied to both inductive and in-road conductive systems. The figure clearly shows the hierarchical nature of the power systems architecture.

Because of the potentially considerable power levels involved, a strong grid is essential (see Chapter 4 for more details), as well as a robust local distribution to the roadside. This results in significant roadside infrastructure being required, with power conversion capability in close proximity to ultimate power transfer equipment (coils, cables or rails). Local power storage (batteries, supercapacitors etc.) has been proposed to alleviate the highly transient nature of the peak power drawn. Proven architecture from light rail applications can be readily adopted, connecting storage units directly to the 750-V DC line. To ensure compatibility with the different methods of power transfer, it is not possible to define a more detailed architecture. However the individual architectures of FABRIC solutions are described in detail in the relevant sub-sections.

The architecture of in-road sections of inductive power transfer has also been considered from the aspect of road construction. Due to the immaturity of viable solutions, and the uncertainties of key design aspects of the solutions, it is not possible to define a generic architecture for in-road installation at this stage.

4 INTERFACE WITH THE ENERGY DISTRIBUTION NETWORK ARCHITECTURE

4.1 Introduction

This chapter describes the outcomes of Task 3.5.3 in the frame of Deliverable 3.5.1, “Architecture Definition” as stated in description of work.

The objective of this task is to define the architecture of the grid connection of the charging solutions. Based on the work carried out in WP4.4, this interface with the public distribution grid will be a grid-tied power electronic converter, which in turn might be connected to the grid with a dedicated power transformer.

A specific section is dedicated to the type of power transfer (conductive or wireless). It will be shown that the grid-interface architecture depends mainly on the required power level and not on the power transfer solution (i.e. capturing system) which will be connected to a DC line.

The work presented in this chapter is mainly focussed on the FABRIC test sites, where several solutions will be installed. Therefore, power electronic architectures are proposed for a power range up to 50 kW. Generic architectures are proposed which are representative for the FABRIC solutions. The grid impact of such a converter is analysed with special focus on harmonic distortion, following the same methodology as in D4.4.1. The main difference to the study presented in D4.4.1 lies in the fact that the proposed architectures are optimised regarding harmonic distortion and thus, represent a concrete recommendation in order to comply with grid requirements. Specific control and filter solutions are presented, while in D4.4.1 the objective was to give a wider overview of possible architectures. The main result of D4.4.1 was that harmonic distortion is an important design parameter to be taken into account, as not all architectures will be able to comply with grid requirements.

A detailed study on possible integration of storage solutions into the DC bus of the WPT system has been carried out in D4.4.2. Although it is closely related to grid-connection issues, it is not considered here as part of the grid interface, but rather as part of the charging solution itself. Therefore, in this document no additional details are given on this topic. Nevertheless, it is mentioned explicitly that storage solutions are very useful and actually there are products already on the market for light railway (tramway) applications.

It is acknowledged here that in real installations, power levels of the grid connection will be in the multi-MW range. In PRIMOVE for example, a rectifier substation of 1.5 – 4.5 MW is proposed, connecting via transformer to a 30-kV distribution line. Other solutions such as the conductive “Slide-in Electric Road System” even propose a connection to a 130-kV line, with a dedicated 30-kV distribution to feed the rectifier substations (1 – 1.5 MW each). The architecture of such high power levels is very different from the solutions installed at FABRIC test sites. Nevertheless, this type of installation is well-known technology, already in use in the railway sector. A specific section is dedicated to provide some examples in order to illustrate possible high-power solutions which are suitable for energy supply of a real installation.

Regarding the grid connection, no specific safety considerations are required for the installation at the test sites. Existing standards for electric installation and its protections must be followed and will guarantee the safety of the equipment. Nevertheless, requirements for road-side installed equipment must be taken into account when installed at real roads (see Chapter 3 of this report).

4.2 Methodology

A short discussion on possible differences between conductive and contactless power transfer is included from the point of view of grid connection. It is assumed here that for both solutions – conductive and contactless – a converter station will be installed in order to provide power for a DC line. From this DC line, the charging systems are fed.

Based on this assumption, a generic grid connection can be proposed. Depending on the required power, different scenarios are possible. This generic grid connection is derived from a review of existing inductive and conductive power transfer solutions (based on the review presented in Chapter 3). First, a generic high-power grid connection architecture is presented (from HV down to the 750-V DC line). In this schematic, the actual grid connection interface is identified (road converter station including transformer). In a second step, this interface is analysed in more detail and finally a generic architecture is developed for the solutions which will be installed within FABRIC project. Within this interface, the AC/DC converter is of special interest.

The converter topology depends on the power level. High-power grid connections (multi-MW range) are the scenario of large-scale deployment. Therefore, a separate section of this chapter is dedicated to solutions of high-power applications. Some examples for configurations of grid connections are presented from the railway sector, which is considered a reference for large-scale implementation of electric transport. Also existing on-road power transfer systems are included, in order to show different options of grid connection. For example, high-power configurations might include a dedicated medium voltage (MV) distribution line (20-30 kV), considering the grid-connection point at a substation of the HV distribution system (110-130 kV). These configurations are very interesting, as they prevent possible issues due to weak grid connections (i.e. harmonic distortion and voltage/frequency fluctuations due to large power fluctuations).

High-power converter configurations already exist in rail transport and renewable energies (offshore wind farms) and can be considered as state-of-the-art technology. The main contribution of this report is focussed on topologies of the power electronic (PE) converter which are relevant for the FABRIC test sites. Within FABRIC, tests will be carried out up to 50 kW. Therefore special attention is given to this power level, as it is also relevant for stationary fast-charging. A detailed analysis of expected harmonic distortion (THD) is carried out, according to the methodology applied in D4.4.1.

From all requirements for grid connection, harmonic distortion has been identified as the most critical aspect of the grid interface by far. Other issues such as very steep power ramps are related to the control strategy and integration of storage solutions, and thus, are independent from the power electronic device which interfaces with the grid.

4.3 Conductive or inductive – Which is the most adequate capturing system?

The decision, of which capturing system is best suited for dynamic power transfer – conductive or contactless –is one of the main objectives of the FABRIC project. There are multiple parameters to be considered in order to reach an objective conclusion on this question. In this chapter, the perspective of grid connection is considered. Other aspects, such as social and economic parameters will be analysed within subproject SP5, where the actual feasibility study is carried out. In D5.5.2: "Cost-benefit analysis and business models of large-scale deployment of on-road charging" this question will be specifically discussed (this is part of WP55 “Assessment of Business and Societal Consequences”).

From the point of view of the grid connection, the type of energy capturing – contact or contactless – is of minor importance. When comparing existing proposed capturing systems, for example PRIMOVE, KAIST (contactless) and the “Slide-in Electric Road System” or Siemens eHighway (conductive), all solutions have in common a converter station which converts AC from the grid to DC. The DC voltage is typically 750 V nominal, which in practice may be 600 – 750 V. The rated power of the converter station varies from 100 kW (KAIST) up to 4.5 MW (PRIMOVE). The conductive solutions are conceived at higher power levels, as they are especially focussed on heavy-duty highway transport, while contactless solutions include city traffic (i.e. busses) which requires lower power levels, as converter stations may be closer to each other. It should be mentioned here that conductive on-road charging for buses (trolleybus) have existed since 1882 and currently around 300 systems are in operation worldwide [10]. Interestingly, the feeding system is typically 600 V DC, which is in line with the recently proposed solutions. Therefore, new conductive systems do not include this option, as trolleybuses are already in place.

From the grid-connection perspective, the only difference between all the solutions is related to the power level, which in turn depends on the application and not on the power transfer solution. Hence, feasibility is given for both types of power transfer by exactly the same degree, as the grid-connection interface will be almost identical. Thus, no decision in favour or against a specific solution can be made from the grid-perspective. An important conclusion from this finding is that the technological risk of the grid connection is very low. Other aspects will have to be evaluated in order to compare these two options. Therefore, this question will be further studied in SP5 (D5.5.2), as mentioned above.

It should be mentioned here, that there is one possible drawback of contactless power transfer, which relates to fast power fluctuations (transitions from one power transfer pad to another). Preliminary studies (see D3.2.1) have shown that these fluctuations may be very high (several MW/s) and should be smoothed out with auxiliary systems such as electrical energy storage (e.g. Electrochemical capacitors (supercaps), batteries). This topic has been covered in more detail in D4.4.2 and is considered independent from the grid interface itself. Therefore, in this report, only the grid-tied converter and transformer stations are included. Possible storage systems have been studied in D4.4.2, but they are not the main focus of FABRIC demonstration.

4.4 Review of high-power grid connection

In this section, the same examples of existing proposals for on-road power transfer (see projects presented in chapter 3) will be reviewed, with focus on their grid connection. Grid connections will be displayed, without describing in detail the converter topology, which will be done in subsequent sections.

4.4.1 PRIMOVE

In Figure 109, the layout of the DC distribution is sketched. If for any reason a single station stops working, it is possible to isolate it and to power the correspondent WPCs using the remaining stations. However, the voltage may be too low to provide power transfer in a section if two or more consecutive rectifier stations fail or in the case that more than one third of them stop functioning in random locations. The size and spacing of the rectifier substations are determined by the load, the size of the DC distribution cable, and the allowable voltage drop between the substations and the WPCs.

In Table 12 the relationship between the spacing of the rectifier substations and the conductor size is reported according to the framework of the Sweden report and their simulations, while in Table 13 the properties of the cables are summarised. The Swedish group claims that the existing 130 kV regional grid is stable enough for use on the project. It would be sufficient to install additional transformers. Furthermore, the HV grid could be easily expanded or reinforced if necessary. The distance from the regional grid, and therefore from the transformers, to the road would vary between 2 – 5 km or more, depending on the geography of the site [11].

Table 12: Spacing of the rectifier substation and conductor size.

Substation spacing [km]	Rectifier substation rating [MW]	Main DC distribution feeder (no cables x conductor size in mm^2) per polarity
1.0	1.5	2 x 240
2.0	3.0	3 x 300
3.0	4.5	4 x 400

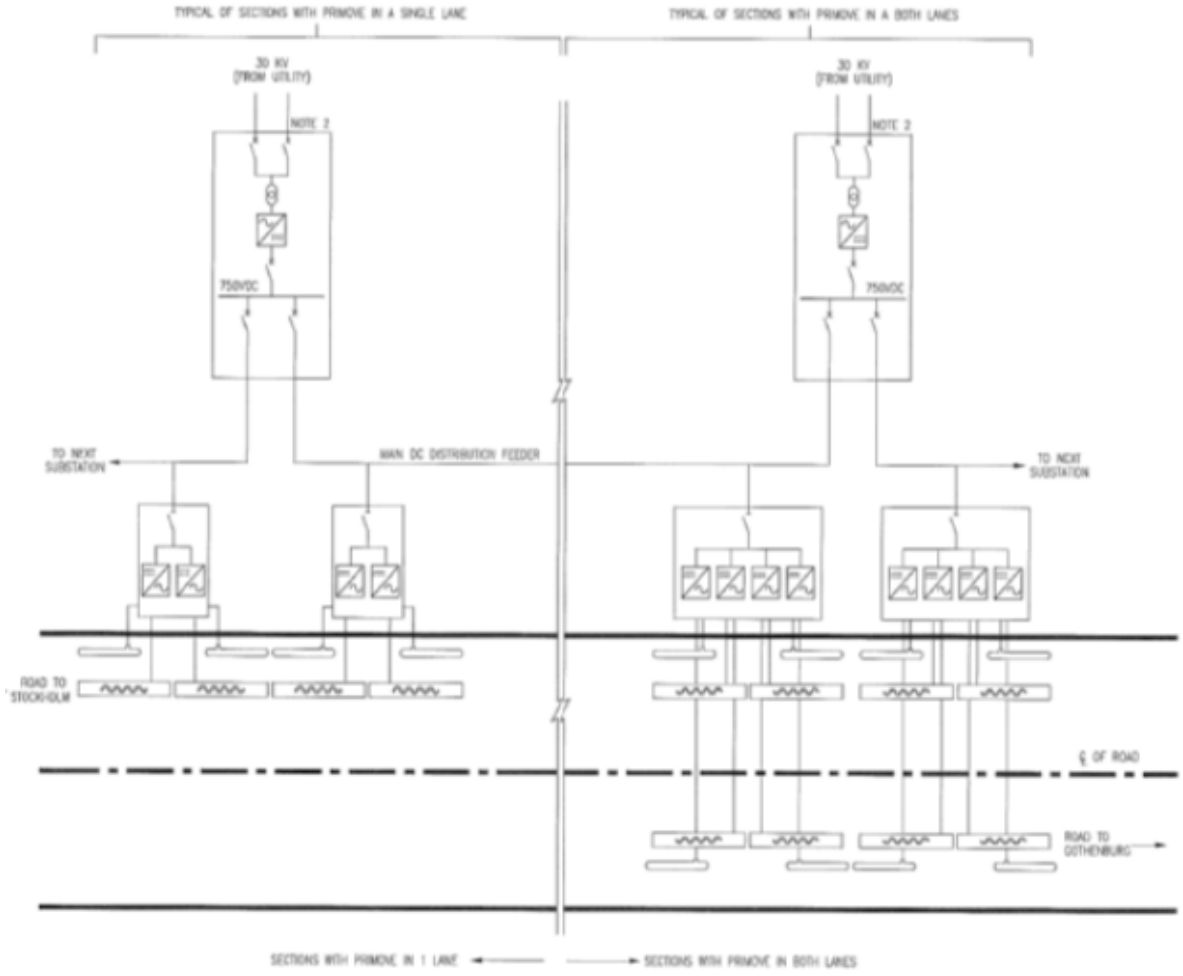

Figure 109: PRIMOVE highway grid connection.

Table 13 Capacity and Resistance of the cable.

Conductor (single conductor insulated cable – stranded copper) [mm^2]	Current carrying capacity [A]	Resistance [mΩs/conductor @ 20°C]
240	~570	75.4
300	~650	60.1
400	760	47.0
1 Current carrying capacity taken from cable manufacturer specifications (Philips Cables) for copper cable in duct **2 IEC 60288 Table 2**		

For the design of connection to the HV grid, the same configuration is adopted as for the Electric Road System (ERS) from Alstom, which is shown in the next section. The design of

the infrastructure from the road transformers down to the power transfer units has also been taken from the ERS proposal, but is adapted to the inductive case (see Figure 110).

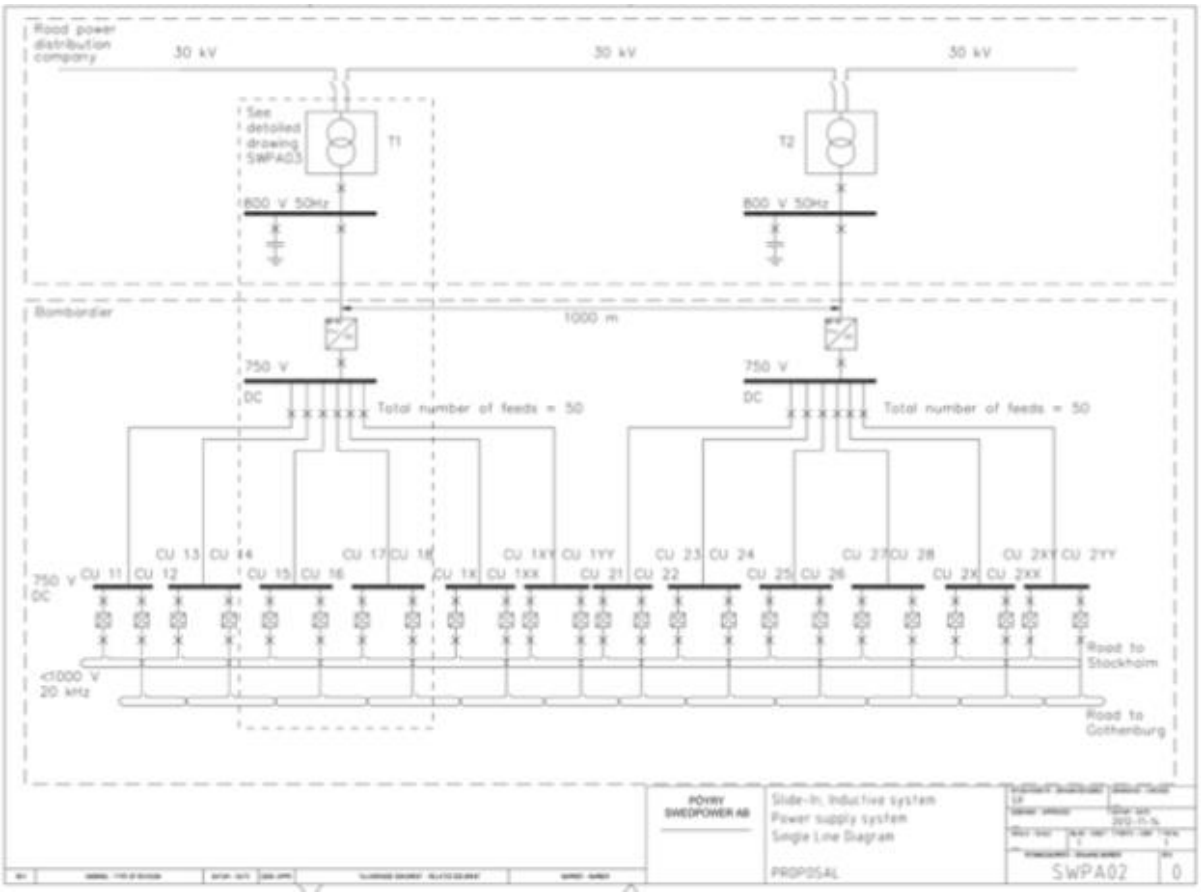

Figure 110: Power grid design from the 30 kV distribution substations to the road integrated 750 VDC distribution system. The diagram is based upon the Bombardier ERS.

4.4.2 Slide-in Electric Road System (ERS) – Conductive

The regional power grid of this system under study is 130 kV. It is therefore necessary to build a grid at 30 kV for supplying the substations, which in turn transform the voltage and feed the road distribution system with 750 VDC. A possible electric layout is described through single line diagrams in Figure 111 and Figure 112.

The proposed configuration consists of road substations including two redundant 130/30 kV transformers, and the road distribution network made of 1 or 1.5 MVA substations each km.

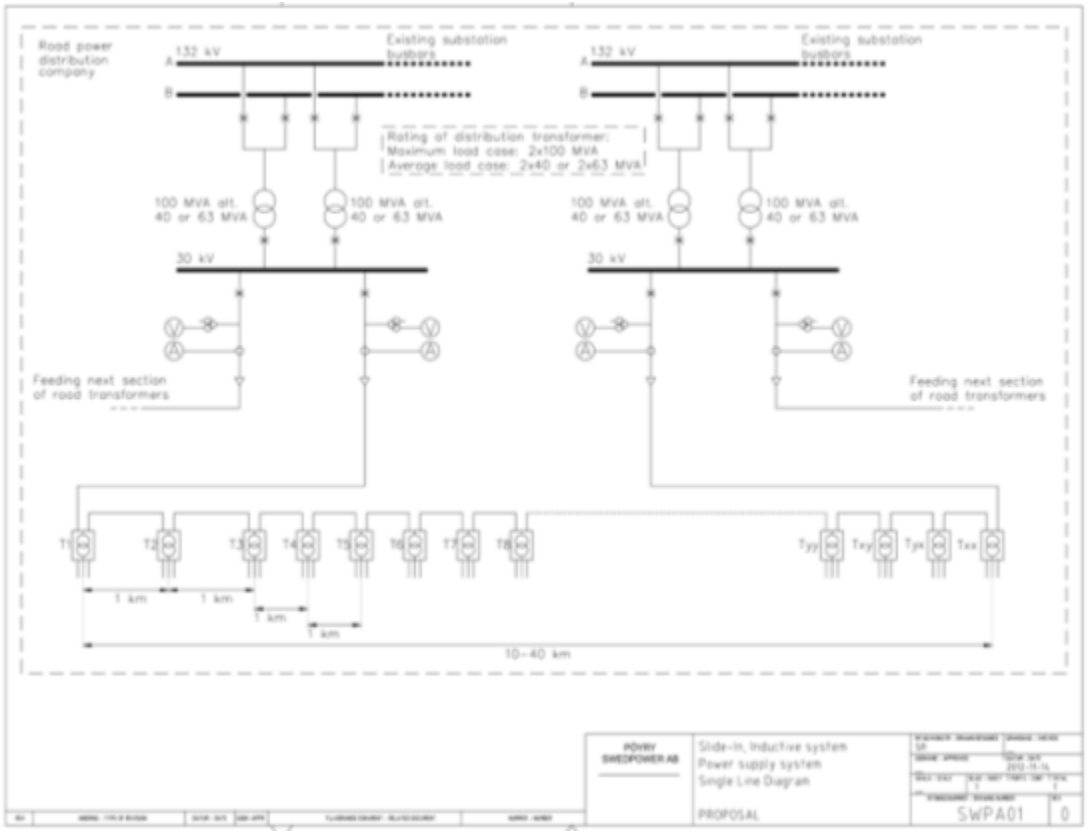

Figure 111: Alstom ERS power grid design from 130 kV down to the distribution (road) substations.

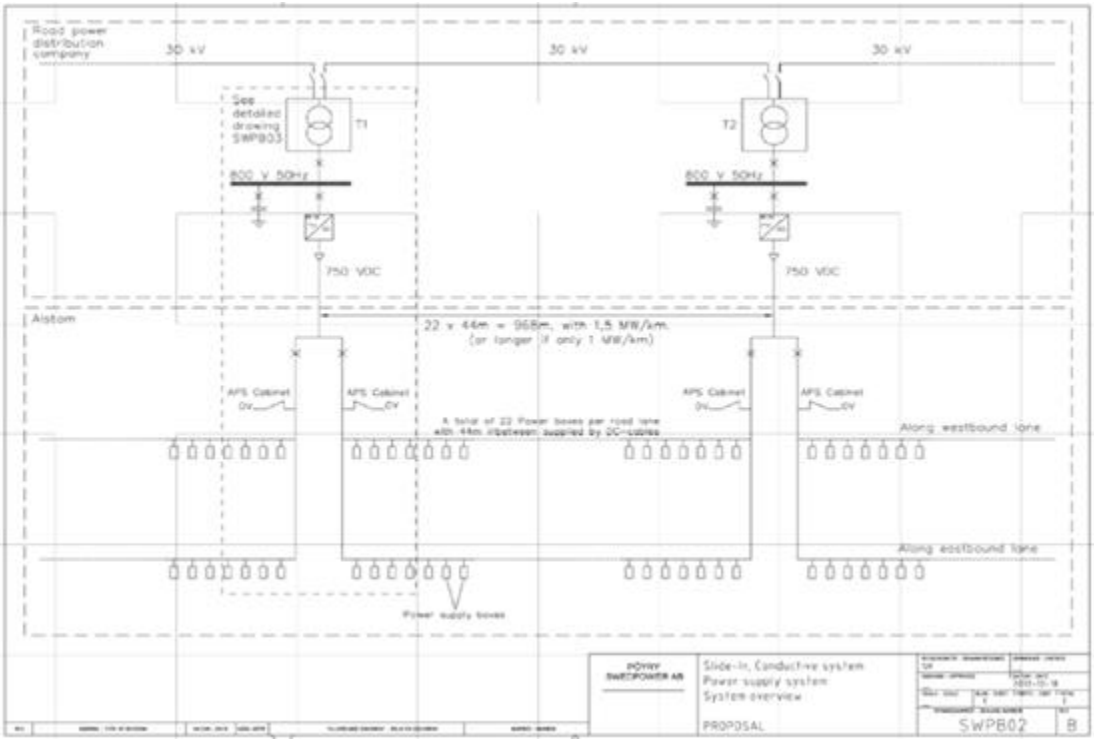

Figure 112: Alstom ERS power grid design from the 30 kV distribution substations down to the road integrated 750 VDC distribution system.

4.4.3 Railway grid connection

Railways are fed from the public grid (50 Hz or 60 Hz) but there are also other feeding systems [12]:

- DC: subways, trolleys, light rail, trams;
- Low-frequency AC: 16.7 Hz in North-western and Central Europe and 25 Hz in Northeast America.

In Figure 113, an overview of Railway electrification systems is given. It may be noticed that high speed lines in France, Spain, Italy, United Kingdom, the Netherlands, Belgium and Turkey operate under 25 kV. As can be seen, 1.5 and 3 kV DC systems are still widely used. Also 25-kV high-power AC systems, running at 50 Hz are widespread. The latter do not need frequency converters and thus can be connected directly to the public network.

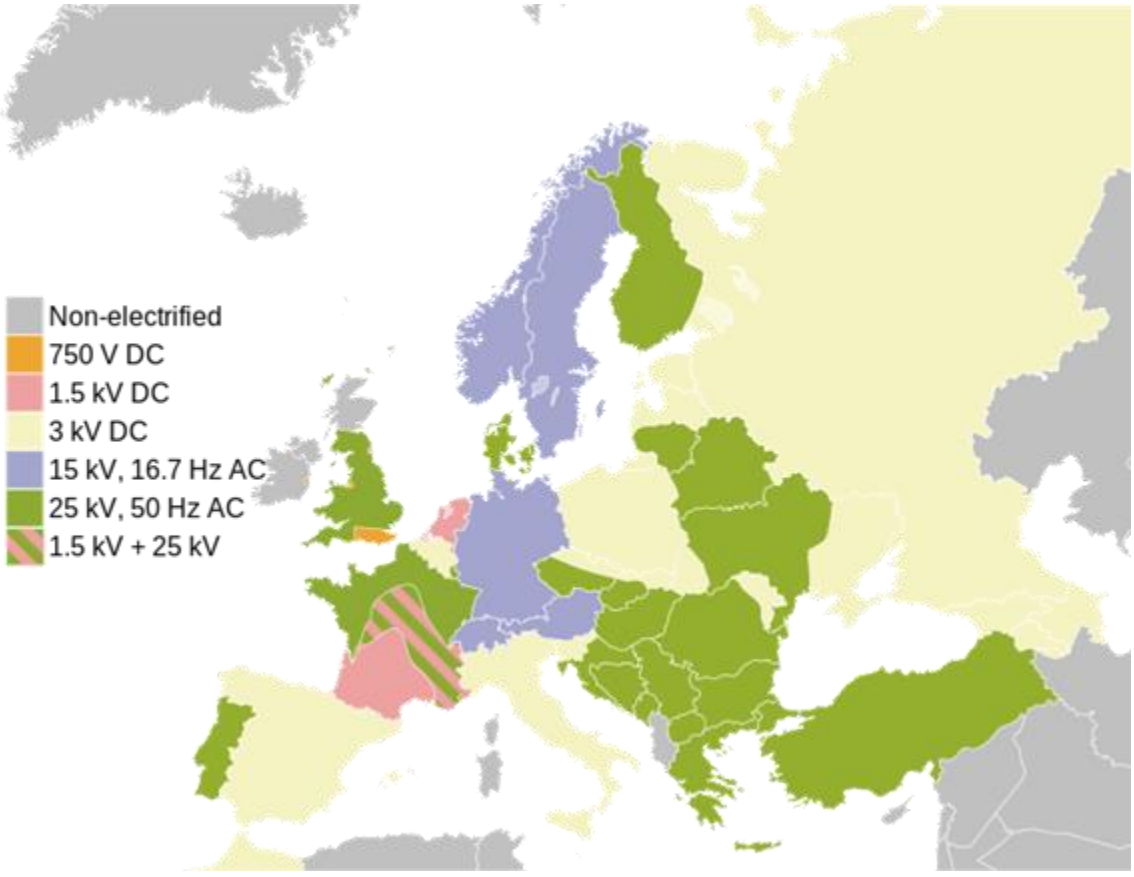

Figure 113: Railway electrification systems in Europe (Source: Wikipedia [13]).

Railway grids which are operated at DC or low frequency need frequency converters or rectifiers to be fed. New installations are connected to the main grid via power electronic converters (also referred to as static converters), although rotary converters are still in use in existing installations.

An example is given in Figure 114 for a commercial 15-MW standard module from ABB [14]. This example demonstrates the availability of high-power configurations, which may be

connected directly to the MV or HV grid. The transformers play an important role as harmonic filters, in addition to the installed filters.

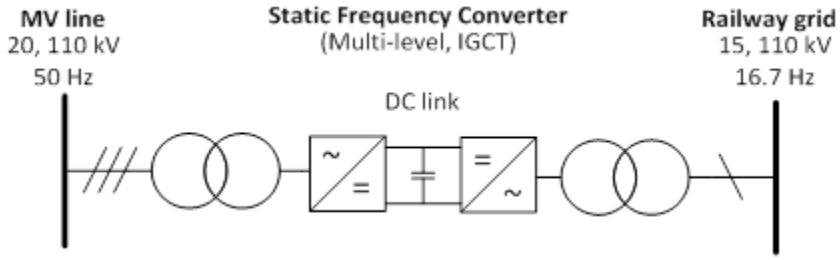

Figure 114: Example of a railway converter station (ABB standard module, 15 MW), Source: ABB [14]

Typical voltages of DC railway grids are 0.75, 1.5 and 3 kV. This is an interesting option in order to feed wireless dynamic EV charging systems directly from those grids [15]. Particularly 0.75-kV DC grids would fit perfectly with the requirements of current proposed DWPT systems (see subsection 4.5.1).

4.4.4 Grid connection topology, solutions from existing light railway systems

The PWT system for charging a FEV during driving conditions requires a distributed power supply along the road. These working conditions are very similar to a Light Railway Transportation (or tramway), the only difference being that tramways use power transfer by contact (normally catenary-pantograph).

The previous investigations showed a maximum power requirement of 1 MW/km, which is very close to the typical peak demand of a tramway system.

It may be mentioned here that the length of a tramway line is usually in the range of 10 to 30 km and the number of vehicles is about 1 to 2 tramway/km, taking account of both directions.

Several converter stations are installed along the track (about 1 station per 5 km). A similar layout can be considered for dynamic PWT system for FEV, although in the PRIMOVE solution, a spacing of 1-3 km was suggested.

Figure 115 presents a typical electric power distribution based on the technology of the electrical power station for tramways. Each power station is connected to the 20-kV distribution grid feeding the common DC distribution line. A specific transformer with 2 secondary windings by a star/delta coupling and the 2 rectifiers connected offer a 12 pulse rectifier system which delivers a smooth and stable DC voltage at 750 V which is highly reliable.

Since beginning of the year 2000 when supercapacitors became commercially available, Siemens was the first company to design and demonstrate the interest of an additional energy storage system directly connected to the 750V DC line (catenary / rail).

The topology shown in Figure 115 assumes a grid connection at reduced power, where the energy storage delivers peak power. The optimized design has to be fitted using the best

knowledge of the road traffic. Please refer to deliverable D4.4.2 where a detailed analysis of possible storage solutions was carried out for this purpose.

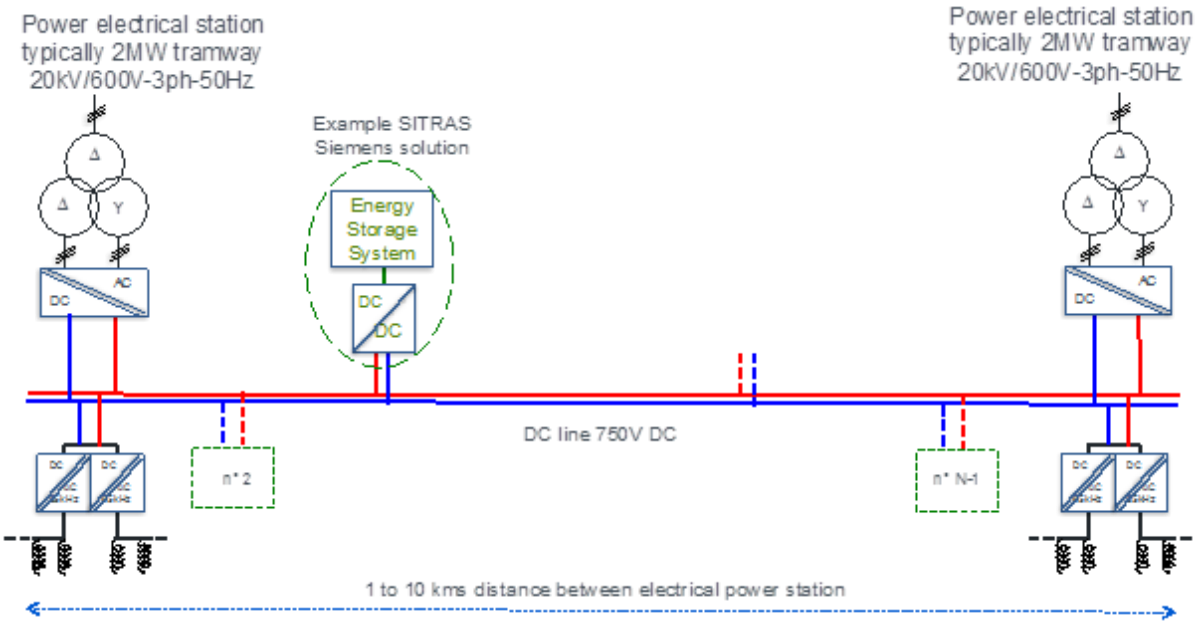

Figure 115: Electric scheme proposed for grid connection and electrical power supply line of a dynamic PWT system based on tramway layout.

Energy Storage System developed for light railway transportation

In order to reduce the typical demand peaks in light railway transportation, when the engine accelerates, innovative energy storage components have been proposed during the last decade. Another objective has been to provide some autonomy to the tramway in order to obtain route sections without catenary in historical town centres. Different technologies have been proposed, such as supercapacitors, NiMH battery, Li-ion battery and hybrid supercapacitors (LiC: Li-ion capacitor). An additional advantage of having storage capacity available is its ability to absorb power peaks from regenerative braking.

Table 14 below presents an overview of the energy storage solutions used today by tramways and electrical buses. As can be seen, 750 VDC is the most common voltage, but there are also tracks with up to 1500 VDC. Therefore, for dynamic WPT the solutions based on 750 VDC are most appealing.

Table 14: ESS solutions uses on tramway and electrical bus.

Railway Energy Storage solutions 750V DC (500-1000)	Symetric Supercapacitor	Hybrid Supercapacitor	Battery Ni-MH, Li-ion
Ground solution	SISTRAS Siemens 1st Dresde 2002, located anyway along the track (2,5 kWh)	?	Komagawa substation 2010, Osaka-Jp, 225kWh-NiMH
	Solutions have been installed in Japan on 1500V-DC lines		500kWh-Li-ion battery block (Saft, ...), since 2014
Embedded solution	MITRAC system 2005, 1-2kWh, Tramway, Bombardier	Energy storage System, 2018 Nice Tramway, Alstom	GreenPower locomotive, USA, 2009
	Supercapacitor storage, Rio tramway 2016, Alstom		Tramway 2009, Japan

4.5 Generic grid connection interface for dynamic power transfer

In this section, topologies for medium-power solutions (up to 50 kW) are proposed based on the review presented before, which are applicable for any solution within the FABRIC test sites in France and Italy.

4.5.1 Generic high-power grid connection derived from review

It is worth noticing that all reviewed solutions are very similar, regarding the design of grid connection (see Table 15). In fact, a generic schema can be extracted, as shown in Figure 116. The diagram shows an example of a possible grid connection of an entire electric road. Note that the MV line (10 – 30 kV) might be owned by a road power distribution company, and this does not necessarily need to be the local DSO.

The principal concept is following classical power distribution principles. From a main substation, one or several MV rings are feeding a set of distribution substations (here: road transformer stations). The difference consists in the fact that the transformer stations are actually converter stations, including an AC/DC converter which feeds a DC line. Voltage levels are standard for all proposed solutions (MV: 10 – 30 kV, LV: 400 V, DC: 750 V). The Slide-in Electric Road System differs slightly, with a non-standard 800 V input voltage level for the AC/DC converter. The information regarding grid-connection of the different solutions is incomplete, as can be observed in the table below. Nevertheless, some interesting conclusions can be drawn. For example, PRIMOVE and ERS solutions expect a power of 1-1.5 MW per km of electrified road. If the distance between converter stations is more than 1 km, higher power levels are needed. Either way, one converter station per km seems to be a good estimate.

Table 15: Summary of high-power solutions for dynamic power transfer.

Solution	MV line (kV)	MV Trafo (MVA)	LV line (V)	DC line (kV DC)	Grid converter power (MW)
Inductive					
PRIMOVE	10-30	40-100	800?	0.75	1.5-4.5
KAIST	–	–	380-440	0.75	N/A
Turki et al. [15]	–	–	0.75-3		0.2
Conductive					
Alstom Slide-in ERS	30	40-100	800	0.75	1-1.5
Siemens eHighway	N/A	N/A	N/A	0.75-1.5	N/A
Railway	20-110	15-100	N/A	0.75, 1.5, 3	15-100
Light Railway	20	2	–	0.6	2

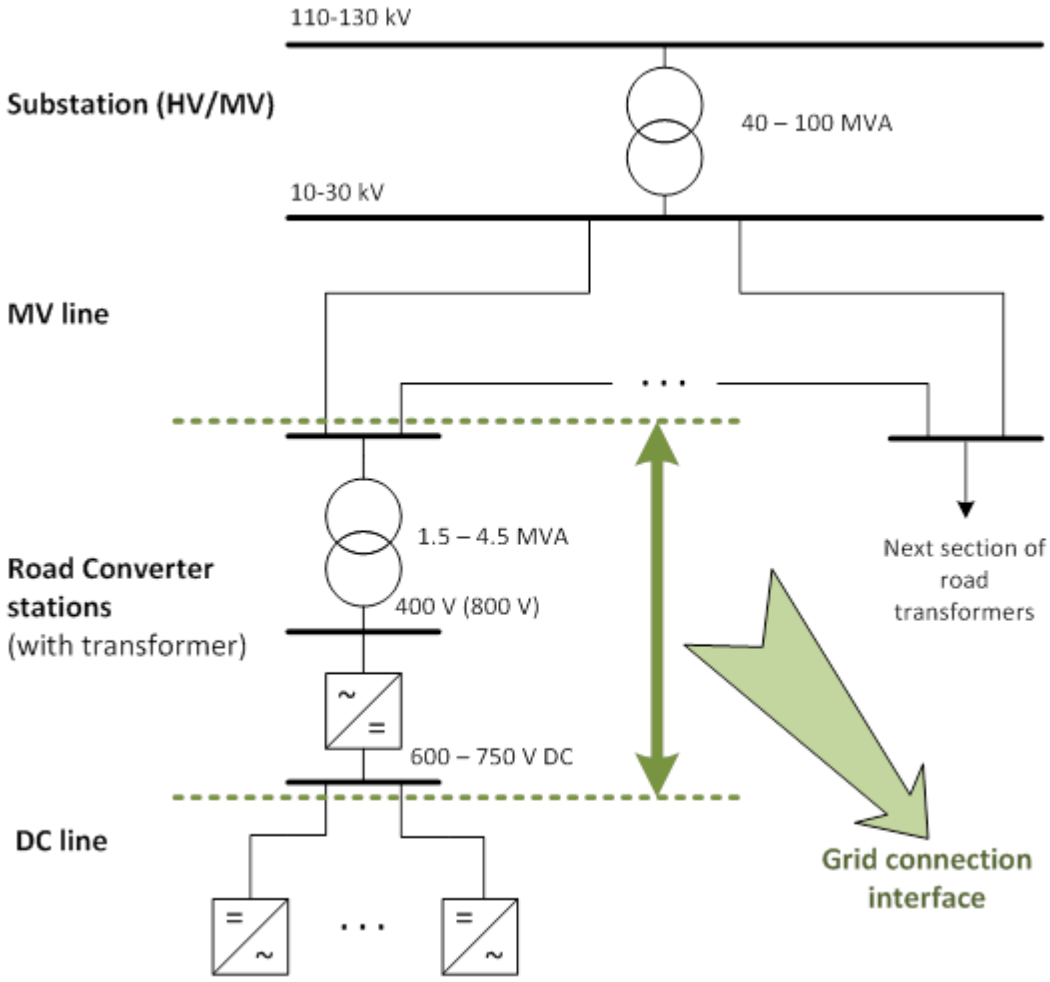

Figure 116: Generic grid connection architecture from HV down to the 750-V DC line.

In Figure 116 the grid connection interface is identified as the road converter station, which includes a transformer and an AC/DC converter. A more detailed analysis of this interface is presented in the next section, with focus on FABRIC solutions.

4.5.2 Grid-connection design

The grid connection interface has been defined above as the road transformer station with converter, which could be termed also as a “road converter station” (see Figure 117). Within this converter station, the main focus here is given to the converter topology itself. Design of the transformer and switches must be carried out according to the well-known standards. It should be noted that the transformer must withstand the typical stress of converter switching. Commercial solutions exist and are used in renewable energy installations (wind and solar power).

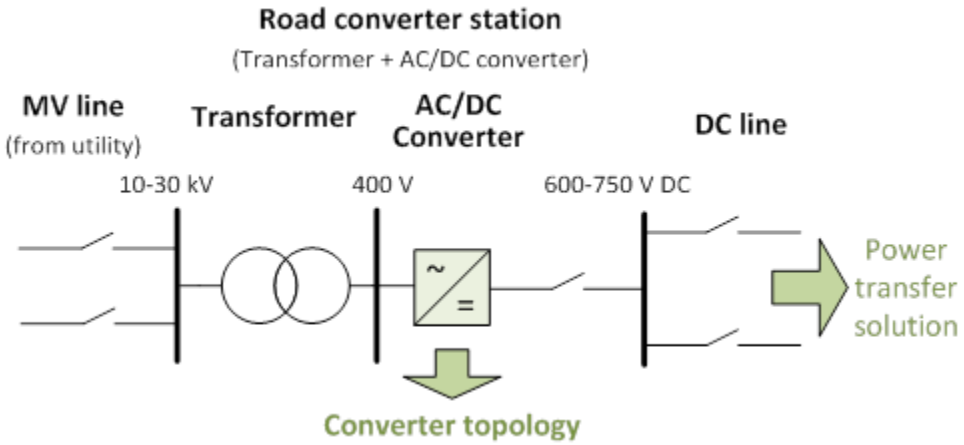

Figure 117: Generic grid connection interface (road converter station).

From D4.4.1, PWM converters with advanced control and filters have been identified as the only candidates who are able to comply with grid requirements regarding harmonic distortion (THD), even in weak-grid conditions. Two examples of possible architectures are proposed here and analysed in detail:

- Two-level PWM converter with LCL filter;
- Three-level PWM converter with LCL filter and NTV control

Harmonic distortion is analysed based on the models presented in Figure 118 and Figure 119. It should be mentioned that LCL filters are very effective, but require special care in control, in order to avoid resonance. Therefore, this seemingly small change, when compared to D4.4.1, actually represents an important technological improvement.

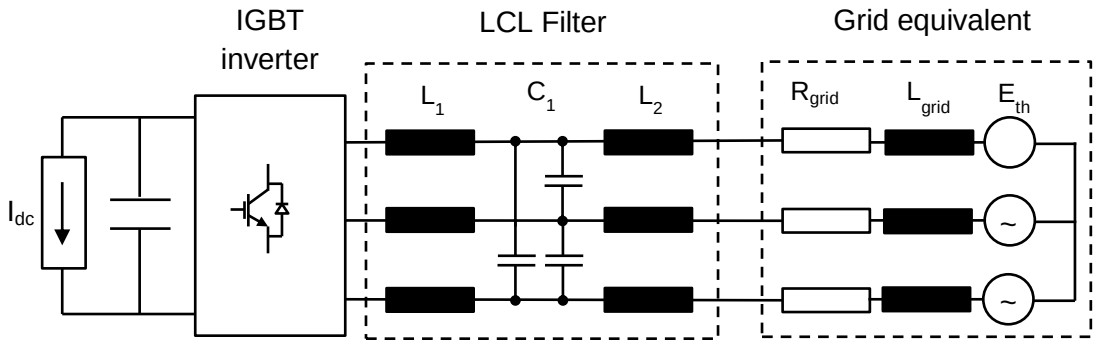

Figure 118: Model used for harmonic simulation. IGBT inverter.

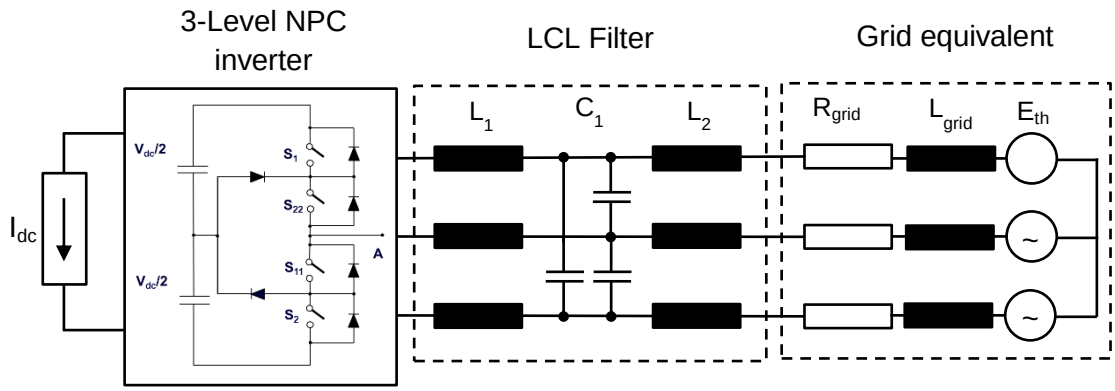

Figure 119: Model used for harmonic simulation. Three-level NPC inverter.

4.5.3 Analysis of harmonic distortion

In this section, an analysis of harmonic distortion in terms of THD is carried out for current and voltage at the grid connection point of the converter. The same methodology is applied as in D4.4.1.

Two-level PWM converter with LCL filter

The two-level PWM converter represents a standard solution for power converters in the range of 50 kW. In D4.4.1 a simple R-L filter was used and results were partly unsatisfactory. Voltage distortion in particular was very large, reaching 50% for weak grid connections. The proposed solution is the improved LCL filter, which implies an advanced control scheme.

Wave forms shown in Figure 120 already indicate that this improved filter provides very good results. This observation is confirmed in Figure 121 where the FFT is shown. THD for current is between 0.5% (strong grid) and 2.6% (weak grid). Voltage THD is between 0.04% (strong) and 0.5% (weak). These values are very low, and encouraging for widespread implementation. Nevertheless, filter inductances are large, which translates in high system costs. Therefore a three-level converter topology is proposed and results are shown below.

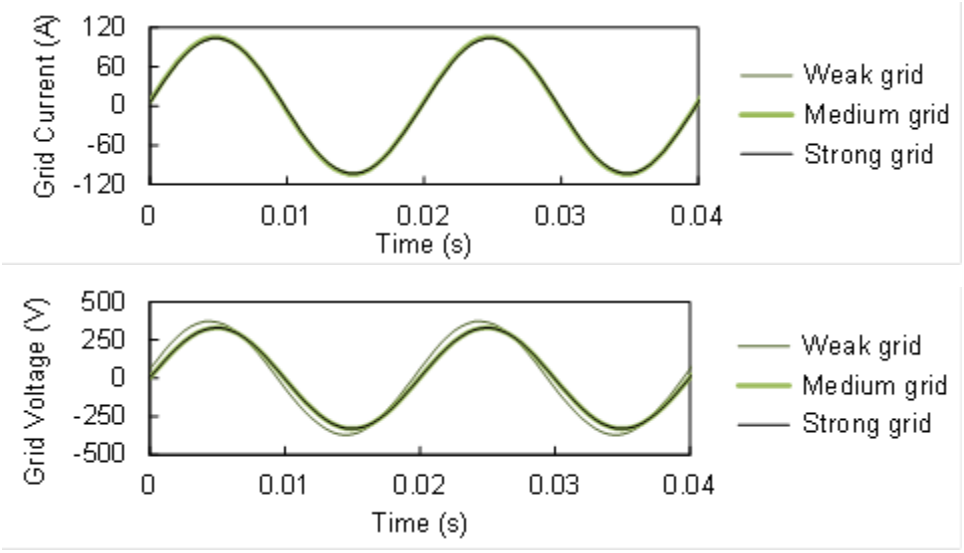

Figure 120: Current (above) and voltage (below) waveform with two-level inverter for different grid strengths.

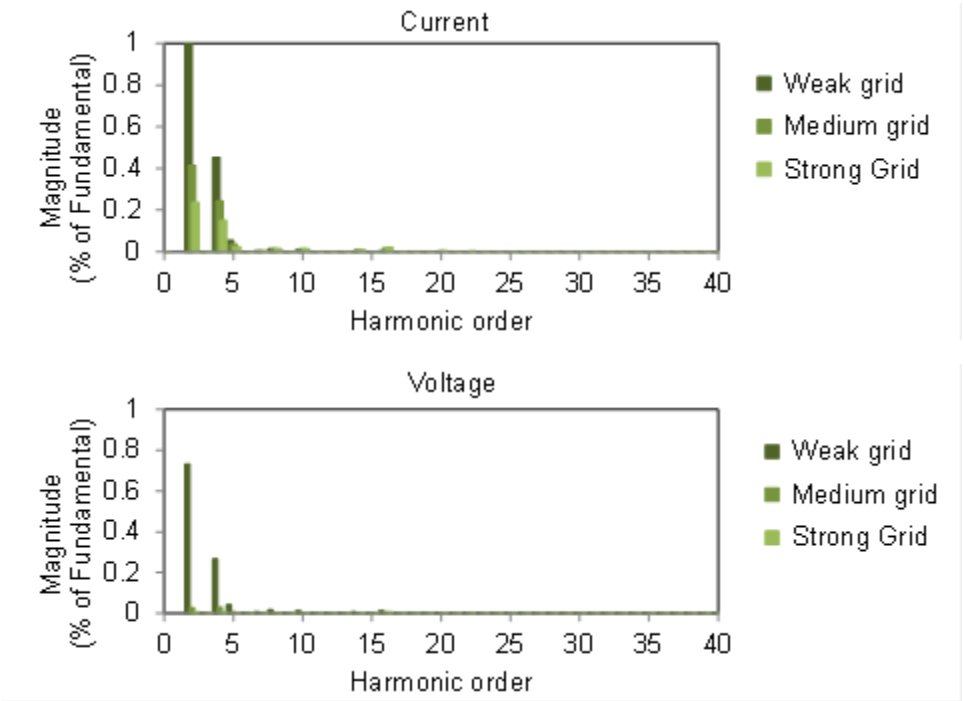

Figure 121: Current (above) and voltage (below) FFT with PWM controlled IGBT inverter for different grid strengths.

Three-level PWM converter with LCL filter

As for the two-level converter, wave forms and FFT spectra are shown in Figure 122 and Figure 123 and as with the two-level converter, very good wave forms are observed for the three-level converter. THD values are between 0.5-4.0% for current and 0.08-2.6% for voltage.

Compared to the two-level converter, results are slightly worse, but the requirements for the filter (especially inductance) are reduced considerably.

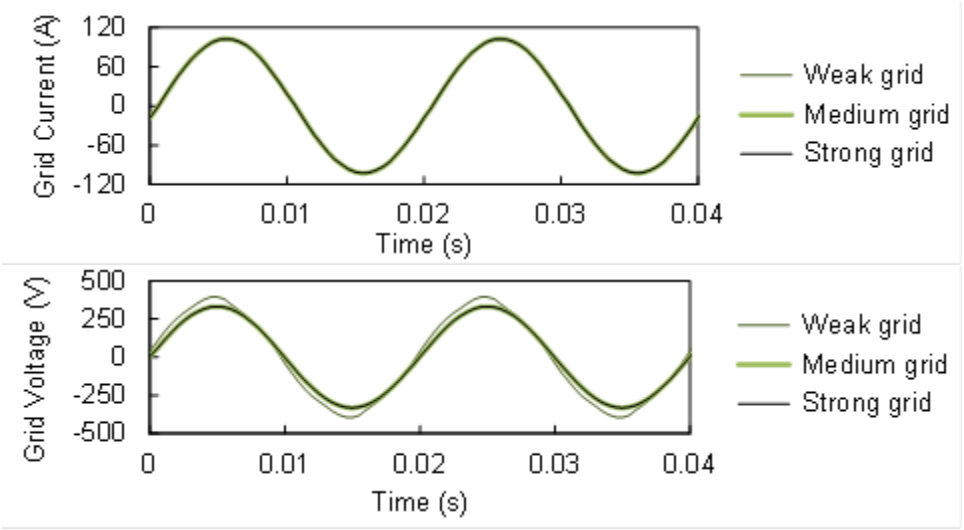

Figure 122: Current (above) and voltage (below) waveform with two-level inverter for different grid strengths

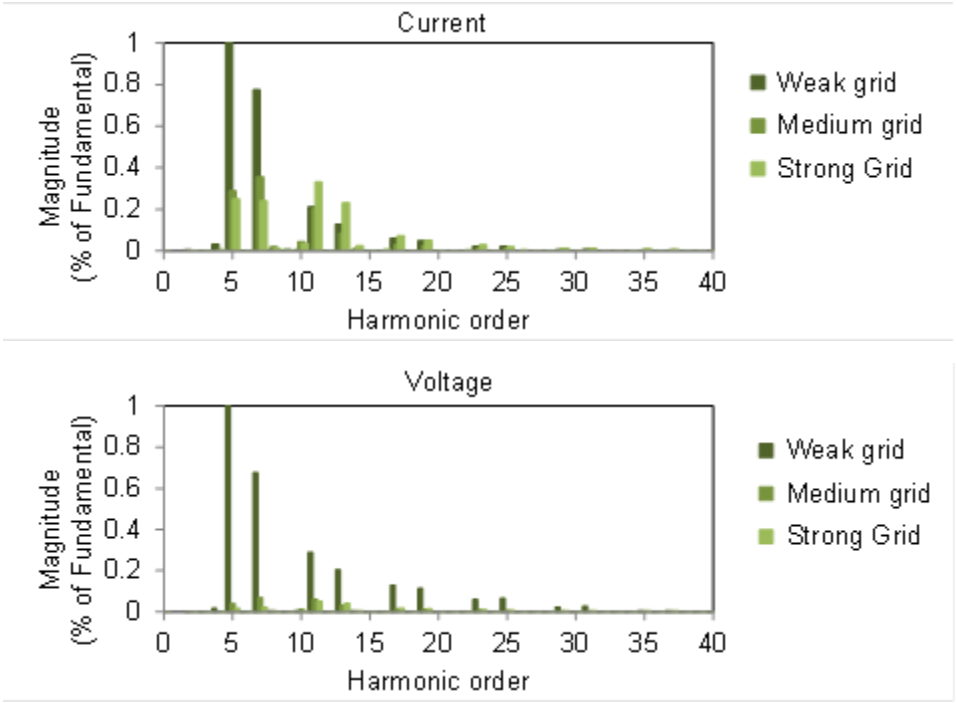

Figure 123: Current (above) and voltage (below) FFT with PWM controlled IGBT inverter for different grid strengths.

4.5.4 Summary

A generic interface for grid connection has been presented. It coincides with the road converter stations, which are mentioned in several proposals of high-power implementation, such as PRIMOVE. Converter power is proposed to be 50 kW, based on IGBT power electronic devices, which is state-of-the-art fast charging standard and proved within the UNPLUGGED project. This is lower power than PRIMOVE (< 1 MW) and KAIST (100-200 kW), but in line with the power level which will be tested during the FABRIC project. Each

solution provider will implement its own solution, but this study shows a bench mark for what it should be possible to achieve.

Special focus is given to harmonic distortion of the grid-tied converter; as in D4.4.1 it has been identified as one of the most critical aspects of grid integration. Particularly with the perspective of large-scale implementation, low THD values are important in order to maintain supply quality. Simulations have been carried out for two possible power electronic topologies in order to quantify total harmonic distortion for different conditions of grid strength. In Table 16, a summary of simulation results is shown. As already shown in D4.4.1, THD depends heavily on the grid strength where the converter is connected. A weak grid will produce higher values of THD. In the case of the two proposed topologies, in any case, very low values of THD are observed.

Table 16: Summary of total harmonic distortion (THD) in percent for different grid strengths and inverter topologies.

	Grid strength		
	Weak	**Medium**	**Strong**
IGBT Bridge (PWM control) LCL			
Current	2.4	0.5	0.3
Voltage	0.8	0.08	0.04
IGBT Bridge (PWM 3-level) LCL			
Current	4.0	0.5	0.5
Voltage	2.6	0.12	0.08

It is worth noting that the 3-level configuration shows higher values of THD, especially if it is connected to a weak grid. Nevertheless, due to the higher effective commutation frequency, passive filter elements, especially coils can be reduced considerably compared to the classical bi-level configuration. In addition, switching losses are reduced, although this aspect has not been the objective of this study.

It should also be mentioned here, that IGBTs cannot be used for converters in the MW range, as are currently in use for railway transport. Therefore, this topology is specific to the power range which will be tested within FABRIC.

4.6 Grid connection design of Italian test site

The distribution of the power on the test site is in DC. This means that whatever power variation is present on the DC line is considered a disturbance. Disturbances are classified into two categories: HF power transmission (i.e. 85 kHz) and load frequencies related to the power load fluctuation due to the vehicle movement over the coils that at constant speed became a periodical load.

The effects of the coil distribution on the power absorbed by the vehicle can be appreciated in Figure 124 which shows the DC current in a simplified model of the physical test site, where the minimal distance among coils has been chosen.

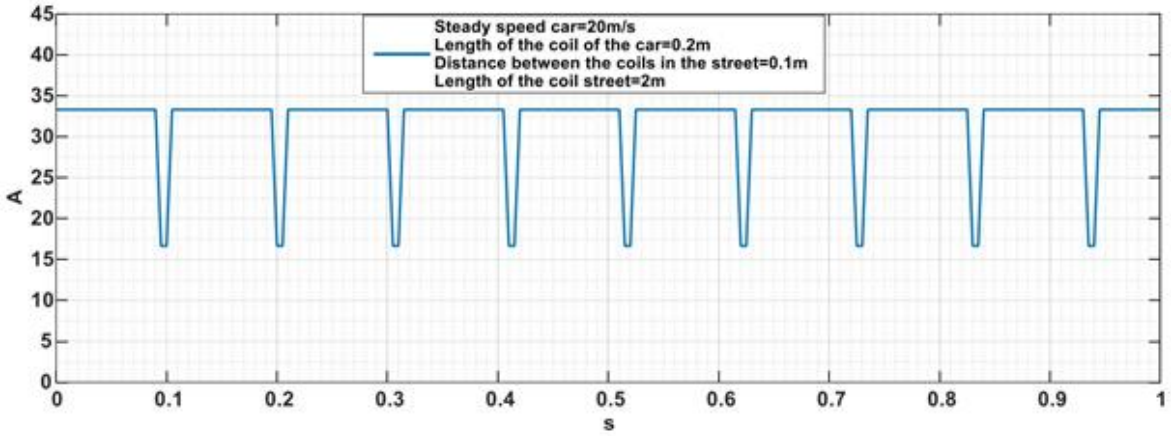

Figure 124: Simulation of the DC current required by one vehicle moving over the coils placed at the smaller possible physical distance.

The HF disturbances will be managed by the single converter so as to avoid any propagation of these frequencies along the DC line.

At the power levels considered within the FABRIC project, a generic PWM controlled rectifier could meet the power quality requirements (EN50160, EN61000) if the load current is free from load frequency components. In order to compensate the distorted current absorbed by the load frequency transmitters placed on the DC bus, two methods have been studied: passive and active.

The passive method in Figure 125 is simple because it is composed of passive components, but the disadvantage of this method is the high capacitance needed to smooth the load current (in the Farad order of magnitude). The frequency of the current absorbed in the DC bus has the same order of magnitude as the grid frequency (Hz) and depends on the car speed, length of the coils and distance between them.

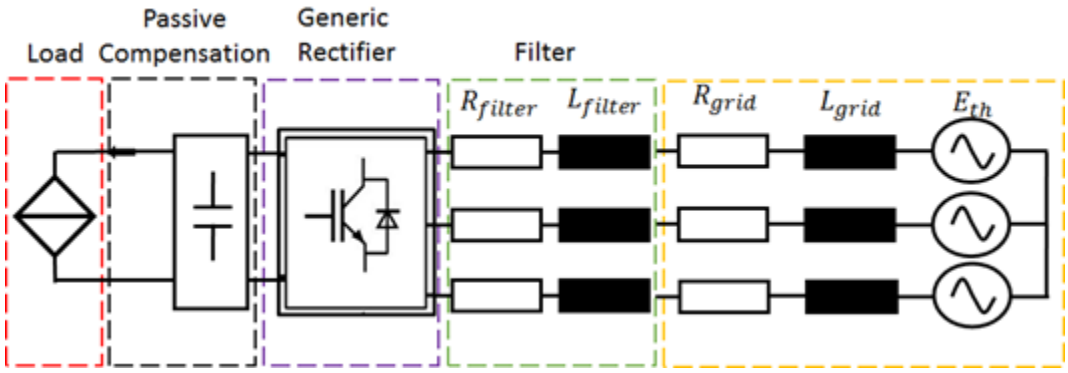

Figure 125: Passive compensation.

The active method in Figure 126 needs an additional converter with increased complexity of the system but the value of the storage capacitor has decreased significantly, with another benefit being the reliability of the service provided by the system.

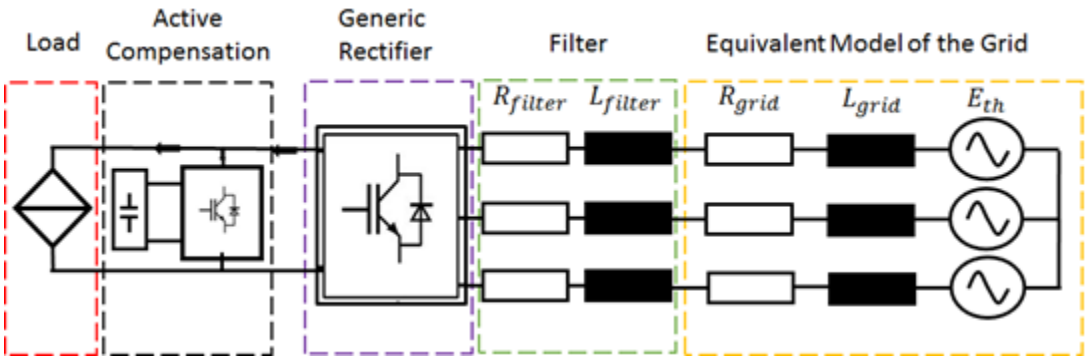

Figure 126: Active compensation.

According to the findings in section 4.5, it is noted that the proposed converter topology is expected to comply with the standards due to the fact that a strong grid connection is expected. Measurements during the test phase will validate this assumption.

4.7 Grid connection design of French test site

4.7.1 Satory test site description

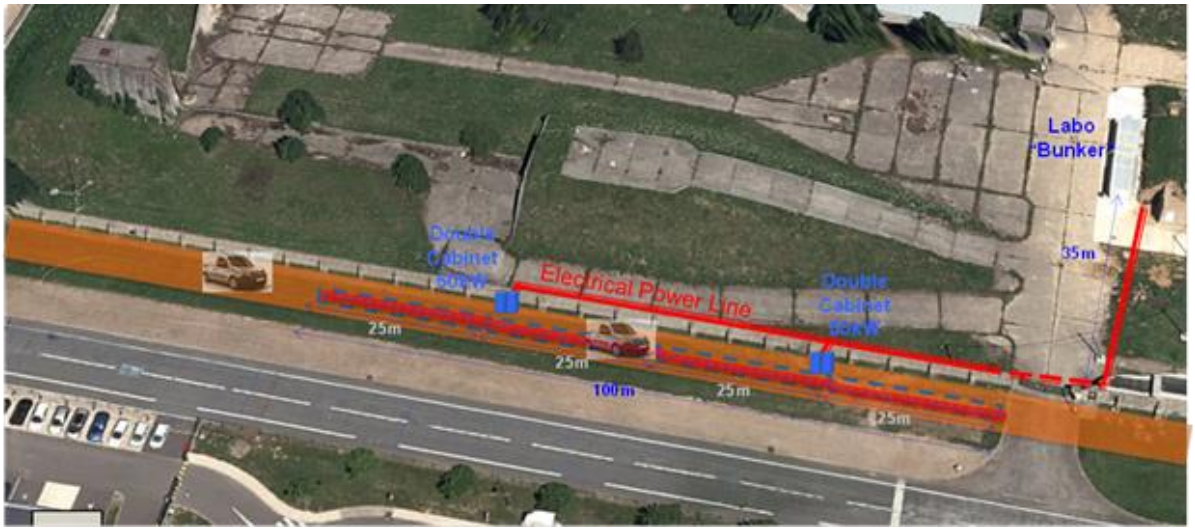

Figure 127: Photograph of the Satory test site with positioning of different converters. AC (50 Hz)/DC is located in the "labo bunker", DC/AC (85 kHz) are located along the track in the double cabinets.

4.7.2 Detailed electrical connection from the grid to the Qualcomm converters

The VEDECOM electrical power supply requirement for the Qualcomm WPT system consists of an AC connexion to the grid which supplies an AC/DC converter localized in an electrical cabinet housed in a special building called the "Bunker". The AC/DC converter delivers a DC voltage of 900 V with a power capacity of 60 kW.

A DC line provided by a two-wired cable delivers the electrical power to the two different locations of the Qualcomm DC/AC 85 kHz converters.

Each converter group is located close to the test track in order to supply power using a special 85-kHz power supply cable which connects the HF converters with the emitter coils implemented in the road of the FABRIC test track.

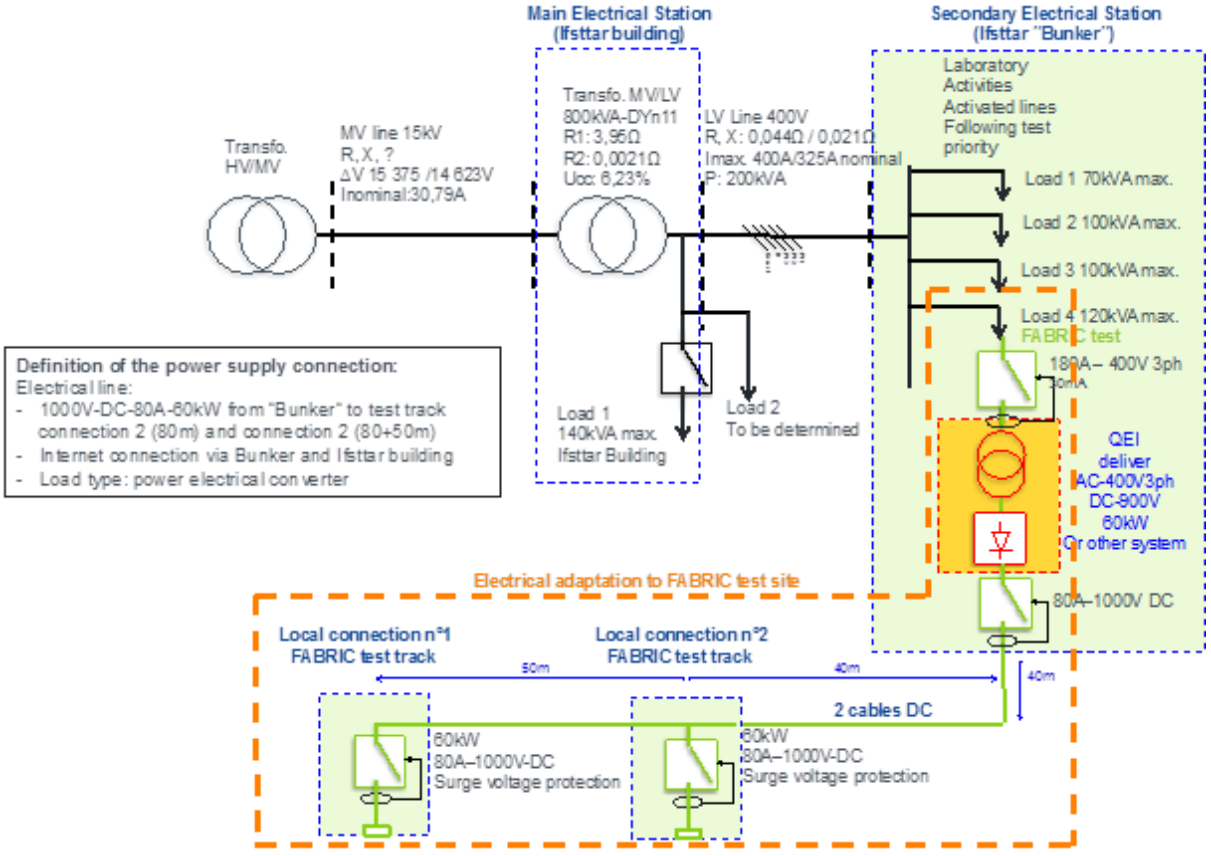

Figure 128: Detailed scheme of the Satory electrical installation.

Figure 128 shows the complete and detailed scheme of the electrical installation in Satory test site:

4.7.3 Technical Specifications

A draft of the electrical grid connection has been defined in January 2015 in agreement with Qualcomm (see Table 17). The solution in the second column was finally chosen (DC 1000 V).

Table 17: AC/DC grid-tied converter.

	DC 1000V IGBT Active rectifier – Power factor 1	AC 3ph-400V-50Hz
Installation	Integrated solution HF transfo DC voltage by Chopper	No
Weight	Example: Regatron Module 32kW: 40kg	No
Volume	Rack 19 “ (500mm)	No
Voltage control	Remote control Voltage control	On / Off
Power factor impact	1	Following BCU load
Harmonics	Following power supply	Following BCU load
Cost DC supply	60k€ min. (about 2 x 30 k€)	0 k€
Cost electrical installation “Bunker“ Installation “Road“	Protection: AC to add 1 DC circuit-breaker to add surge voltage protection	Protection : AC Protection : AC
Summary of Impact for VEDECOM	Easy to install Electrical protection included. Electrical Quality: Yes Add. cost for DC protection But cost cable reduced	Basic solution Electrical Quality: Yes

Table 18: Electric lines.

t	Function	Characteristics
DC cables	Power supply DC/AC	60 kW, 1000 VDC, 80 A
AC cables	Auxiliary power supply 230V-1ph+N+T, 32A	230 V, 50 Hz, 32 A

5 General Aspects

5.1 Shielding Architectures for WPT

Wireless energy transfer using inductive coupling has led to convenient EV charging that does not require charging cables. Magnetic field resonance offers increased efficiencies and higher transmission power among other wireless energy transfer techniques. In such systems, shielding from the suppression of electromagnetic interference is required in order to conform to limits set by international standardisation bodies, and this is combined with specific coil designs for low levels of energy losses.

During wireless energy transfer the current flowing through the system's primary coils generates an electromagnetic field around them. Electronic devices and the human body can be affected by EMF emissions. Acceptable levels of EMF emissions have been defined by the International Commission on Nonionizing Radiation Protection (ICNIRP). The physical quantity used to specify the basic restrictions on exposure to EMF is the internal electric field strength Ei. Since the internal electric field is difficult to measure, exposure limits are related to the measurable quantity that generates this field; i.e. the magnetic induction B.

Two versions of ICNIRP standards are available publicly. ICNIRP 1998 is the initial version of the standard, according to which, two reference levels are defined; occupational and public exposure. At the range of 0.8–150 kHz, which spans a big range of possible EV WPT frequencies, the limit for general public exposure is 6.25 μT. In the case of occupational exposure, limits differ. At a frequency of 0.82–65 kHz, the limit is 30.7 μT. Whereas at the 0.065–1 MHz range, the limit is derived according to the 2/f formula, f denoting the frequency in MHz. Since solutions, derived in FABRIC span the 20-200 kHz frequency range, the maximum occupational exposure at the maximum frequency is 10μT. At the same frequency the approximate limit for general exposure, according to the linear degradation occurring in the 150 kHz- 10 MHz region is 6.16μT.

Several WPT experimental architectures have been setup in S&T literature, in order to evaluate electromagnetic emissions. Indicatively, according to [16], magnetic field exposure at a 1500 mm height body, was measured to be 4.36 μT at a lateral distance of 820 mm from the centre of the coils, for a 5 kW static EV WPT system. For a 35 kW dynamic EV WPT system, that includes ferrite cores at the secondary coil, [17] report that the magnetic flux density, at a lateral distance of 1 m from the centre of the road, is 2.8 μT which is well below the 1998 ICNIRP limits.

The revision of the ICNIRP standard in 2010 resulted in a significant increase in the reference levels. The general public reference value has risen from 6.25 to **27 μT**. For occupational exposure, the reference level is set to 100 μT. In addition to the aforementioned standards, IEEE Std. C95.1-2005 is a relative standard proposed by the IEEE International Committee on Electromagnetic Safety. According to the standard, maximum permissible exposure of head and torso is 205 μT in the case of general public exposure and 615 μT for occupational exposure. The maximum permissible exposure for the limbs is set to be even higher at the level of 1130 μT for both the general public and in terms of occupational exposure. [18] Conducted tests with an 8 kW reference WPT system,

according to the ICNIRP 2010 procedures for both occupational and general public exposure. The results are shown in Figure 129.

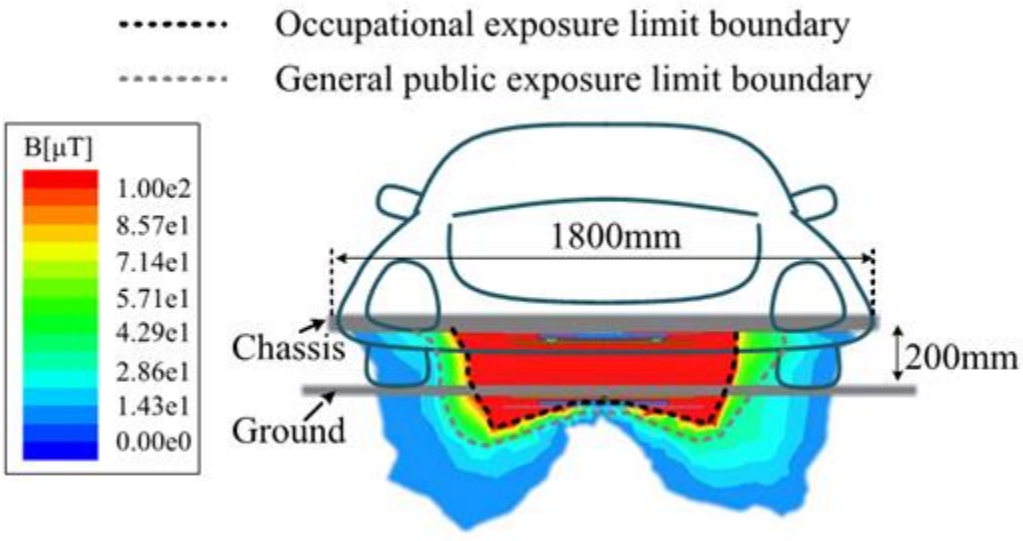

Figure 129: Public and occupational boundaries for electromagnetic exposure. Excerpt from (Li & Chris, 2015).

As depicted, EMF emission boundaries are limited below the cabin and within the space occupied by the vehicle (for perfect primary-secondary coil alignment). Moreover tolerance for higher power WPT system is available without compromising general public safety issues.

5.2 Methodologies for shielding

Several methodologies for shielding have been proposed in S&T literature. In passive shielding, magnetic materials are used to form the magnetic flux or to produce a reverse magnetic field. A typical example of such a material, is ferrite which has high relative permeability (1500 to 3000) and can be used to guide magnetic flux. Such an approach has multiple advantages since it improves the self /mutual inductance of coupled coils and reduces leakage thus minimising energy losses due to the eventual production of stray induced currents. However, special caution is required in order to avoid hysteresis losses; maximum values of the magnetic field intensity must be controlled in order to be smaller than the saturation region of ferrite. The following image depicts an architecture where ferrite has been used to form the magnetic field [18]. Two WPT base pad architectures are demonstrated; circular and doubled base pads. Below the coil, a ferrite layer is inserted in order to enhance and guide the flux. The final layer of the pads consists of a conductive shielding material.

Another passive shielding approach that is generally considered in shielding applications, is the use of metallic materials to cancel electromagnetic fields. The physical principle in this case is that time varying magnetic fields induce electric currents in such shielding metallic materials, due to Faraday's law, and then these currents in turn produce their own magnetic fields which cancel the fields that penetrate the metallic material, thus creating a reduction in

the overall field at the opposite side of the magnetic material. However; special care must be taken when placing metals close to coils as they can cause a decrease in the self/mutual inductances of the WPT system. In this case, it is permissible to introduce a ferrite core between the coil and the shielding, in order to reduce the aforementioned effect and preserve WPT efficiency. This type of shielding is also depicted in image 2 in Figure 130, where the base layer of pads installed within the roadside infrastructure, consists of metallic material shielding and ferrite on top.

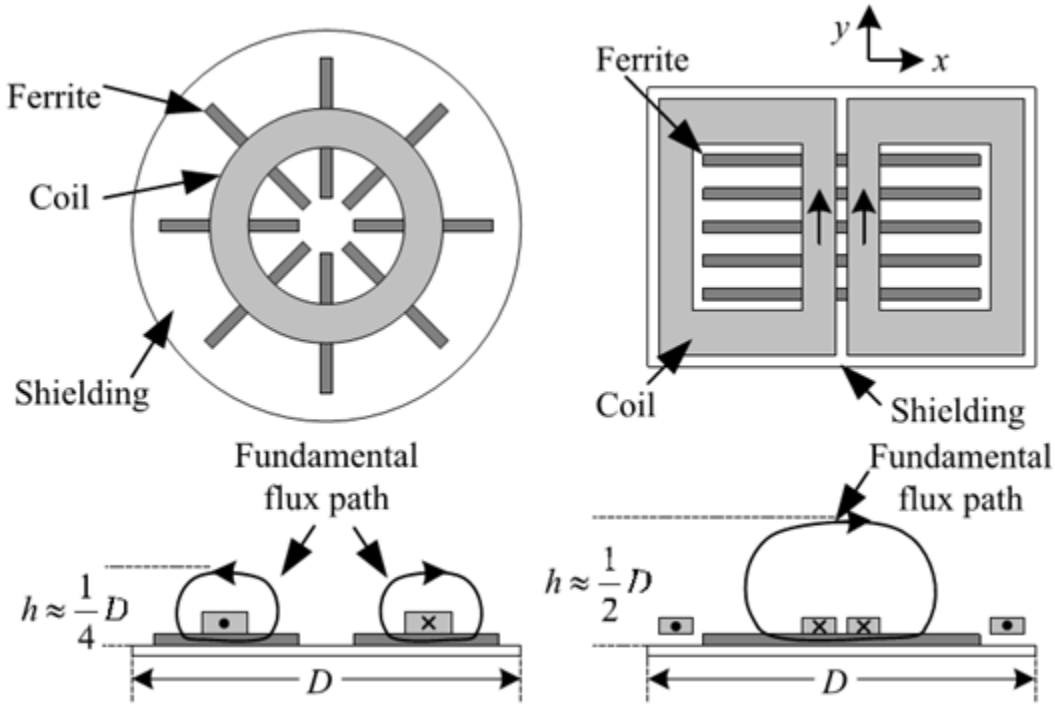

Figure 130: Architecture of WPT transmission bases. Excerpt from (Li & Chris, 2015).

Another category of shielding methodologies includes active shielding where electromagnetic noise can be cancelled out with the use of an additional current source that creates an opposite magnetic field to the one generated during WPT. In this case, a detailed design of the cancelling current source must be determined, in order to ensure cancelling effects, thus making the overall WPT system design process more complicated.

Such a methodology has been implemented in the OLEV project as outlined in [19] and combines aspects of both passive and active shielding (see Figure 131). In this case a resonant reactive loop cancels the generating magnetic field without requiring additional power supply. Reactive resonant current loops have been placed perpendicular to the receiving coils of the Online Electrical Vehicle, thus leading to an overall reduction of the field at a level below 6,25μT, at measurement points defined as per IEC 62110 “Electric and magnetic field levels generated by AC power systems - Measurement procedures with regard to public exposure”. The following image shows the placement of the reactive compensation loops on the Online Electric Vehicle (OLEV).

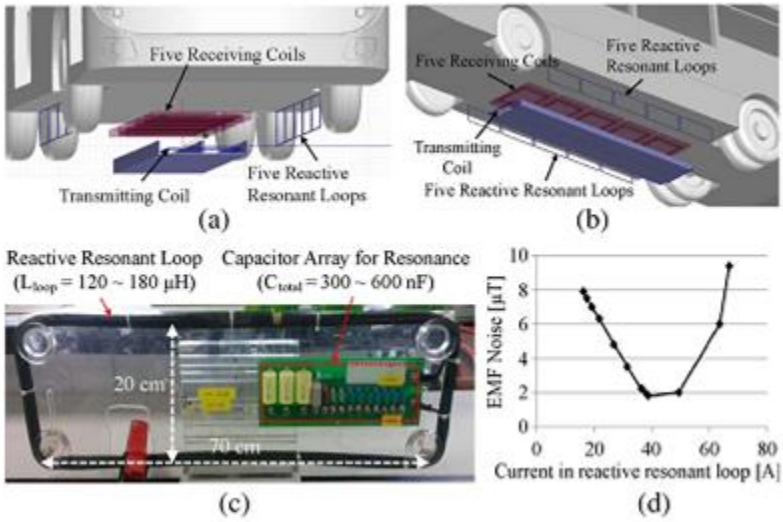

Figure 131: Application of the reactive current loop on the Online Electric Bus (OLEV). Excerpts from Kim, et al.).

The design of WPT transfer systems for overall electromagnetic noise suppression can additionally benefit from optimum coil design, in addition to passive or active shielding techniques. [20] reports that the minimisation of the near field produced by WPT coils can be achieved by appropriately defining their geometry. By designing the average winding diameters and the diameter of the ferrite shields equal to √2 and 3 times the air gap between the primary and secondary coil, the authors report, a reduction of over 29.12% with a negligible loss in power transfer efficiency.

5.2.1 Shielding methodologies considered in FABRIC

Within FABRIC, four WPT architectures will be considered; the case of the French test site, the Italian test site, where two different architectures regarding the roadside equipment will be evaluated and finally the Swedish test site case.

5.2.2 French test site

In the case of the French test site, interference will occur at the frequency of 85 kHz.

This frequency is within the range of operational frequencies defined by current static wireless charging standardisation, as defined by IEC 61980-3, ISO19363, SAE J2954. Additional interference occurs at the base side inverter of the vehicle; however shielding for these emissions will be constructed in order to cancel them out.

On the vehicle side, the architecture for shielding targets needs to meet the ICNIRP 1998/2010 guidelines for basic restrictions for the occupants of the passenger vehicle and secondly to limit unwanted heating effects from the base magnetic materials on the vehicle components. The shielding methodology is based on the passive shielding approach where a conductive material creates an opposing electromagnetic field that cancels electromagnetic noise created by the WPT process. In this case a 3 mm thick aluminium

plane covering the biggest part of the vehicle's floor plan will create an opposing field to any intersecting flux thus reducing undesired electromagnetic noise effects.

In addition to the protective measures for vehicle passengers, the flux of the WPT is designed in a manner that aims at reducing the emissions for pedestrians. The following image in Figure 132 demonstrates an indicative simulation setup for the WPT charging system of the French test pilot.

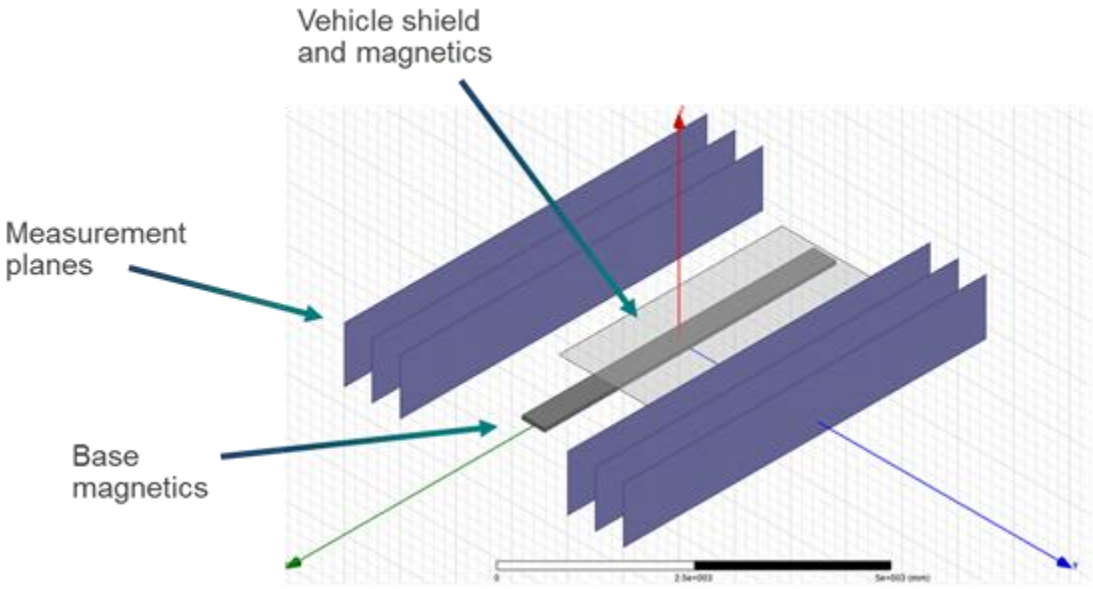

Figure 132: Maxwell model of wireless charging magnetics for emissions.

In this case the simulation setup consisted of a 5.25 m section of roadway, comprising of a vehicle shield of 4 x 1.6m. Two vehicle pads were included under the shielding and the base coils were energised at maximum current amplitude. Results from the simulations demonstrated that at 2.5 m distance from the pads (along the y axis shown below), the peak flux density is less than 2.5 μT; at 2 m the peak flux density is less than 4 μT, and at 1.5 m the peak flux density is less than 8.5 μT. In this case the magnetic field beyond a 2.0 lateral distance from the vehicle, is below the reference values for public exposure as defined in the ICNIRP 1998 guidelines. Indicative results for the 2.0 m measurement plane are demonstrated in Figure 133.

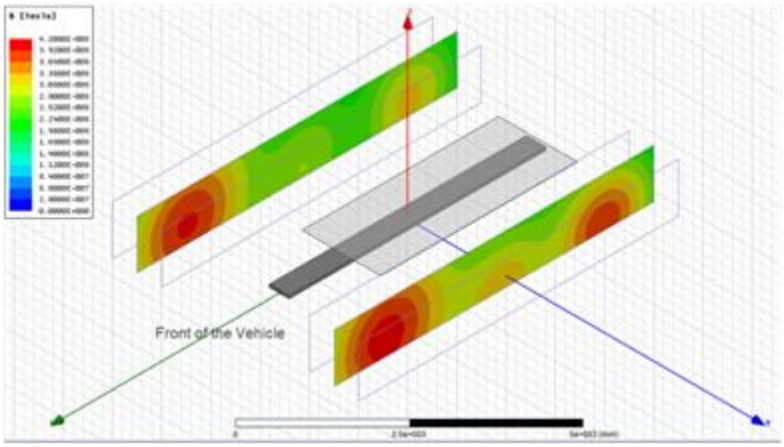

Figure 133: Emissions at 2.5 m from the roadway centre (ISO).

The aforementioned simulations target only indicative cases, which address the static scenario. More simulations regarding EM measurements inside the vehicle and outside the vehicle, during dynamic WPT operations will be carried out by Qualcomm.

5.2.3 Italian test site

The shielding design for the Italian test site follows the passive shielding methodology as presented in the first paragraph of this chapter. In this case a combination of shielding with conductive materials and ferromagnetic cores is used to both shape the magnetic field and create an opposing magnetic field that compensates electromagnetic noise. Figure 134 depicts the architecture for shielding of both the vehicle side and the infrastructure side.

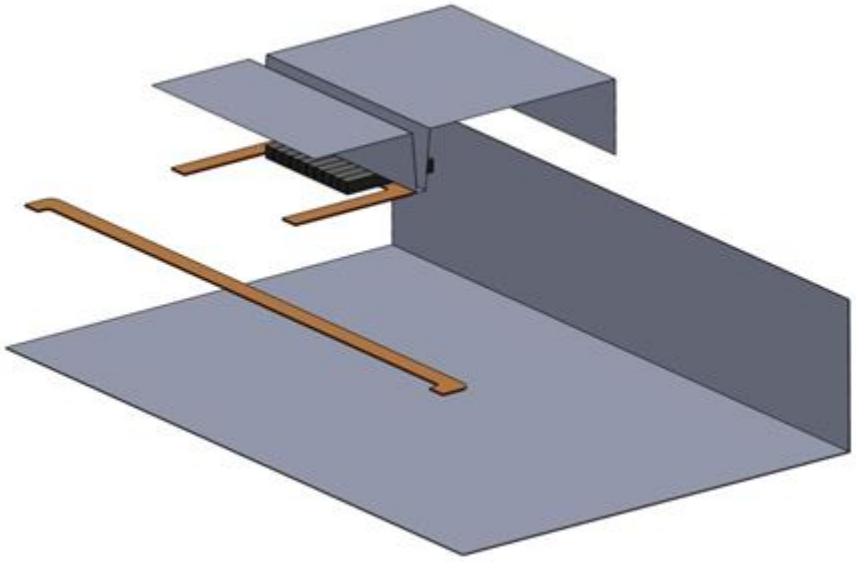

Figure 134: 3D model (half on the lateral dimensions) of the complete shielding system. Simplified structures from the 3D simulations.

The vehicle side is shielded with a ferromagnetic core that increases the magnetic coupling and minimises the losses due to the conductive aluminium shield. In addition to the receiving side coil conductive shielding, an additional conductive plane covering the bottom plane of the vehicle is considered as viewed above. Preliminary simulations show that in the case of

the double shielding architecture on the receiving side of the vehicle, the calculated magnetic induction from a side view perspective (perpendicular to the movement of the vehicle) is below 6.25 μT at measurement points as defined by ICNIRP 1998 guidelines.

A floor plan view of the magnetic field, when considering an offset along the axis that is perpendicular to the movement of the vehicle, is depicted in Figure 136. In this case the magnetic field is evaluated at a 0.1 m offset from the ground at a distance of 0.4 m by the side of the vehicle. The results confirm the compliance within the ICNIRP limits.

The aforementioned scenarios demonstrate the case where vehicles are positioned over a given charging pad, with primary and secondary coils being perfectly aligned. However, this case is not totally representative of the situation during dynamic wireless charging, as misalignments between primary and secondary coils are possible.

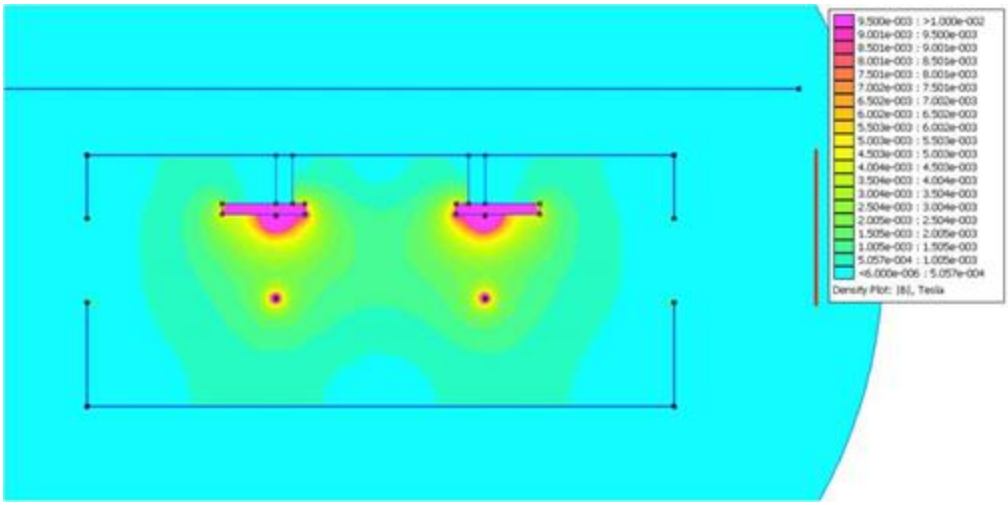

Figure 135: Map of the rms value of the magnetic induction B.

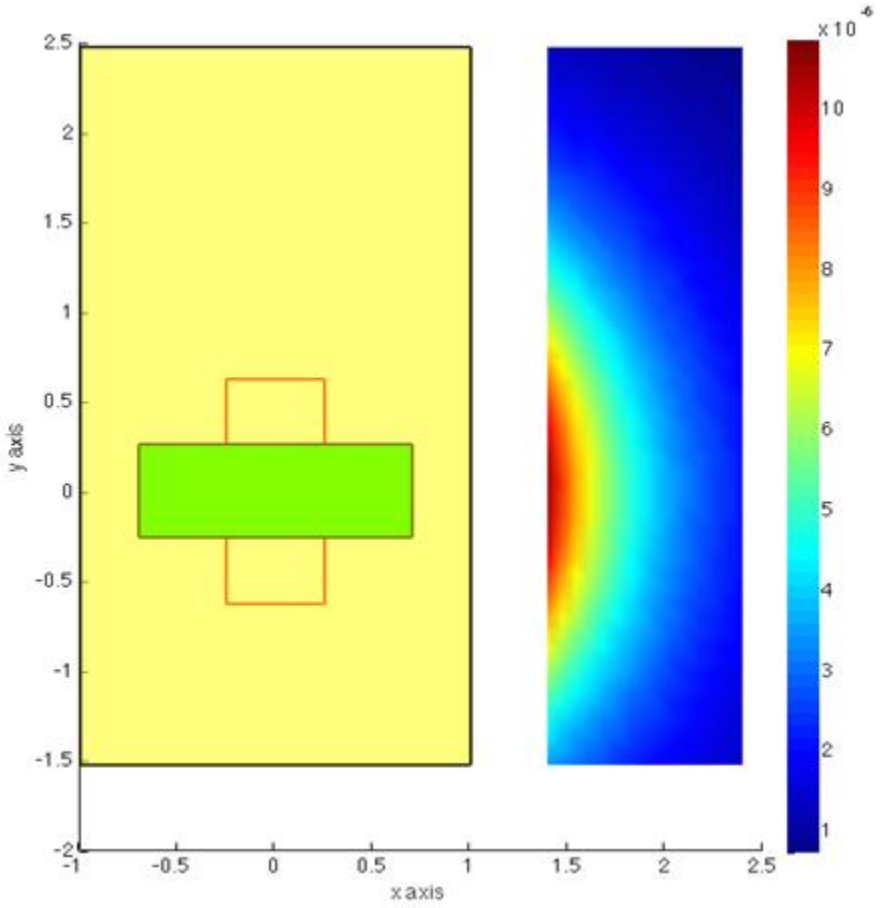

Figure 136: Colour map of induction B in Tesla on a plane z=0.1 m.

Such a case has been simulated as shown above. In the worst case misalignment case (see Figure 137, note the different scales), the ICNIRP-2010 reference limit of 27μT is exceeded by 44% at the point of maximum field strength. This fact highlights the need for further investigation of the magnetic field distribution during dynamic wireless charging conditions.

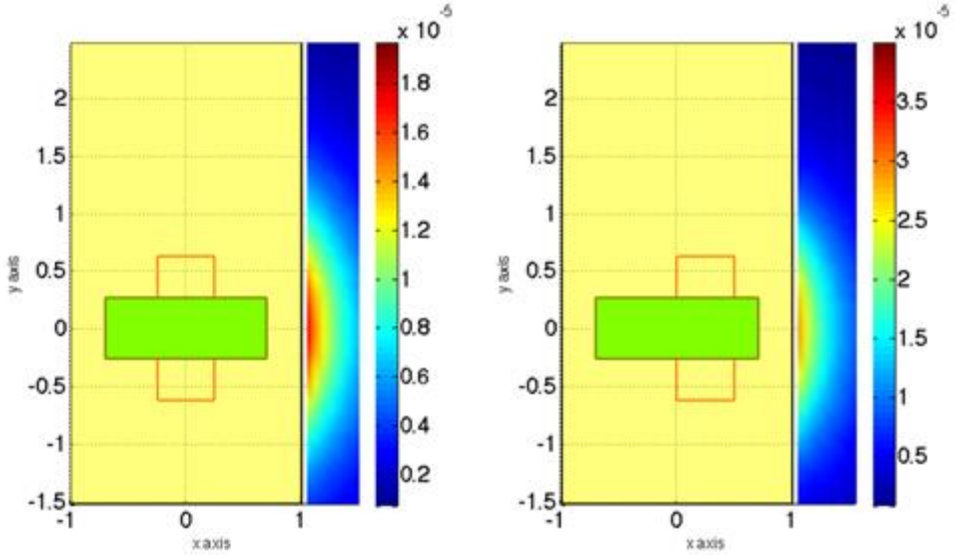

Figure 137: Map of the magnetic field density in a plane z=0.01 m (plane of worst condition).

Within the Italian test site, an additional primary side (infrastructure side) coil design for WPT will be considered. In this case, the design for shielding follows the passive shielding pattern with a combined effect of ferrite magnetic material for flux shaping and conductive material loss reduction, in addition to a conductive material case targeting the creation of an opposite electromagnetic field suppressing electromagnetic noise. In this case, primary coils buried 5 cm below the road surface, comprise a plasto-ferrite substrate that acts as a flux concentrator, with an aluminium plate under it. Findings from simulation results, demonstrate the necessity of reducing the original width of the coils to 1200-1300 mm, with an optimised shielding structure that surrounds them, in order to assure the energy transfer is in compliance with the ICNIRP public reference guidelines.

Figure 138 shows a side view of the solution along the axis perpendicular to the direction of movement of the vehicles, for a passive shielding architecture comprising of a high permeability ferrite substrate with its aluminium shielding structure as demonstrated in the image below.

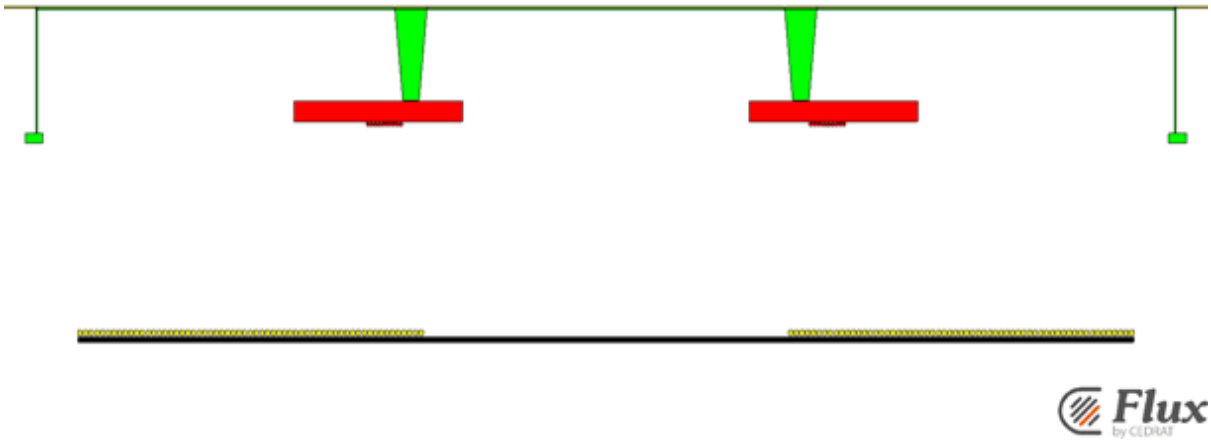

Figure 138: Original SAET InnovaLab solution geometry.

The corresponding values of the magnetic field are shown in Figure 139.

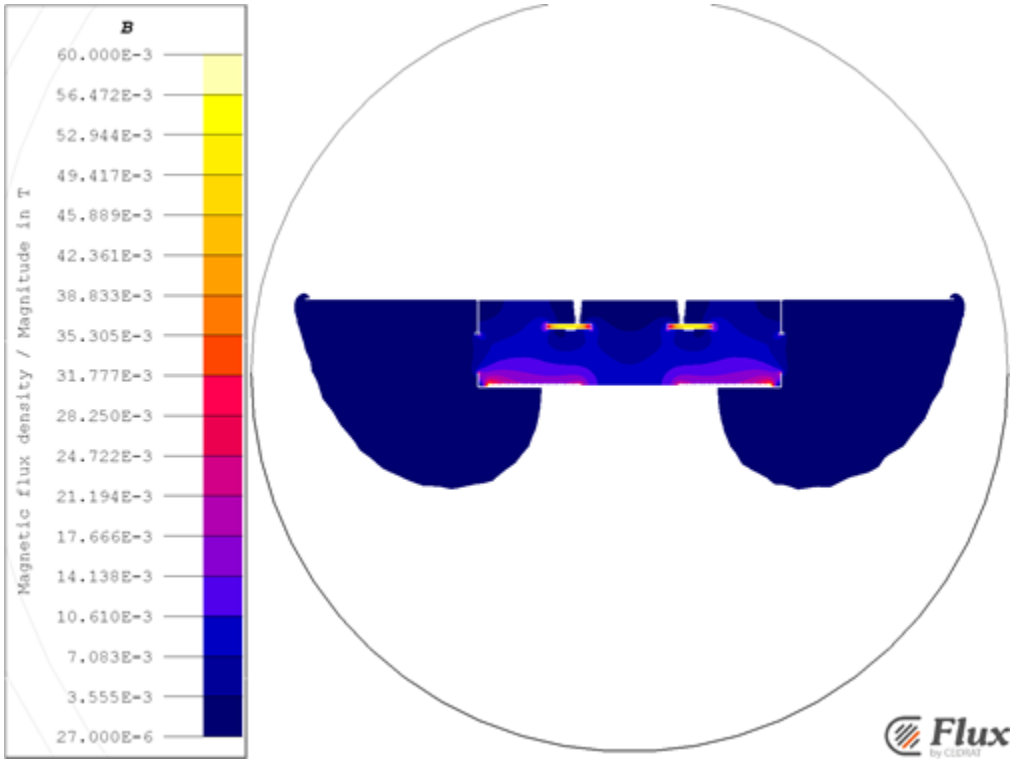

Figure 139: Colour map of induction B in the analysis domain.

As depicted in Figure 139, the overall shielding of the system suppresses electromagnetic noise in the cabin and outside the area of the vehicle. However, results from the simulation on the lateral side of the vehicle show that this solution has to be improved in order to reduce the magnetic field on the lateral axis.

5.2.4 Bombardier test site for Swedish system

The goal of the WPT design is to transmit power at a level of up to 200 kW, within the limits of the magnetic field being below 6.25 μT in all public areas and in the driver cabin. During tests, safety with respect to magnetic fields has been measured, both inside the truck (driver cabin and load area) as well as next to the truck. In all test cases, the EMF was below the ICNIRP 1998 limit of 6.25 μT. As previously mentioned this field level is lower than the recommended level for public exposure in the latest ICNIRP 2010 standard and is safe for all modern pacemakers (VDE, 2002). The following image indicates the methodology for testing and the respective emissions from the PRIMOVE solutions along the axis perpendicular to the vehicle, at a height of 0.1 m.

It is important to note that the system does not activate WPT unless the vehicle is over the emitting charging pad and therefore, electromagnetic emissions do not occur otherwise. Such a proactive approach creates a basic requirement in the design of WPT supporting ICT systems which must ensure that power is transferred only when a vehicle is over a given charging pad.

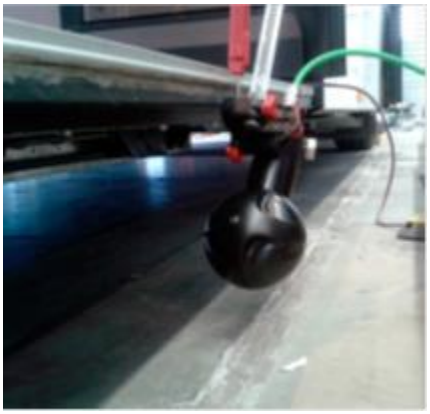

Figure 140: Magnetic flux calculation experimental setup.

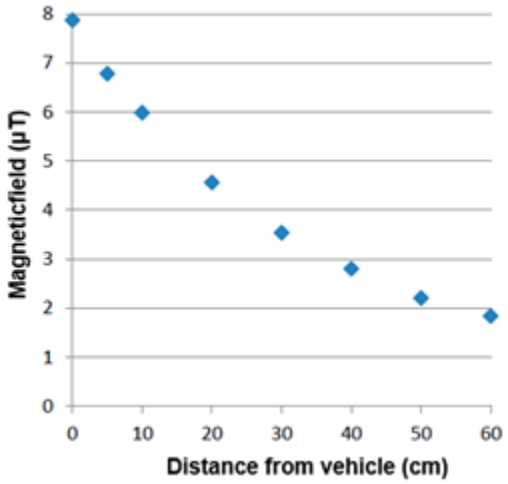

Figure 141: PRIMOVE magnetic field density.

5.3 Discussion

Current technologies and test setups for EMC and safety have focussed on static WPT configurations, which have often neglected issues that may appear during wireless charging operations. Aspects such as vehicle and consequently coil misalignment, could lead to increased electromagnetic emissions, thus a more detailed analysis is required in order to tune coil design parameters accordingly and specify the impact of such an environment on humans. Moreover, the overall design must take into consideration the cumulative electromagnetic noise that could occur due to neighbouring installations such as parking lots etc. In addition to optimised coil designs, ICT systems should enhance the suppression of electromagnetic noise where possible. Such systems could ensure the transmissions of power from the primary to secondary coil when a set of shielding criteria meet the criteria for safety and EMC.

6 CONCLUSIONS

6.1 General comments

The work presented in this deliverable is the outcome of WP3.5 activities, aimed to define vehicle equipment architecture and on-road equipment architecture definition and evaluation. The investigations also focussed on the definition of interface between charging systems and energy distribution networks.

The results of this activities specify which architecture aspects can be utilised from existing solutions and vehicles, and which aspects are required for further design, starting from a single vehicle perspective.

On-road dynamic power transfer architecture and the architecture of each solution are tailored to meet the specifications and capabilities of the test site that it will be tested on.

Evaluation results are summarised in the following sections, related to vehicle and on-road equipment architecture.

6.2 Vehicle equipment architecture

In Chapter 2 of this deliverable the vehicle equipment architecture has been analysed and discussed.

A detailed layout study has been carried out to define the correct installation of the system on the vehicle, and performance analysis, both in terms of NVH and Passive Safety for the CRF vehicle, has been carried out to check the developed layout, with the CRF Partner support.

The performed evaluations lead to the conclusion that there were no structural problems of the system, in normal vehicle operation conditions.

The most critical point of architecture definition, in term of components, materials and assembly, is the need to satisfy electromagnetic, thermal and mechanical requirements by means of the best compromise solution. For a shielding with additional structural and thermal functions; the case has to be completely hermetic.

First of all it would be very advantageous to obtain a significant weight reduction of the system, for example by means of integration between the receiving system and the structure.

Generally speaking, out of the scope of a feasibility study, the choice of materials must be revised from a manufacturing point of view.

6.3 On-road equipment architecture

In Chapter 3, the on-road architecture has been analysed and discussed. Both systems installed in previous trials, as well as the systems being evaluated in FABRIC, have been considered.

All wireless systems considered have a high-level architecture similar to that shown in Figure 142 – in this case the POLITO system architecture.

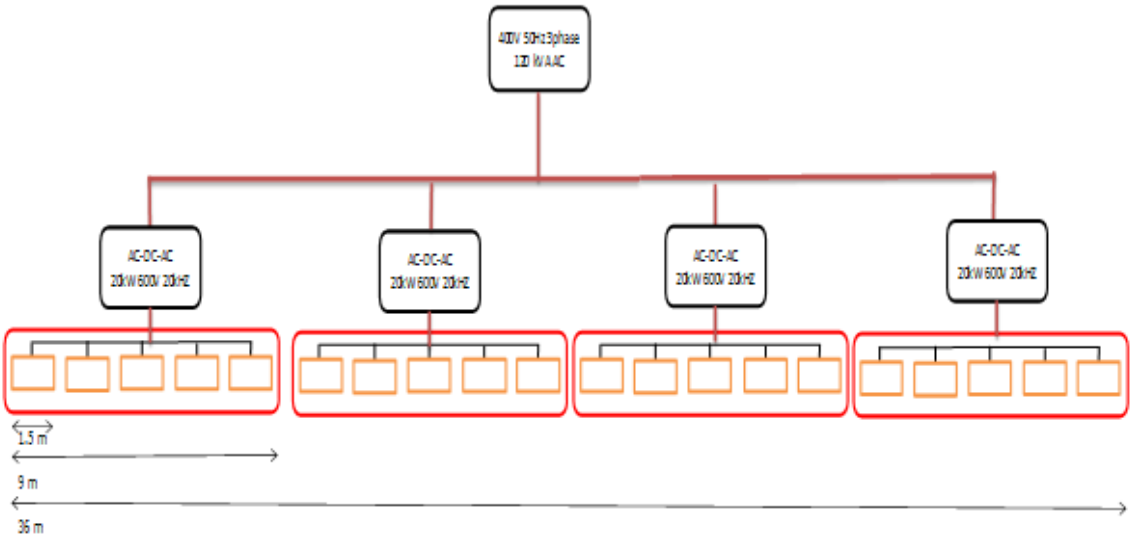

Figure 142: DWPT high-level architecture.

This shows how a low-voltage supply from a sub-station (which is connected to the high-voltage grid) is fed to a number of roadside controllers where the power is again converted to a format suitable for use by the power transfer system. This will typically take the low-voltage supply, rectify it and convert it to a high-frequency AC supply.

Typically, a controller will supply one or two power transfer segments (shown in red), and each segment will consist of one or more loops (shown in orange). While the size of segments, size of loops and number of loops per segment varies between systems, the high-level architecture tends to follow this basic format. There are a number of good reasons for using this architecture:

1. Power should only be transferred while a vehicle able to receive the power is over the power transfer area. From both a safety and efficiency point of view, power transfer equipment should be disabled when either a non-equipped vehicle, or any other object, could be affected by the power. Hence all solutions considered use power transfer segments or loops which are only activated when a suitable vehicle is in a suitable position to receive the power.
2. Long runs of power cables carrying high-frequencies and high-power should be avoided to minimise losses, hence power controllers are positioned close to the segments they feed.
3. Long runs of low voltage power should also be avoided to minimise losses in the power cables used, hence the sub-stations feeding the power controllers should not be too far from the controllers.

The power transfer loops in each segment are normally closely spaced to allow a near continuous transfer of power. Some systems activate loops on a rolling manner where at least two adjacent loops are activated at any one time, allowing the vehicle to draw continuous power from the charging infrastructure.

The positioning of power transfer loops within the road surface varies from solution to solution, their position being a compromise between the requirements of maximum efficiency, costs of components and installation, and durability and safety of the road surface. Therefore all solutions need to be embedded in such a way as not to compromise the structural integrity of the road, while maintaining a reasonable efficiency of power transfer.

Various techniques for embedment can be used, including trench construction where the equipment is installed into a trench machined into the road and covered over, pre-fabricated construction where power modules (typically concrete) are embedded into the road surface, or even pre-fabricated road lanes where an entire lane width of road is pre-fabricated with the power transfer equipment already embedded, and installed. As there has been no wide-scale deployment of dynamic wireless power transfer systems, it is not clear at this stage what the optimal embedment method is, or even if there is an optimal solution.

In-road conductive solutions are likely to have similar architectures to wireless systems. Again segmentation will be required for safety reasons, and local power distribution will be similar to that shown in Figure 142. Options for embedment are limited however, as the conductive rail must be exposed and level with the road surface. Roadside infrastructure is however different, as these typically transfer power using either medium voltage DC, or 50Hz AC, so the high-frequency inverters are not required.

Overhead conductive solutions are architecturally quite different to in-road solutions – they are typically not segmented, and being typically higher voltage (up to 1500v) do not require as regular road-side infrastructure. It should be noted that overhead conductive system are not suitable for use with cars and light trucks due to the required height clearance to overhead cables.

6.4 Interface with the energy distribution network architecture

In Chapter 4, the expected architecture of the interface of dynamic wireless power transfer solutions with the public grid has been described. It has been pointed out that the architecture of this interface will depend mainly on the power level of the installation and not on the power transfer technology (conductive or wireless). The reason lies in the fact that it can be expected that any of these solutions will include a power converter which rectifies in a first step the AC current from the grid to DC, as several examples of ongoing projects are suggesting. Therefore, from the point of view of the grid interface, no preference can be derived towards one particular solution. This intrinsic compatibility or interoperability of the grid-tied converter with any subsequent power transfer options is an important fact to be taken into account for any feasibility analysis.

Furthermore, it has been shown that high-power grid connection interfaces based on power electronics are already in operation for railway, tramway and trolley bus transport. This means that for large-scale implementation, existing converter technology can be readily adopted. Examples show that depending on the demand, even proprietary MV grids may be installed in order to feed the charging demand directly from HV distribution (> 100 kV).

In addition it is emphasized that from the experience of tramway applications, the integration of energy storage systems directly connected to the DC distribution line will be beneficial, reducing power peaks and thus power rating of the grid connection.

After this outlook towards possible solutions for large-scale implementation, a design is proposed which is thought to give support to the solutions which will be installed at the FABRIC test sites. The selected power level is 50 kW. Two topologies, based on IGBT power electronic devices have been presented. Dynamic simulation demonstrated that both solutions show very low harmonic distortion and acceptable THD even if connected to a weak grid. Three-level topologies are recommended in order to reduce the size of passive elements in the grid-side filter. Nevertheless, if a strong grid connection is available, simple PWM converters will also be able to fulfil current standards.

6.5 ICT interface to the energy distribution System.

Distribution System Operator (DSO) to charging system operator (CIO) information regarding available capacity and consumed capacity is transferred in real time between the aforementioned entities. Focus on the exchange of information regarding capacity (Power), between the aforementioned entities has been made in order to enable demand response as a means of avoiding peak power overloading. This particular use case has been identified as a scenario where "Smart charging" can intervene and result in satisfactory usage of current grid infrastructure, smaller investments of future grid infrastructure, cost minimisation due to thermal supply unit operations and support of distributed generation by the position paper reported by Eurelectric "Smart Charging: steering the charge, driving the change". The grid capacity is then disaggregated by the load balancing module which is installed within the charging infrastructure operator into charging levels allocated to EVs. In order to provide low latency responses to grid capacity emergencies or alternatively, intermittent power supply, a low latency transport protocol (RFC 6455) has been chosen for the DSO to CIO communication link. Though this transport layer mechanism differs from the proposal of the current OSCP specification [21], insights regarding the relative performance of RFC 6455 to HTTP web-services will be a valuable output of FABRIC. Nevertheless, the data model of OSCP will be implemented wherever possible. A detailed analysis regarding the DSO to Charging infrastructure operator implementation has been reported in Chapter 2 of D2.5.3, "Load Balancing for Dynamic Wireless Charging: ICT standardisation and approach". Moreover details regarding the implementation of load balancing, have been reported in chapters 2-6 of D2.5.3.

7 References

[1] P. FABRIC, D3.4 Specification Document, 2015.

[2] C. Lanczos, An iteration method for the solution of the eigenvalue problem of linear differential and integral operators, J. Res. Nat'l Bur. Std. , 1950.

[3] Viktoria Swedish ICT, "Slide-in Electric Road System, Inductive project report," Scania CV, 2013.

[4] California PATH Program, Roadway Powered Electric Vehicle Project Track Construction and Testing Program Phase 3D, California: University of California, 1994.

[5] I. Suh, "Application of shaped magnetic field in resonance (SMFIR) technology to future urban transportation," 21st CIRP Design Conference, 2011.

[6] TfL, "Street furniture guide".

[7] Department for Transport, "Manual for Streets," 2007.

[8] "Design Manual for Roads and Bridges, Volume 6: Road Geometry," 2005. [Online]. Available: http://www.standardsforhighways.co.uk/ha/standards/DMRB/vol6/section3.htm. [Accessed 20 10 2015].

[9] "Streetlayout," 04 2015. [Online]. Available: http://transportblog.co.nz/tag/dominion-road/page/2/.

[10] M. Webb and M. W. J. Clarke, IHS Jane's Urban Transport Systems 2012-2013, Jane's Information Group, 2012.

[11] S. Andersson and E. Edfeldt, Electric road System for trucks, Stockholm: KTH School of Industrial Engineering and Management, 2013.

[12] L. Abrahamsson, T. Schütte and S. Östlund, "Use of converters for feeding of AC railways for all frequencies," Energy for Sustainable Development, vol. 16, pp. 368-378, 2012.

[13] Wikipedia, "Railway electrification system," [Online]. Available: https://en.wikipedia.org/wiki/Railway_electrification_system. [Accessed 20 10 2015].

[14] G. Linhofer, P. Maibach and N. Umbricht, "The Railway Connection," ABB Review, vol. 3, 2008.

[15] F. Turki, V. Staudt and A. Steimel, "Dynamic wireless EV charging fed from railway grid: Grid connection concept," in Proc. of International Conference on Electrical Systems for Aircraft, Railway, Ship Propulsion and Road Vehicles (ESARS), 2015.

[16] H. Wu, A. Gilchrist, K. Sealy and D. Bronson, "A high efficiency 5 kW inductive charger for EVs using dual side control," IEEE transactions on industrial informatics, pp. 585-595, 2012.

[17] H. Jin, L. Sungwoo, P. Changbyung and C.-T. R. Gyu-Hyeoung C, “High performance inductive power transfer system with narrow rail width for on-line electric vehicles,” in IEEE ECCE.

[18] S. Li and C. Chris, “Wireless Power Transfer for Electric,” IEEE JOURNAL OF EMERGING AND SELECTED TOPICS IN POWER ELECTRONICS, 2015.

[19] J. Kim, J. Kim, S. Kong, H. S. I.-S. Kim, N. P. Suh, D.-H. Cho, J. Kim and S. AHN, “Coil Design and Shielding Methods for a Magnetic Resonant Wireless Power Transfer System,” Proceedings of the IEEE.

[20] H. Kim, C. Song, J. Kim, D. Jung, S. Eunseok, S. Kim, J. Kim and J. Kim, “Design of magnetic shielding for reduction of magnetic near field from wireless power transfer system for electric vehicle,” in International Symposium on Electromagnetic Compatibility, Gothenburg, 2014.

[21] OCA, “Open Smart Charging Protocol,” 2015.

[22] HEMIS, “Current EMC standards and gaps detected regarding FEVs,” 2012.

[23] Design Manual for Roads and Bridges, “Volume 6,” 2005.

[24] “streetlayout,” 04 2015. [Online]. Available: http://transportblog.co.nz/tag/dominion-road/page/2/.

[25] s. a. a. E. Edfeldt, Electric road System for trucks, Stockholm: KTH School of Industrial Engineering and Management, 2013.

[26] M. Budhia, J. T. Boys, C. A. Covic and H. Chang-Yu, “Development of a single-sided flux magnetic coupler for electric vehicle IPT charging systems,” IEEE transactions on Industrial Electronics, p. 318–328, 2014.

[27] J. Jae and K. Dae, “System architecture and mathematical model of public transportation system utilizing wireless charging electric vehicles,” in IEEE IESC, 2012.

[28] P. EcoFEV, D300.5 System design, integration and technical evaluation.

[29] “Streetlayout,” 04 2015. [Online]. Available: http://transportblog.co.nz/tag/dominion-road/page/2/.

[30] “Design Manual for Roads and Bridges, Volume 6: Road Geometry,” 2005. [Online]. Available: http://www.standardsforhighways.co.uk/ha/standards/DMRB/vol6/section3.htm. [Accessed 20 10 2015].